Energy Systems Research

Volume 1 • Number 4 • 2018

Published by
Melentiev Energy Systems Institute
Siberian Branch of Russian Academy of Sciences

Available online: esrj.ru

ISSN 2618-9992

Energy Systems Research

Volume 1 • Number 4 • 2018
International scientific peer-reviewed journal
Available online: http://esrj.ru

About the journal

Energy Systems Research is an international peer-reviewed journal addressing all the aspects of energy systems, including their sustainable development and effective use, smart and reliable operation, control and management, integration and interaction in a complex physical, technical, economic and social environment.

Energy systems research methodology is based on a system approach considering energy objects as systems with complicated structure and external ties, and includes the methods and technologies of system analysis. The system approach is also necessary to address complex energy issues and challenges.

Within this broad multi-disciplinary scope, topics of particular interest include strategic energy systems development at the international, regional, national and local levels; energy supply reliability and security; energy markets, regulations and policy; technological innovations with their impacts and future-oriented transformations of energy systems.

The journal welcomes papers on advances in power engineering and heat supply, energy efficiency and energy saving, renewable energy and clean fossil fuel generation, and other energy technological issues.

Energy Systems Research is also concerned with energy systems challenges related to the applications of information and communication technologies including intelligent control and cyber security, modern approaches of system analysis, modeling, forecasting, numerical computations and optimization.

Topics

- Energy production, conversion, transport and distribution systems
- Integrated energy systems
- Energy technologies
- International, regional, local energy systems
- Energy system protection, control and management
- Smart energy systems, smart grids
- Energy systems reliability and energy security
- Electricity, heating, cooling, gas and oil systems
- Energy system development and operation
- Demand-side management
- Energy economics and policy
- Renewable energy and clean fossil fuel based systems
- Distributed energy systems
- Sustainable energy transitions
- System problems of power and thermal engineering
- Artificial intelligence in energy systems
- Information and communication technologies in energy systems
- Energy systems analysis and modelling
- Computational methods and optimization in energy systems

Contacts

Scientific secretary:	Alexey Mikheev, Dr. of Eng.
E-mail:	info@esrj.ru
Tel:	+7 (3952) 950980 (English, Russian)
Fax:	+7 (3952) 426796
Address:	130, Lermontov str., Irkutsk, 664033, Russia

Contents

Distributed Ancillary Services in Smart Distribution Grids: Demand, Requirements and Benefits

Marc Richter[1,*], Przemyslaw Trojan[2], André Naumann[1], Przemyslaw Komarnicki[3]

[1] Fraunhofer Institute for Factory Operation and Automation IFF, Magdeburg, Germany
[2] Otto von Guericke University, Magdeburg, Germany
[3] Magdeburg-Stendal University of Applied Sciences, Magdeburg, Germany

***Abstract* — The progressing distribution of the electricity supply necessitates redesigning the mechanism for providing ancillary services particularly by the distribution grid. Methods of voltage regulation and congestion management particularly have to satisfy new standards since, although the development of renewables is increasing the number of resources with an impact, these resources' individual contribution is comparatively slight. Taking the state-of-the-art and the basic regulatory conditions in Germany as a point of departure, this paper analyzes the requirements for algorithms and communication systems that provide distributed support to distribution grid operation. A novel mathematical method that prevents voltage range deviations and feeder overloads based on sensitivities is presented and validated in simulations by a case study. An analysis of the communications systems for monitoring and control technologies for distributed energy resources, including the available communication channels, serves as the basis for an evaluation of the suitability of current control mechanisms in the future. The findings of a live field test in a real 110 kV distribution grid corroborate the necessity for coordinated grid support by distributed energy resources and demonstrate the limits of current methods.**

***Index Terms* — Ancillary services, distribution network, active/reactive distributed power control, renewables integration, communication standards for distributed energy resources, live test.**

* Corresponding author.
E-mail: marc.richter@iff.fraunhofer.de

http://dx.doi.org/10.25729/esr.2018.04.0001
Available online February 28, 2019.

I. Using distributed energy resources to support the grid

A. Introduction

Electrical grids and distribution grids in particular are currently undergoing a transition. Distributed sources, flexible loads and (stationary and mobile) storage systems will affect their operation in the future [1]. The growing number of distributed energy resources [2] will be operated primarily based on market factors [3]. This is the case in Germany in particular. Resources will supply energy at times when it is not necessarily expedient in terms of benefit to the grid and sometimes even detrimental to grid stability [4]. Distribution grids will have to be made smarter [5] and be able to use distributed electricity generation, loads and storage systems optimally for the current grid situation [6]. Distribution grid control centers will have to coordinate optimal operation and the requisite data exchange between control centers and distributed resources will have to be integrated [7], [8]. Good observability of the distribution grid will also be essential.

This paper presents the requirements that smart distribution grids ought to meet and methods for implementing them technically. Optimization algorithms and concepts for linking information systems of distributed resources are also presented. Although some aspects of observability are examined, readers are primarily referred to other literature.

B. State-of-the-Art Power System

An analysis of the situation in Germany reveals a rated generating capacity of 183.6 [9] at a peak demand of 82 GW. Around 94 GW (51%) of this rated capacity comes from renewable and thus distributed energy resources alone. They are supplemented by distributed energy resources operated with fossil fuels. The trend is toward an increasing share of renewables, thus making generation even more important on the distribution grid level [10]. For comparison, the rated capacity of storage systems

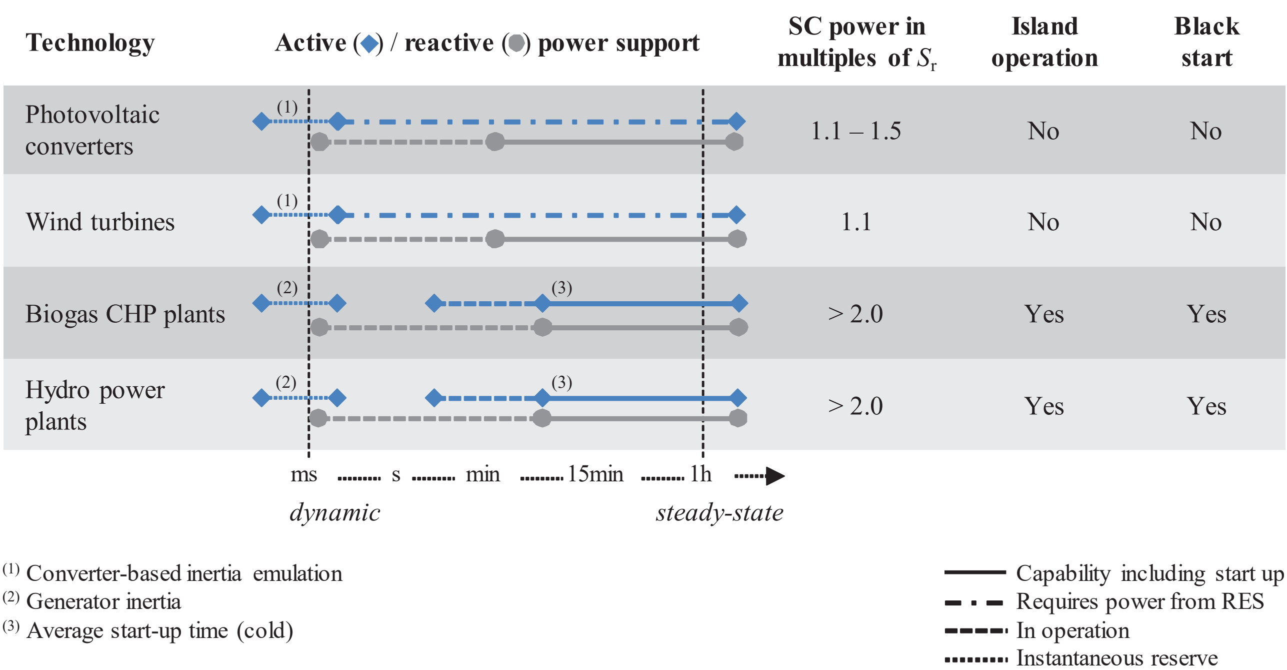

Fig. 1. Overall structure of the proposed aggregator.

is relatively low, the largest number being conventional storage systems such as pumped-storage power stations with 37 GWh in Germany [11], [12]. While technologies such as compressed air energy storage and battery systems are in use, their numbers are insignificant at present [13], [14], [15], [16]. Around 34000 battery energy storage systems with PV systems were installed in Germany in 2015. Assuming an average storage system has a capacity of 15 kWh, the total capacity of PV energy storage systems is approximately 510 MWh [12], equivalent to merely a fraction of energy storage capacities.

Distributed resources injecting power into the grid are primarily operated to maximize energy output and commercial profit. Benefit to the grid thus plays a subordinate role and grid operators can only take action to prevent equipment overloads in critical situations. In Germany, such actions are regulated in Section 13 of the Energy Industry Act [17]. This law stipulates that grid operators first have to perform appropriate switching operations, take market-related actions or activate additional reserves in order to ensure an electrical grid's reliability. Only when such actions are insufficient, grid operator may take-grid-related actions to curtail (the active power of) energy resources. Market factors are subordinate in this second step.

A grid operator usually takes action in the context of grid stability management, solely reducing the active power injected by resources [18]. Other potential capabilities of resources, e.g. supplying reactive power for voltage backup or microgrid capability, are not utilized at present. There is no regulatory and economic framework to offer system operators an incentive to provide resources for this. Moreover, sufficient measurements for system state estimation and thus suitable dynamic control algorithms for integration of distributed resources beneficial to the grid are not always available for grid operation.

C. Analysis of Ancillary Service Capabilities of Distributed Energy Resources

Relevant requirements ought to be listed first in order to assess distributed resources' capabilities. In principle, resources should be able to contribute to providing ancillary services [19] [20]. Their contribution is relevant on every level of the electricity supply and has increasingly to be covered by the growing number of distributed resources in the distribution grid. The typical features of each resource technology are crucial to capability. An overview of researchable capabilities beside storage systems as in [21] is presented in Fig. 1.

RES power plants are already able to supply active and reactive power within a very short time. Synthetic inertia emulation even enables converters to contribute instantaneous reserves [22]. Regardless of a resource size, they are not necessarily conditional on the availability of incoming power since power can be drawn from the intermediate circuit. Conventional generator systems still obtain this power from their inertia. Frequency support as well as grid restoration capabilities are nevertheless the domain of non-volatile resources alone [23], [24].

Reactive power is normally injected within a few grid cycles [24] regardless of its generation [25]. Increased use of converters decreases short-circuit power in the electrical grid. Protection necessitates usually limiting short-circuit current to 1.1 - 1.5 times the nominal current for [26], [27]. Only generator resources are able to supply much more nominal current [28].

Other services, e.g. supplying short-circuit current, improving power quality, and supplying microgrid capability and black-start capability, will presumably gain importance in the future. This will also generate new opportunities for the use of renewable and distributed energy resources, appropriate control algorithms having to be created and suitably adapted to the regulatory framework.

II. Active and Reactive Power Adjustment Beneficial to the Grid

A Three-Level Approach

An analysis can be performed on three different levels corresponding to the increasing contribution to ancillary services to utilize distributed resources capability to benefit the grid. On the simplest level, a distributed resource can be controlled so that it selects an optimized operating point at its connection point from the available measurements. To do this, the resource's local control system must continuously record voltage and frequency values at the connection point. These values are used to adjust the resource's operation to attain active and reactive power values that maximize system support based on the situation at the resource's connection point.

On the second level, the resource is run not only optimized, given the local connection point, but also with the goal of benefitting the grid in the section of the distribution grid with which it is connected. For voltage regulation, this can mean that voltage level is monitored along the grid branch (or ring) and distributed resources are controlled locally and regionally so that the voltage level has an optimal value within the grid branch (or ring). The active power supply is controlled in keeping with the requirements of the primary substation. Local and regional grid segments are incorporated for restoration of supply and microgrid capability to ensure a stable supply to these sections in the event of a malfunction.

The control of distributed resource on the third level goes beyond a local and regional analysis and is utilized to contribute to ancillary services in coordination with the primary grid. Direct or indirect communication must be ensured to transfer setpoints required for active and reactive power between primary grid operators and the particular resource, possibly in the form of a schedule. Whereas only the surrounding grid up to the primary substation is relevant for the operation of distributed resource on the other two levels, this does not constrain contributions to ancillary services on this level. Coordination with other distributed resources is essential to obtain optimal results since this maximizes the contributions to ancillary services [29], [30]. This requirement and the resultant requirements of requisite information and communications technologies (ICT) and coordination additionally makes this the most complex option of all.

The third level, which contributes most to global system stability, always ought to be striven for to stabilize operation. Moreover, the requirements of the two lower levels are taken into account during operation on these levels so that local and regional stability as well as the contribution to global ancillary services can be implemented.

B. Iterative Control Algorithm Using Sensitivity Analysis

An optimization algorithm that provides distributed support to the electrical grid is presented here. It ascertains an optimal setpoint value for individual resources in order to provide an ideal value for voltage response in the grid and to ensure that no equipment is overloaded. It is based on a method based on standard network theory, which depicts the distribution of flows of different resources between loads and lines. Approaches based on demand response using sensitivity matrices have been studied in [31]. Priority is given to renewable energy sources. Network structure parameters can employ diversity factors to identify the power diversity. This method can be used for economic dispatch and power flow analysis.

The active and reactive power adjustment necessary in each case is determined based on the Jacobian matrix J determined with the Newton–Raphson method for power flow studies. This matrix depicts the correlation between the active and reactive power buses and the electrical system state variables (voltage magnitude U and angle θ):

$$\begin{bmatrix}\Delta \boldsymbol{P}\\ \Delta \boldsymbol{Q}\end{bmatrix} = \begin{bmatrix}\boldsymbol{J}_{P\theta} & \boldsymbol{J}_{PU}\\ \boldsymbol{J}_{Q\theta} & \boldsymbol{J}_{QU}\end{bmatrix}\begin{bmatrix}\Delta \boldsymbol{\theta}\\ \Delta \boldsymbol{U}\end{bmatrix} \quad (3)$$

The following correlation results for the influence of purely reactive power control on the bus voltage level:

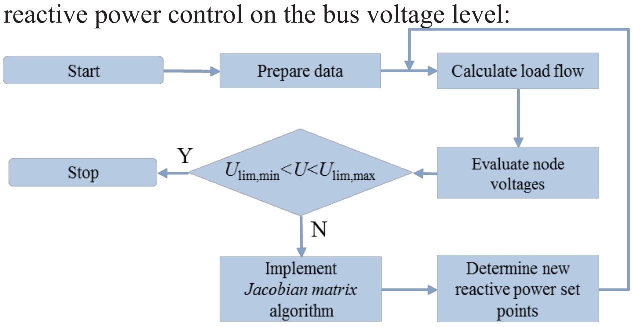

Fig. 2. Iterative optimization method for grid support

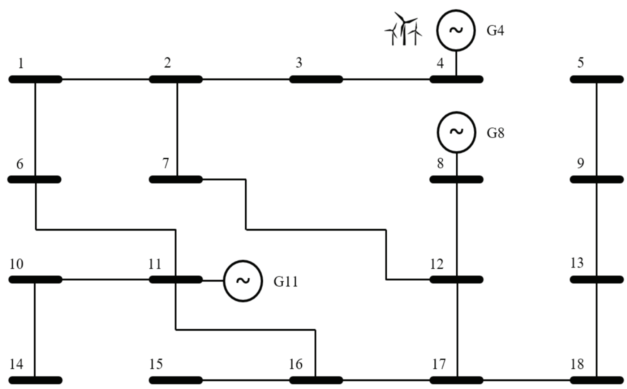

Fig. 3. Distribution grid structure for the field test

$$\Delta \boldsymbol{Q} = \left(\boldsymbol{J}_{QU} - \boldsymbol{J}_{Q\theta}\boldsymbol{J}_{P\theta}^{-1}\boldsymbol{J}_{PU}\right) \cdot \Delta \boldsymbol{U} = \boldsymbol{J}_R \cdot \Delta \boldsymbol{U} \tag{2}$$

The influence of reactive power control $\Delta \boldsymbol{Q}$ in the grid area analyzed can consequently be ascertained by inverting $\boldsymbol{J_R}$ according to (X).

$$\Delta \boldsymbol{U} = \boldsymbol{J}_R^{-1} \cdot \Delta \boldsymbol{Q} \tag{3}$$

The coefficients in the matrix $\boldsymbol{J}_R^{-1}$ indicate which buses have the greatest sensitivity to other buses, a higher value indicating a greater correlation. An analogous approach can be applied to active power control.

The optimization function is flowcharted in Fig. 2. The algorithm uses the Jacobian matrix in every iteration to verify the voltage values. In the event of voltage problems at the system buses, the reactive power adjustment is retrieved selectively until the grid malfunction has been eliminated. This algorithm runtime has proven practicable in tests since it completes the calculation in 0.5 s. This applies to the analyzed grid computed on a standard computer. It can be scaled up for larger systems. This also makes the algorithm suitable for operative use by CHPs controlled with parameters for a control strategy considering forecasts in less than one second [32].

C. Simulation Evaluation

Since thresholds were not exceeded during the entire period, the control algorithms did not automatically activate. Different operating points were therefore created in an 18-bus test system (see Fig. 3) to verify the algorithm developed to regulate voltage. At the start of every scenario, every dispatchable generator (at buses 4, 8 and 11, designated G4, G8 und G11) is assumed to supply 10 Mvar of reactive power. The outcomes of the simulations are presented in Table 1. Supplying reactive power stabilizes high voltage more efficiently. Adjusting active power would additionally entail undesired actions in the electricity market.

The simulation results presented in Table I (scenarios 1 to 6) confirm the optimization algorithm effectiveness. In scenario 1, generator G8 is selected to support the grid actively by supplying reactive power. The reactive power setpoints are adjusted to 1.13 Mvar. The voltage at bus 1 has already returned to the feasible value of 1.1 pu after the third iteration. Similar effects are observable in scenarios 2, 3 and 4. In the latter, generators with low sensitivities are additionally included for support since the technical limits of G8 have been reached. The number of iterations needed to calculate new setpoints rises to eleven loops. Scenarios 5 and 6 confirm the method effectiveness even when voltage is unduly low. Increase in reactive power at G4 and G8 also eliminates the stability problem.

D. Remote Control and Monitoring of Distributed Energy Resources

1) Introduction

Distributed energy resources integrated in an existing grid have to meet standard technical specifications and communications interface specifications, thus ensuring that they can be monitored with sufficient accuracy and time resolution, and controlled when necessary [33]. The interface of communications systems has to be designed accessibly so that different systems are interoperable [34]. Using open standards and standard interfaces is expedient [35], [36]. Practicable methods for this are presented below.

2) IEC 60870 and IEC 61850 Interface

Established and advanced remote control protocols such as IEC 60870 and IEC 61850 improve distributed resources' interface [37], [38]. This enables every relevant measurement to be continuously transmitted to a control center [39]. Any setpoint value desired can also be implemented within the limits of a particular resource technical capability. This means that both active and reactive power setpoint values can be varied dedicatedly in fine steps [40]. For instance, power electronic converters in advanced wind and PV systems can contribute substantially and flexibly to the local supply of reactive power. This can only be activated for grid operation with a proper communications interface, though. Although advanced and large resources have such interfaces, grid operators do not take full advantage of them at present [41]. Moreover, since the number of resources equipped with interfaces is very limited, conventional solutions still have to be employed.

Table 1. Simulation results

Before optimization			**After optimization**					
Scenario	Min. bus voltage in pu.	Max. bus voltage in pu.	Q_{G4} in Mvar	Q_{G8} in Mvar	Q_{G11} in Mvar	Min. bus voltage in pu.	Max. bus voltage in pu.	Iteration
1	U_{17} = 1.028	U_1 = 1.102	10.00	1.13	10.00	U_{17} = 1.028	U_1 = 1.100	3
2	U_{17} = 1.028	U_1 = 1.107	10.00	-22.65	10.00	U_{17} = 1.028	U_1 = 1.100	7
3	U_{17} = 1.028	U_1 = 1.108	10.00	-29.64	10.00	U_{17} = 1.028	U_1 = 1.099	8
4	U_{17} = 1.028	U_1 = 1.114	3.49	-30.00	-10.00	U_{17} = 1.028	U_1 = 1.099	11
5	U_1 = 0.899	U_{17} = 1.028	10.00	18.25	10.00	U_1 = 0.901	U_{17} = 1.028	2
6	U_1 = 0.885	U_{17} = 1.028	40.00	30.00	10.00	U_1 = 0.900	U_{17} = 1.028	7

3) Grid Stability Management Interface

Since the majority of distributed resources can only be controlled by a grid stability management interface, upgrades of installed equipment must be allowed. Such an upgrade enables the transmission of current measurements so that previously "blind" control systems of resources also deliver current measurements by wireless control signal and the grid operator is immediately notified of the resource's response. Even though this interface only facilitates relatively rough control of active power, while not permitting any control of reactive power, it improves the use of distributed resources to apply the aforementioned algorithm.

The additional technology that has to be installed to implement this control system and to transmit measurements basically consists of an additional current and voltage transformer measurement logger and an interface to the existing grid stability management interface, which normally consists of four main switching contacts. Every contact corresponds to one of four stages (100% - 60% - 30% - 0%). Conventional control systems (programmable logic controllers) provided by remote control interfaces can both log measurements and connect switches. MODBUS/TCP, IEC 60870, IEC 61850 or DNP3 can be used as the communications protocol for a remote control interface, thus enabling the grid operator to access resource parameters directly. A biomass CHP plant serves as an example in the design for upgrading existing resources diagrammed in Fig. 4.

4) Adding RTUs

Retrofitting with an RTU is a more flexible but also more expensive way of equipping an existing resource with a suitable remote monitoring and control system than that described in section 3). An additional RTU provided by such interfaces as IEC 61850 and IEC 60870 is subsequently integrated in the distributed resource's process control system. Normally, this is done by using Profibus, CAN bus or EtherCAT to link the retrofit RTU with the distributed resource's existing process control system. This makes the retrofitted RTU a gateway that exchanges defined data (measurement and setpoint values) between the resource's process equipment and the grid operator's remote control system. The RTU must be carefully configured since, in the worst case, direct access to the resource control system can damage the resource if the RTU has been configured incorrectly. The grid operator has to configure and test the IEC 61850 or IEC 60870 interface based on the resource features and the specifications.

E. Selecting Appropriate Communication Channels

1) Dedicated Lines through Grid Operators

A line installed by the electrical grid operator and dedicated to transmitting the resource measurement data and setpoint values can be used to connect distributed resources. This is a state-of-the-art approach to interfacing the communications system of substations but is inconsistently employed for distributed energy resources. The advantage of this approach is its provision of a very reliable interface explicitly established for this purpose, which is highly reliable and available. The relatively high installation costs are a drawback.

2) Public Network DSL or ISDN Line

The advantage of using existing lines of operators of public telecommunications networks such as DSL or ISDN is that they are already virtually ubiquitous and can be used to connect distributed resources. A landline telecommunications infrastructure may inadequately cover rural regions where the majority of distributed resources are installed. While ISDN lines and DSL suffice for the quantities of data normally transmitted, they may also be used for other public communication purposes, thus causing congestion. A factor viewed critically by grid operators in particular is property rights to the respective lines and thus also monopolies on lines. This can cause trouble in the event of a malfunction. Data security is more serious. Since public telecommunications networks are physically linked directly with the public Internet, actions have to be taken to prevent unauthorized access to the resource's or the grid operator's data network. Complex security measures and gateways have to be planned between the grid operators' internal network and the public network.

3) Mobile Broadband

Along with landline public telecommunications networks, public cellular networks can also be employed to monitor and control distributed resources. Since this does not necessitate installing additional lines to the particular resource, the capital expenditures are relatively low. This communication channel is the most unreliable in practice though. Cellular coverage may be inadequate in rural regions and is heavily dependent on weather conditions. Packets may be transmitted incompletely or the transmission bandwidth may not suffice at times, depending on the connection quality. Since this telecommunications network is public, the security constraints and associated additional security measures for landline public telecommunications networks also apply (see section 2)).

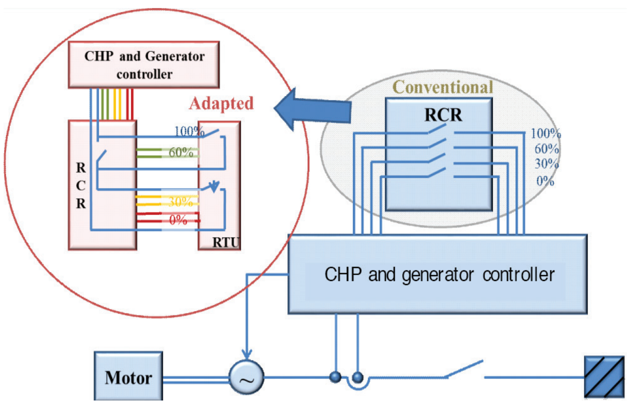

Fig. 4. Interface design.

4) Selections in Comparison

The relevant features of the different technologies are compared in Table II.

5) Future Communication Channels

Additional communication channels can be expected to gain importance in the future. Power-line communication systems, for instance, can transmit data from a distributed resource to the nearest substation where other technologies forward them. This approach could grow more prevalent in the future [42], [43], [44], [45].

Efforts are also made to regulate radio frequency bands dedicated to transmit data for electrical grid operation [46]. Frequencies of 400 MHz and 450 MHz that provide a channel bandwidth sufficient to transmit a sufficient payload are especially relied on here. The band frequency should be low enough to expand physically (with appropriately low free-space path loss) to connect to respective distributed resources reliably.

III. Practical Limits of Active Power Adjustments

A. Field Test Environment

A 110 kV voltage section of an 18-bus distribution grid (see Fig. 3) served as the field test area. The grid is highly saturated with RES (160 MW of wind and 40 MW of photovoltaic power) and has a peak load of 220 MW. An 80 MW wind farm was used to test actions using active power to stabilize voltage. Two high voltage transformers connect it with the grid. The large electrical distance to the 110/380 kV connection point (bus 14) minimizes influences from the high voltage system.

Voltages were recorded directly at the wind farm connection point U_4 to analyze the effects of active power control on the rest of the grid and additionally at substation U_2 approximately 20 km away. The wind farm is represented by generator G4.

B. Findings

The recorded curves of the incoming power supplied by the wind farm and the related voltage values at the wind farm U_2 and at the adjacent station U_2 are presented in Fig. 5.

The active power was curtailed when the load was low for monetary reasons. The control signal was sent at t_1 = 30 min. Instruments verified the complete cessation

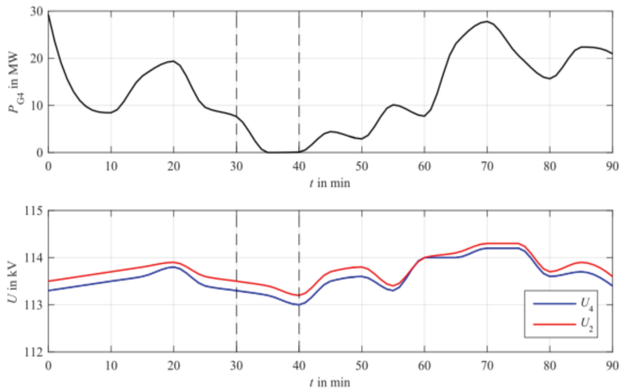

Fig. 5. Active power and voltage curve in the field test.

of active power injection after about 4 min. The curtailed power was 8.1 MW and accompanied by a voltage drop of 0.3 kV at both the connection point and the nearby substation. The grid stability management interface was reactivated at t_2 = 40 min.

C. Evaluation

A correlation k [47], [48] of the voltage curves with the active power curve can be discerned. The mathematical correlation factors of the active power P_{G4} with the voltage at the wind farm connection point U_4 or the active power P_{G4} with the nearby substation voltage U_2 at bus 2 are as follows:

$$k_{PG4-U4} = \frac{\sum_{i=1}^{n}\left(P_{G4,i} - \overline{P_{G4}}\right)\left(U_{4,i} - \overline{U_4}\right)}{\sqrt{\sum_{i=1}^{n}\left(P_{G4,i} - \overline{P_{G4}}\right)^2 \cdot \sum_{i=1}^{n}\left(U_{4,i} - \overline{U_4}\right)^2}} = 0{,}84 \quad (4)$$

$$k_{PG4-U2} = \frac{\sum_{i=1}^{n}\left(P_{G4,i} - \overline{P_{G4}}\right)\left(U_{2,i} - \overline{U_2}\right)}{\sqrt{\sum_{i=1}^{n}\left(P_{G4,i} - \overline{P_{G4}}\right)^2 \cdot \sum_{i=1}^{n}\left(U_{2,i} - \overline{U_2}\right)^2}} = 0{,}73 \quad (5)$$

Factoring in a potential range of the correlation factor from -1 (completely negative correlation) to 0 (no correlation) to +1 (completely positive correlation), the field test demonstrated that:

1. the active power control influences voltages both at the connection point and in the nearby grid,
2. the voltage effect diminishes greatly as distance increases, and
3. although an active power variation–voltage causality is

Table 2. Telecommunication technologies in comparison.

Parameter	Dedicated network operator lines	Public lines (ISDN, DSL)	Public wireless (GPRS, UMTS, LTE)
Availability (space)	Limited	High	Variable
Availability (time)	Constant	Very high	Variable (weather-dependent)
Reliability	Very high	High	Low
Cost	High	Medium	Low
Security	Very high	Low	Medium

present, its impact is unduly low.

Consequently, the standard grid stability management interface is “not suited” for limiting active power. On the one hand, economic losses ensue since available renewable power cannot be injected into the electrical grid. Therefore, additional battery storage systems could be used to minimize impacts [49]. On the other hand, the simulation tests have demonstrated that smart and coordinated reactive power control by distributed resources has a greater impact on the grid while keeping costs the same.

IV. Conclusion

The capabilities of renewable energy plants and distributed energy resources to play a role in certain ancillary services was scrutinized and the technical, communication and regulatory requirements for this were analyzed. Capabilities to eliminate voltage problems by adjusting reactive power in selected resources while minimizing the impact on ongoing grid operation and not taking market-related actions were presented in simulations. A field test demonstrated the technical limits of conventional curtailment of renewable energy plants. The moderate influence of unilateral control of active power on voltage as well as the shortfall renewable energy at equal cost caused by it was decisive.

An increasing response to critical situations directly at the local level and with more intensive coordination (among distribution grid operators as well) will therefore be expedient in the future. This approach will guarantee a globally optimized result while minimizing the impact on grid operation and components [50]. Advanced renewable energy plants already have the technical capabilities to implement fine operating points while employing advanced communications standards [51], [52]. More intensive monitoring of low voltage levels and the use of available communication channels to interface field devices are therefore an important prerequisite for a more dynamic and accurate control system [53]. Germany requires few regulatory changes to implement such a system. Part of the standards have already been incorporated in amendments (e.g. to the 2017 German Renewable Energy Act [19]) and regulations (e.g. 2015 Regulation of Ancillary Services by Wind Turbines [54]).

Acknowledgment

This paper was written as part of the research project SECVER funded by the German Federal Ministry for Economic Affairs and Energy.

Mathematical Symbols

k	Correlation factor
J	Jacobian matrix
P	Active Power
Q	Reactive power
S	Apparent power
t	Time
U	Voltage

Abbreviations

CHP	Combined heat and power
DER	Distributed energy resource
DSL	Digital subscriber line
DSO	Distribution system operator
EEG	Erneuerbare-Energien-Gesetz (German Renewable Energy Sources Act)
GPRS	General Packet Radio Service
ISDN	Integrated Services Digital Network
LTE	Long Term Evolution
RCR	Remote Control Relay
SDLWindV	Verordnung zu Systemdienstleistungen durch Windenergieanlagen (Regulation of Ancillary Services by Wind Turbines)
TSO	Transmission system operator
UMTS	Universal Mobile Telecommunications System

References

[1] J. Wang, “Smart grids, renewable energy integration, and climate change mitigation – Future electric energy systems,” *Applied Energy*, pp. 1-3, 2012.

[2] J. Wu, “Integrated Energy Systems,” *Applied Energy*, pp. 155-157, 2016.

[3] J. Winkler, M. Pudlik, M. Ragwitz and B. Pfluger, “The market value of renewable electricity – Which factors really matter?,” *Applied Energy*, pp. 464-481, 2016.

[4] N. Ederer, “The market value and impact of offshore wind on the electricity spot market: Evidence from Germany,” *Applied Energy*, pp. 805-814, 2015.

[5] N. I. Voropai and B. Bat-Undraal, “Multicriteria reconfiguration of distribution network with distributed generation,” *Journal of Electrical and Computer Engineering*, 2012.

[6] C. F. Calvillo, A. Sanchez-Miralles and J. Villar, “Optimal planning and operation of aggregated distributed energy resources with market participation,” *Applied Energy*, pp. 340-357, 15 11 2016.

[7] J. Yan, Y. Zhai, P. Wijayatunga, A. M. Mohamed and P. E. Campana, “Renewable energy integration with mini/micro-grids,” *Applied Energy*, pp. 241-244, 2017.

[8] S. B. Myungchin Kim, “Decentralized control of a scalable photovoltaic (PV)-battery hybrid power systems,” *Applied Energy*, pp. 444-455, 2016.

[9] Bundesnetzagentur, “Kraftwerksliste,”

Bundesnetzagentur, 2017. [Online]. Available: https://www.bundesnetzagentur.de/cln_1411/DE/Sachgebiete/ ElektrizitaetundGas/Unternehmen_ Institutionen/Versorgungssicherheit/Erzeugungskapazitaeten/Kraftwerksliste/kraftwerksliste-node.html. [Zugriff am 24 April 2017].

[10] H. U. Heinrichs and P. Markewitz, "Long-term impacts of a coal phase-out in Germany as part of a greenhouse gas mitigation strategy," *Applied Energy*, pp. 234-246, 2017.

[11] J. L. Peter Stenzel, "Concept and potential of pumped hydro storage in federal waterways,"*Applied Energy*, pp. 486-493, 2016.

[12] J. Schmidt-Curreli, A. Knebel und L. Lawrenz, "Energiewendeatlas Deutschland 2030," Agentur für erneuerbare Energien e.V., Berlin, 2016.

[13] P. A. Lombardi and F. Schwabe, "Sharing economy as a new business model for energy storage systems," *Applied Energy*, pp. 485-496, 2017.

[14] C. Guo, L. Pan, K. Zhang, C. M. Oldenburg, C. Li und Y. Li, "Comparison of compressed air energy storage process in aquifers and caverns based on the Huntorf CAES plant," *Applied Energy*, pp. 342-356, 2016.

[15] R. Madlener and J. Latz, "Economics of centralized and decentralized compressed air energy storage for enhanced grid integration of wind power," *Applied Energy*, pp. 299-309, 2013.

[16] M.-A. Hessami and D. R. Bowly, "Economic feasibility and optimisation of an energy storage system for Portland Wind Farm (Victoria, Australia)," *Applied Energy*, pp. 2755-2763, 2011.

[17] Bundesrepublik Deutschland, "Gesetz über die Elektrizitäts- und Gasversorgung (Energiewirtschaftsgesetz - EnWG)," Berlin, 2017.

[18] V. M. Michael Waite, "Modeling wind power curtailment with increased capacity in a regional electricity grid supplying a dense urban demand," *Applied Energy*, pp. 299-317, 2016.

[19] Bundesrepublik Deutschland, "Gesetz für den Ausbau erneuerbarer Energien (EEG)," Berlin, 2017.

[20] VDE, "TAB Hochspannung (VDE-AR-N 4120)," VDE, Frankfurt, Germany, 2015.

[21] S. Balischewski, C. Wenge, P. Komarnicki and M. Wolter, "Optimized operation of energy storages for primary control reserve," in Proc. of 2018 NEIS Conference on Sustainable Energy Supply and Energy Storage, Hamburg, Germany, 2018.

[22] F. M. Gonzalez-Longatt, "Activation schemes of synthetic inertia controller on full converter wind turbine (type 4)," in Proc. of 2015 Power & Energy Society General Meeting, Denver, CO, USA, 2015.

[23] A. Hoke, M. Shirazi, S. Chakraborty, E. Muljadi and D. Maksimovic, "Rapid Active Power Control of Photovoltaic Systems for Grid Frequency Support," IEEE *Journal of Emerging and Selected Topics in Power Electronics*, 2016.

[24] Sandia National Laboratories, "Reactive Power Interconnection Requirements for PV and Wind Plants - Recommendations to NERC," *Sandia National Laboratories, Albuquerque*, NM, 2012.

[25] SMA, "Technical Information: Q at Night," SMA, Kassel, Germany.

[26] D. Turcotte and F. Katiraei, "Fault Contribution of Grid-Connected Inverters," in Proc. of IEEE Electrical Power Conference, Montreal, Quebec, Canada, 2009.

[27] E. Muljadi, N. Samaan, V. Gevorgian, J. Li and S. Pasupulati, "Short Circuit Current Contribution for Different Wind Turbine Generator Types," in Proc. of 2010 IEEE PES General Meeting, Providence, RI, USA, 2010.

[28] WA notstromtechnik GmbH, "Stromerzeuger-Lexikon," [Online]. Available: http://www.stromerzeuger-lexikon.de/lexikon/kurzschlusleistung. [Zugriff am 24 April 2017].

[29] D. Wang, S. Parkinson, W. Miao, H. Jia, C. Crawford and N. Djilali, "Hierarchical market integration of responsive loads as spinning reserve," *Applied Energy*, pp. 229-238, 2013.

[30] P. A. Ostergaard, "Ancillary services and the integration of substantial quantities of wind power," *Applied Energy*, pp. 451-463, 2006.

[31] O. Homaee, A. Zakariazadeh, S. Jadid and P. Siano, "A new approach for real time voltage control using demand response," *Applied Energy*, vol. 117, pp. 157-166, 2014.

[32] M. Short, T. Crosbie, M. Dawood and N. Dawood, "Load forecasting and dispatch optimization for decentralied co-generation plant with dual energy storage," *Applied Energy*, vol. 186, pp. 304-320, 2017.

[33] B. M. Buchholz and Z. A. Styczynski, Smart Grids - Fundamentals and Technologies in Electricity Networks, Berlin Heidelberg: Springer-Verlag, 2014.

[34] G. Ghatikar, S. Mashayekh, M. Stadler, R. Yin and Z. Liu, "Distributed energy systems integration and demand optimization for autonomous operations and electric grid transactions," *Applied Energy*, vol. 167, pp. 432-448, 2016.

[35] W. Shi, X. Xie, C.-C. Chu and R. Gadh, "Distributed Optimal Energy Management in Microgrids," IEEE Transactions on Smart Grid, pp. 1137-1146, 05 2015.

[36] G. Zapata, A. Salazar, D. Moreno and R. Garcia, "Supervision of a distributed energy resources generation system using IEC and ISA standards," Robotics and Automation (CCRA), IEEE Colombian

Conference, 2016.

[37] N. Higgins, V. Vyatkin, N.-K. C. Nair and K. Schwarz, "Distributed Power System Automation With IEC 61850, IEC 61499, and Intelligent Control," IEEE Transactions on Systems, Man, and Cybernetics, Part C (Applications and Reviews), pp. 81-92, 2011.

[38] T. Dethlefs, C. Brunner, T. Preisler, O. Renke, W. Renke and A. Schröder, "Energy Service Description for Capabilities of Distributed Energy Resources," *Lecture Notes in Computer Science*, 6 01 2016.

[39] C. Wenge, A. Pelzer, A. Naumann and P. Komarnicki, "Wide area synchronized HVDC measurement using IEC 61850 communication," in 2014 IEEE PES General Meeting | Conference & Exposition, National Harbour, MD, USA, 2014.

[40] N. Etherden, V. Vyatkin and M. H. J. Bollen, "Virtual Power Plant for Grid Services Using IEC 61850," IEEE Transactions on Industrial Informatics, pp. 437-447, 2016.

[41] S. Alepuz, S. Busquets-Monge, J. Bordonau and J. Gago, "Interfacing Renewable Energy Sources to the Utility Grid Using a Three-Level Inverter," *IEEE Transactions on Industrial Electronics*, pp. 1504-1511, 10 2006.

[42] F. R. Yu, P. Zhang, W. Xiao und P. Choudhury, "Communication systems for grid integration of renewable energy resources," *IEEE Network*, 2011.

[43] Y.-s. Son, T. Pulkkinen, K.-d. Moon und C. Kim, "Home energy management system based on power line communication," *IEEE Transactions on Consumer Electronics*, 2010.

[44] U. Braun, "Bridging the gap with Broadband Powerline (BPL) technology," in Innovative Smart Grid Technologies (ISGT Europe), Manchester, UK, 2011.

[45] L. Karg und M. Wedler, "E-Energy Abschlussbericht - Ergebnisse und Erkenntnisse aus der Evaluation der sechs Leuchtturmprojekte," B.A.U.M Consult GmbH, München, Berlin, 2014.

[46] D. Marger, J. Riedl, J. Tusch, C. Wietfeld, I. Wolff und W. Zeittler, "Kommunikationsnetz für das Smart Grid - Positionspapier des VDE zur weiteren Ausgestaltung der Energiewende," *VDE Verband der Elektrotechnik Elektronik Informationstechnik e.V.*, Frankfurt am Main, 2015.

[47] K. Pearson, "Notes on the History of Correlation," Biometrika, pp. 25-45, 1920.

[48] J. Hauke and T. Kossowski, "Comparison of values of Pearson's and Spearman's correlation coefficients on the same sets of data," *Quaestiones Geographicae*, 2011.

[49] S. Balischewski, I. Hauer, M. Wolter, C. Wenge, P. Lombardi and P. Komarnicki, "Battery storage services that minimize wind farm operating costs: A case study," in Proc. of 2017 IEEE PES Innovative Smart Grid Technologies Conference Europe, Torino, Italy, 2017.

[50] M. Bae, H. Kim, E. Kim, A. Y. Chung, H. Kim and J. H. Roh, "Toward electricity retail competition: Survey and case study on technical infrastructure for advanced electricity market system," *Applied Energy*, pp. 252-273, 2014.

[51] T. J. Hammons, "Integrating renewable energy sources into European grids," *International Journal of Electrical Power & Energy Systems*, pp. 462-475, 2008.

[52] P. N. Vovos, A. E. Kiprakis, A. R. Wallace and G. P. Harrosin, "Centralized and Distributed Voltage Control: Impact on Distributed Generation Penetration," *IEEE Transactions on Power Systems*, pp. 476-483, 2007.

[53] S. U. Taha, C. Ozansoy and A. Zayegh, "Modeling of a Centralized Microgrid Protection System and Distributed Energy Resources According to IEC 61850-7-420," *IEEE Transactions on Power Systems*, pp. 1560-1567, 08 2012.

[54] Bundesrepublik Deutschland, "Verordnung zu Systemdienstleistungen durch Windenergieanlagen (SDLWindV)," Berlin, 2015.

Marc Richter holds a PhD in electrical engineering from the Otto von Guericke University of Magdeburg. He is currently an expert scientist in the Convergent Infrastructures business unit at the Fraunhofer Institute IFF. His main research interest is in demand side management and electric energy system studies. In recent years, Marc Richter has also focused on the development and operation of innovative technologies, such as digital twins and artificial intelligence, in modern power systems.

Przemyslaw Trojan received his PhD degree in electrical engineering from Otto von Guericke University Magdeburg, Germany in 2013 and 2018 respectively. He is currently research assistant at the Otto von Guericke University Magdeburg at the Chair of Electric Power Networks and Renewable Energy Sources. His research interests are agent-based approaches for power system management, modelling of power systems, real-time simulations, and communication technologies.

André Naumann received his PhD at Otto von Guericke University Magdeburg in 2012. He is now group manager at Fraunhofer Institute for Factory Operation and Automation IFF. His special field of interest include protection systems in electrical energy systems as well as substation automation and communication technologies for energy systems. He is a member of the German Association for Electrical, Electronic and Information Technologies (VDE), active in the standardization process for Power Network Operation in the DKE German Commission for Electrical

Przemyslaw Komarnicki earned a dual Master's of Science from Wroclaw University of Technology in Poland and Otto von Guericke University of Magdeburg in Germany in 2004. Since 2008, he has been the manager of the Electric Power Systems Group in the Convergent Infrastructures business unit of the Fraunhofer Institute IFF. Parallel to his work, he earned

Development of Mongolia's Electric Power Industry and its Role in Shaping the Northeast Asian Super Grid

Bayar Bat-Erdene*, Sereeter Batmunkh, Altain Erdenebaatar

Mongolian State University of Science and Technology, Mongolia

***Abstract* — The paper presents the background of creation and development of Mongolia's electric power industry and its current state. Despite considerable energy resources, the country suffers from electric power shortage that is covered by electricity supplied from Russia and China. The expected considerable power consumption growth can be met by doubling generating capacities, enhancing electrical networks and by interconnecting the five existing electric power systems (EPSs) into an Integrated Power System (NPS) of Mongolia as a future component of the Northeast Asian Super Grid. To accomplish these tasks, we propose a number of conceptual structural and technological models for the development of Mongolian electric power systems that can form a basis for the future Integrated Power System of Mongolia.**

***Index Terms* — Electric power generating industry, energy resources, electric power systems, power plants, transmission lines, forecasting, structural models of the system, electric power interconnection.**

I. Introduction

Until the early XX century, Mongolians remained nomads occupied largely with livestock breeding. Energy demand was reduced to heating by open fire of conventional household stoves; there was no idea of the energy supply in the most general sense. The first electric lighting was used in Ulaanbaatar, the capital of Mongolia, in 1912. The emergence and development of electric power industry within a little more than 100 years can be divided into four phases:

1. 1912-1940. The economy of Mongolia is mainly a livestock economy; industry is predominantly represented by small trades. This is the time when the first 2.5 MW cogeneration plant was put into operation in Ulaanbaatar.
2. 1940-1960. Manufacturing industry comes into being, the first large processing plants are constructed, and urban population grows. The need arises to establish electric power systems, and the groundwork for the accomplishment of this task is laid.
3. 1960-1990. A new economic policy is pursued to transform the country's economy from agrarian-industrial to industrial-agrarian one. The implementation of this economic policy primarily required development of new heat and power generating facilities, and they were constructed. This is the period when four independent EPSs that covered almost the entire country were constructed and further developed.
4. 1990- until now. This period is characterized by technological advancements in the electric power industry, by its furnishing with modern machinery and equipment, development of new technologies, implementation of a number of advanced projects. Nevertheless, some urgent problems remain. They include expansion of generating capacities (including maneuverable ones); construction of transmission lines; establishment of an Integrated Power System (IPS) of Mongolia and its integration into the Northeast Asian Power Grid, International Power Pool in Northeast Asia, and others. All these challenges require

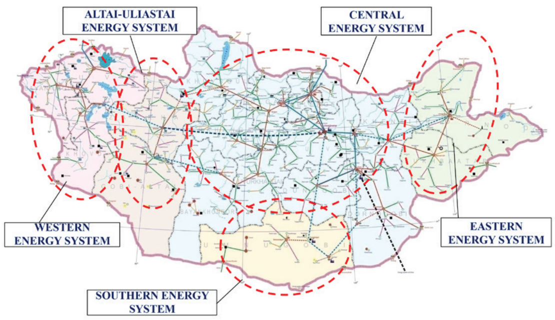

Fig. 1. Electric Power Systems of Mongolia.

* Corresponding author.
E-mail: batmunkh_acad@yahoo.com

http://dx.doi.org/10.25729/esr.2018.04.0002
Available online February 28, 2019.

Table 1. Characteristics of electric power systems of Mongolia.

No.	EPS	Power plants		Length of transmission lines, km					Note
		Name	Installed capacity, MW	220	110	35	15	10-6	
1	CEPS	CHP-2	21.5 (1.99%)						CEPS supplies power for people in 13 aimags and covers 60 percent of Mongolian territory.
		CHP-3	198 (18.39%)						
		CHP-4	723 (67.14%)						
		NEEPS	50 (4.64%)						
		ECP	36 (3.34%)						
		DarCHP	48 (4.46%)						
		BUPVS	0.4 (0.04%)						
		Total	1076.9 (100%) (92.6%)	1434	3439	6197	1694	9619	
2	WEPS	Durgen HPP	12 (100%)						110kV transmission line 800 km long works in parallel with Krasnoyarsk EPS (the Russian Federation).
		Total	12 (100%) (1.03%)	-	779	951	960	1207	
3	SEPS	DCP	9 (33.3%)						Mining industry is rapidly developing in this province, including Oyu Tolgoi copper-molybdenum mine, and Tavan Tolgoi coal basin
		TTCPP	18 (66.7%)						
		Total	27 (100%) (2.32%)	-	-	431	161	236	
4	AUEPS	Taishir HPP	11 (100%)						It is connected to WEPS by a single-circuit 35kV TL and to CEPS by a single-circuit 110kV transmission line.
		Total	11 (100%) (0.95%)	-	253	929	533	525	
5	EEPS	DorCHP	36 (100%)						It is connected to CEPS by a single-circuit 110kV transmission line.
		Total	36 (100%) (3.1%)	-	849	990	292	722	
Total:			1162.9 (100%)	1434	5321	9498	3640	12309	

both technical implementation and development of an appropriate methodology for modeling and for feasibility studies on the complex development of rapidly growing electric power industry and EPSs of Mongolia.

II. The Current State of Mongolia's Electric Power Industry and Prospects for its Development

1. The Current State of Mongolia's Electric Power Industry

The area of Mongolia is 1.5 million square kilometers; its population is about 3 million people. The country is rich in different mineral resources, including coal and oil shale. In the foreseeable future they will remain the major fuels for the power industry. There are also some other prospective energy resources to be taken into account when making decisions on strategic development of the national EPSs [1].

At present there are five independent EPSs in Mongolia:

1. Central Electric Power System (CEPS)
2. West Electric Power System (WEPS)
3. South Electric Power System (SEPS)
4. Altai-Uliastai Electric Power System (AUEPS)
5. East Electric Power System (EEPS)

Present-day structure of Mongolian EPSs is given in Fig. 1, while some quantitative characteristics of five independent EPSs are given in Table 1, where NEEPS is Northeast EPS, DarCHP is Darkhan CHP, ECP is Erdenet CHP, TTCPP is Tavan-Tolgoi CPP, DCP is diesel CHP, DorCHP is Dornod CHP.

The data given in Table 1 show that 92.6% of Mongolia's generating capacities are concentrated in CEPS that covers more than 60% of the country's territory. Almost all the power plants of CEPS (with the exception of 50 MW Salkhitiin wind mill and 0.4 MW Buyant-Uhaa photovoltaic system – BUPVS) are combined heat and power plants (CHPs) designed for heat and power cogeneration. In the structure of CEPS generating capacities, the cogeneration plants account for 92.15%; condensing power plants (Ukhaa-Khudag CPP) fired by brown coal make up 1.54%; wind mills - 4.3%; hydro power plants (HPP) - 1.97%, and solar power plants account for 0.04%. The share of renewable energy sources in the total power generation does not exceed 6.3%.

The presented structure of generating capacities does not take into account back-up diesel power plants of aimag and somon centers, and local hydropower plants. According to the data available, diesel power plants of aimag and somon centers in 2014 generated about 0.15% of the total electricity generated in the country.

Electricity demand of almost all the consumers distant from the centralized electricity system has been satisfied owing to the "100 000 Solar Ger Electrification" programme launched in the early 2000s. The Project implied the use of small-size power sources. This project has been successfully implemented and electricity demand of local households has been almost 100% met. Due to lack of reliable statistical data it is difficult to assess quantitative results of the "100 000 Solar Ger Electrification" programme. Nevertheless, assuming that power consumed by one herder family in the decentralized areas (provided they use energy-efficient domestic appliances) is approximately equal to 100 W, the power consumed by 180 000 nomadic families will make up 18 MW. Thus, electricity generation by solar power plants reaches 1.4% of the total power generation in the country.

At present 80% of consumed electricity is generated in Mongolia and 20% is imported from Russia and China. On the average, 14.4% of electric power generated by CHP are used for auxiliary needs; power losses in the system on the average are 13.7%. These figures are by 1.3-1.7 times higher than those for developed countries [2]. In the future, they should be made equal to the world indicators.

Electric power systems of Mongolia are composed of overhead transmission lines for the voltage levels of 110 kV, 220 kV, as well as of 0.4 kV, 6 kV, 10 kV, (15), and 35 kV. Transfer capability of a transmission line depends on the wire cross-section, the number of circuits and the distance the line covers [3].

Technical characteristics of the lines, including their transfer capability, and the largest power transmission distance are given by voltage level in Table 2 [3].

An analysis of a scheme of Mongolia's electric power systems (Fig. 1) and the data in Table 2 reveal that 220 kV transmission lines are within feasible limits in terms of transmitted power and extension, whereas the distance covered by 110 kV and 35 kV transmission lines exceeds the recommended values given in Table 2, which reduces transfer capability of the lines and disturbs their normal operating conditions. As an example, 110 kV transmission line Bulgan-Muren-Uliastai-Altai covers the distance of 1000 km. Excessive (above recommended size) length of this line has a negative impact on its operation, reduces its transfer capability and complicates its operation.

In Mongolia's electric power systems, the length of 220 kV transmission lines in CEPS alone is 1434 km, that of 110 kV lines is 5321 km, including 3439 km within CEPS. Due to poorly informed technological policy in the national electric power industry, the electric power systems of Mongolia have not been appropriately developed. Ultra-long low-voltage transmission lines built in the late 1990s were, on the one hand, of high social value as they supplied power to a large community but, on the other hand, they produced some negative effects. In particular, the quality of transmitted power deteriorated, the systems could not operate efficiently, and the dispatching and emergency control capabilities diminished.

According to the calculations of power flows of the ultra-long low-voltage transmission lines, it was necessary to install compensators at the terminal substations but due to a considerable increase in the total costs, this was not done. Improper decisions on the transmission line length, voltage, and technical implementation negatively affect the coordinated operation of relay protection and automatic

Table 2. Transfer capability of transmission lines.

Rated voltage, kV	Highest transmitted power per circuit, MW	Largest distance of transmission, km	Actual transmitted power, MW
35	5-15	30-60	3
110	25-50	50-150	30
220	100-200	150-250	120

Table 3. Mix and characteristics of the existing substations.

Voltage, kV	CEPS	WEPS	AUEPS	EEPS	SEPS	Total
220	6					6
110	56	9	4	13		82
35	207	18	12	17	15	269
15	94	39	21	34	11	199
6-10	3811	431	132	206	117	4697

devices, lead to the adverse changes in the functional properties and operation principles of earthing protection in the lines with insulated neutral. Moreover, the increasing length of the transmission lines makes it more difficult to detect faults; the error of their detection increases, and it takes more time to restore the lines.

The total length of transmission lines is given in Table 1. The number of substations in each individual system is given in Table 3. Quantitative characteristics of the country's electric power systems are assumed based on the data published by the Energy Control Committee of Mongolia in 2014 [4].

Eighty eight 110 kV (and above) substations are currently in operation in five EPSs of Mongolia, of which 18 substations are major substations, and the remaining 70 are intermediate and terminal substations. Long distances between substations have a negative impact on power flows. Thus, it becomes necessary to construct additional major substations and power plants. Raising the transmission line voltage can be an alternative to construction of substations and power plants and a way to tackle the pressing problems.

Due to a rapid urbanization process, 70% of population is concentrated in the cities of Ulaanbaatar, Erdenet, and Darkhan. These are central provinces where power consumption grows and power flows increase causing overload of transmission lines and substations, which reduces the reliability of CEPS as a whole [4]. Lack of sufficient generating and backup capacities results in electric power shortage, which diminishes energy security of Mongolia.

Table 4. Forecast of per capita power consumption.

Years	Forecast of per capita power consumption, kWh		
	Low	Medium	High
2012	1.739	1.739	1.739
2015	2.269	2.269	2.269
2020	3.914	4.232	5.015
2025	4.994	5.408	6.425
2030	6.172	6.692	7.959

2. Power consumption forecast

As Mongolia's industry develops, the power consumption grows annually by approximately 10%. According to estimations, electricity demand in 2030 will be as high as 3.5 GW, whereas total present-day generating capacity is 1GW. The expected demand for electricity and power in terms of reliability and security cannot be met by imported electricity alone, therefore, construction of new power plants, substations and transmission lines is required.

The development of electric power systems was stipulated in the "State Energy Policy for 2015-2030" approved by the Decree of Great Khural No. 63 of June 19, 2015 [6]. Objective of the Policy is to establish an Integrated Power System of Mongolia. Paragraph 1.2 of the Decree indicates that "Governmental energy policy pursues the objective to provide continuous and reliable power supply in the country and to convert Mongolia into an electricity-exporting country". Implementation of this policy will require construction of new power plants, electric networks, and substations.

All the five above-mentioned operating electric power systems should be interconnected into an Integrated power system of Mongolia. Reliable operation of each individual power system should be provided to ensure reliability of the entire Integrated power system. A feasibility study of optimal sites and required capacities of new power plants and substations should be conducted, given the increase in electricity demand. Based on the note to Table 1, we can suppose that some of the five existing power systems are interconnected but more careful consideration makes it obvious that for efficient operation of this interconnection certain technical requirements should be met to provide their joint operation.

Three most probable scenarios of per capita power consumption growth are given in Table 4. The annual growth, depending on scenario, is on the average 15-20% and during the period under review, it will increase by 3.5-4.6 times.

The estimated growth of power consumption requires

Table 5. Projected power facilities, expansion of existing facilities.

No.	Power plants	Location	Installed capacity, MW	Date of commissioning
1	CHP-3	Ulaanbaatar	250	2019-2020
2	Darkhan CHP	City of Darkhan	35	2019
3	Erdenet CHP	City of Erdenet	50	2019-2020
4	CHP-5	Ulaanbaatar	450	2019-2021
5	Tavan-Tolgoi CHP	South-Gobi aimag	450	2019-2021
6	Baganuur CHP	City of Baganuur	700	2019-2021
7	Telmen CPP	Zavkhan aimag	100	2019-2021
8	Choibalsan CHP	City of Choibalsan	100	2019-2021
9	Nuurst-Khotgor CPP	City of Ulan-Gom	100-600	2019-2021
10	Eg HPP	Selenge aimag	325	2019-2022
11	Chandgana CPP	Khentii aimag	600	2019-2022

Table 6. Projected transmission lines and substations.

No.	Names of substations (SS) and transmission lines (TL)	Voltage, kV	TL length, km	Note
1	CHP-5-Songino 2-circuit TL and SS	220		FS and FEED
2	Baganuur-Choir 2-circuit TL and SS	220	178	FS and FEED
3	Choir-Saynshand-Zamyn-Uud 2-circuit TL and SS	220	406	FS and FEED
4	Baganuur-Underkhan-Choibalsan 2-circuit TL and SS	220	519	FS
5	Oyu-Tolgoi-Tsagaan-Suvarga 3-circuit TL and SS	220	160	FEED
6	Nariinsukhait TL and SS	220	270	
7	Ulaanbaatar-Mandalgovi TL and SS	330	260	FS and FEED
8	Baganuur-Ulaanbaatar 2-circuit TL and SS	500 minimum	157	
9	“Baganuur-Choir” TL and SS	500 minimum	190	

Note: FS - Feasibility Study; FEED - Front End Engineering and Design; SS - substation

construction of new power plants, given their technical characteristics and geographical location of consumers.

3. Prospects for Mongolia’s Integrated Power System Development

To meet the rising power demand of the economy and social sphere and to provide the required technical and technological reliability of power supply it is necessary to concurrently put into operation new generating capacities, transmission lines and substations. A presumable mix of new power plants, transmission lines and substations for the years to come is given in Tables 5 and 6. All these measures were developed in different years, for different conditions and very often were not interrelated, therefore, additional comprehensive studies are necessary to justify the investment and motivate investors.

An analysis of operating electric networks within EPSs shows that transfer capability of some existing transmission lines does not match the output capacities of power plants. This fact indicates the necessity of raising the voltage levels and increasing the number of circuits in transmission lines. According to the calculations, new 330kV and 500kV overhead power lines need to be constructed. These voltage levels are new for Mongolia. However, they have been scientifically grounded and tested in other countries, and have all the prerequisites for being implemented.

4. Structural Models of Prospective Integrated Power System in Mongolia

In 2013, the Asian Bank for Reconstruction and Development proposed a Master Plan for development of

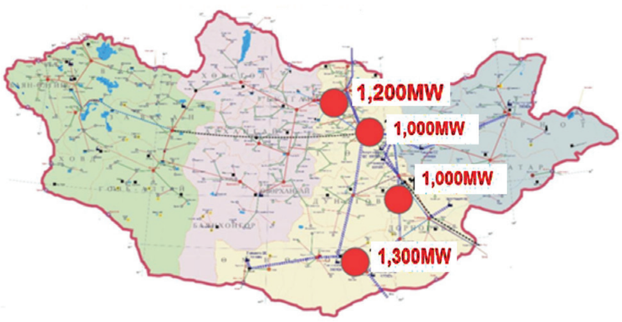

Fig. 2. Prospective industrial zones of Mongolia.

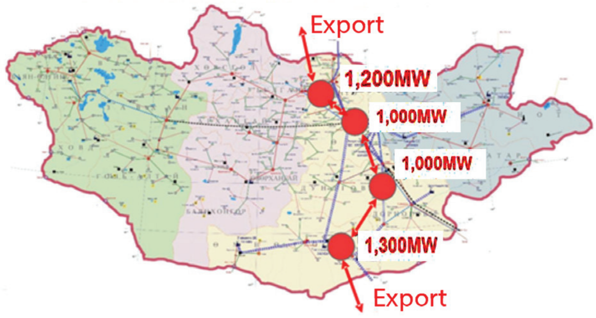

Fig. 3. Export-oriented model (vertical).

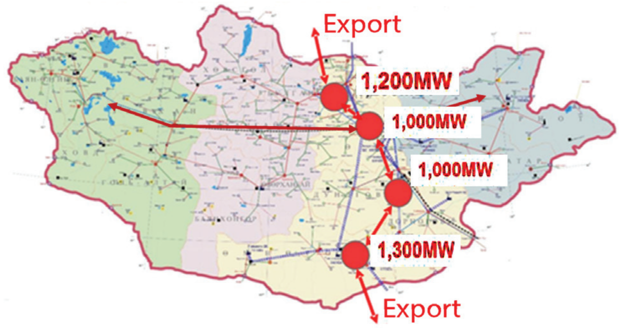

Fig. 4. Time-zone model (horizontal).

Mongolia's electric power industry. In the long term, this Plan suggests creation of four industrial zones with power consumption of about 1000 MW each (Fig. 2). One zone is proposed to be located in the neighborhood of Ulaanbaatar; the so-called "northern industrial zone" is proposed to be located in Darkhan-Erdenet; the "central industrial zone" is proposed to be located in Sainshand or Choir, and the "southern industrial zone" - in Tavan Tolgoi.

To meet energy demand of the future industrial zones it is advisable to have several conceptual models of EPS development and to select the most optimal one. There can be three options of initial conceptual models.

Export Model (power export-oriented) suggests construction of an interconnected power system connecting four developing industrial zones through high-voltage (400 kW minimum) transmission lines and cross-border lines to Russia and China. It has exporting and importing transmission lines spatially oriented along the vertical axis of Mongolian territory (Fig. 3).

Time-zone model suggests construction of EPSs around the HV (400 kV minimum) transmission line extending along the horizontal axis of Mongolian territory (Fig. 4). This model takes into account time differences between western and eastern provinces of the country. This and the previous model ensure the participation of Mongolia in the energy cooperation with NEA countries, primarily with China and Russia.

Radial model, the so-called "pitchfork", represents a mixed system integrating the above-considered models (Fig. 5). This model is the most advantageous but requires the highest investment.

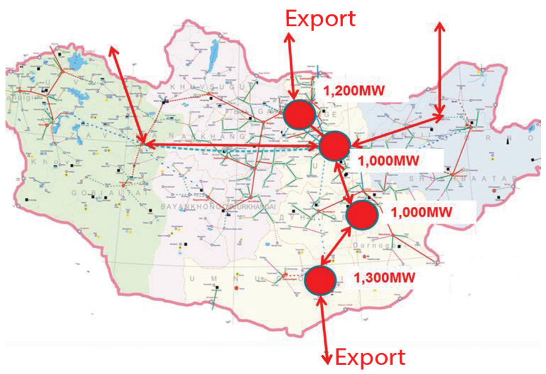

Fig. 5. Radial model, a "pitchfork".

Apart from the largely available technical capabilities of the EPSs development and establishment of Mongolia's integrated power system, it is necessary to prepare the scientific and methodological grounds to make it part of the Northeast Asian energy infrastructure.

Relevant scientific and methodological procedures should be developed to determine optimal location of generating capacities, select their type and size, and determine location of transmission lines and substations.

III. Mongolia's Potential for Interstate Energy Cooperation

1. Characteristic of the Potential

Against the background of different levels of development of the world countries, availability of renewable (wind, solar, and hydro) and conventional energy sources, power import and export have become an indispensable part of the energy policy in many countries. In this context, the energy market expands, as a rule, to the neighboring countries. Energy market expansion is primarily based on the construction and development of International Power Pools (IPPs) [7].

Creation of an IPP as an integrated engineering system will benefit electricity trade, provide sustainable power supply to the regions, enhance the efficiency of installed capacities, boost technological advancement of the energy infrastructure, contribute to the development of environmentally friendly power generation, help to solve environmental problems, and encourage joint construction of power generating facilities in the countries within the power pool.

An analysis of international experience shows that international power pools are, as a rule, established on a bounded territory covering two or more states, or in the off-shore zones [8]. Studies on creation and expansion of interstate power pools focus on large capacities based on renewable energy sources (solar, wind, hydro). This is done, on the one hand, to compensate for the shortage of generating capacities of conventional power sources and, on the other hand, to ensure the sustainable environment. For example, China deploys solar and wind facilities, Mongolia studies possibilities for constructing similar facilities in the Gobi Desert [8,9] with a view to their future integration into the Northeast Asian Super Grid (Fig. 6) [10].

2. Prerequisites for Mongolia’s Participation in the Energy Cooperation in Northeast Asia

For participation in the Northeast Asian Super Grid, Mongolia can offer construction of large-scale power plants by making use of rich renewable energy potential in the Gobi Desert, and construction of high-voltage AC and DC transmission lines to ensure sustainable development of the electric power industry in the region. It is worth noting that Russia, China, Japan and South Korea are interested in this project, and comprehensive studies on the prospects for the development of the region are currently under way [10, 11]. Some of these countries border one another; they have a multi-year experience of mutually beneficial trade and have sufficient financial potential for investing into construction of large-scale power plants of different types. Russia together with China and Japan, and China together with Democratic People's Republic of Korea have launched some joint large-scale energy projects [12, 15] that can form a basis for the future Northeast Asian Super Grid. Mongolia’s potential for participation in the Asian Super Grid Project [16, 17] requires a scientifically grounded assessment of capacities and sites for new power plants considering spatial distribution of energy resources throughout the country, and an analysis of energy markets.

In the recent years investors very often refused to finance construction of coal-fired power plants as they pollute the environment. After large accidents at nuclear power plants (NPPs) followed by negative consequences, public in many countries of the world is against NPP construction and operation. These circumstances require revision of the energy policy in many countries and its switch to renewable energy sources. Similar tendencies are observed in Mongolia as well, as along with considerable amount of conventional fuels the country has rich potential of renewable energy sources. The forecast coal reserves in the country are estimated at 175 billion t, oil reserves make up 205 million t, and those of uranium - 68 million t [18, 19]. According to the estimates of the US National Laboratory on Renewables, Mongolia has high wind resource potential, its forecast capacity equals 1100 GW (only as little as 10% of Mongolian territory has specific power of above 600 W/h) [9]. According to the Report of the Energy Charter Treaty issued in 2014, the forecast solar-based capacity can amount to 2500 GW [9, 16, 17]. This potential is graphically presented in Fig. 7.

The country has considerable energy resources, both

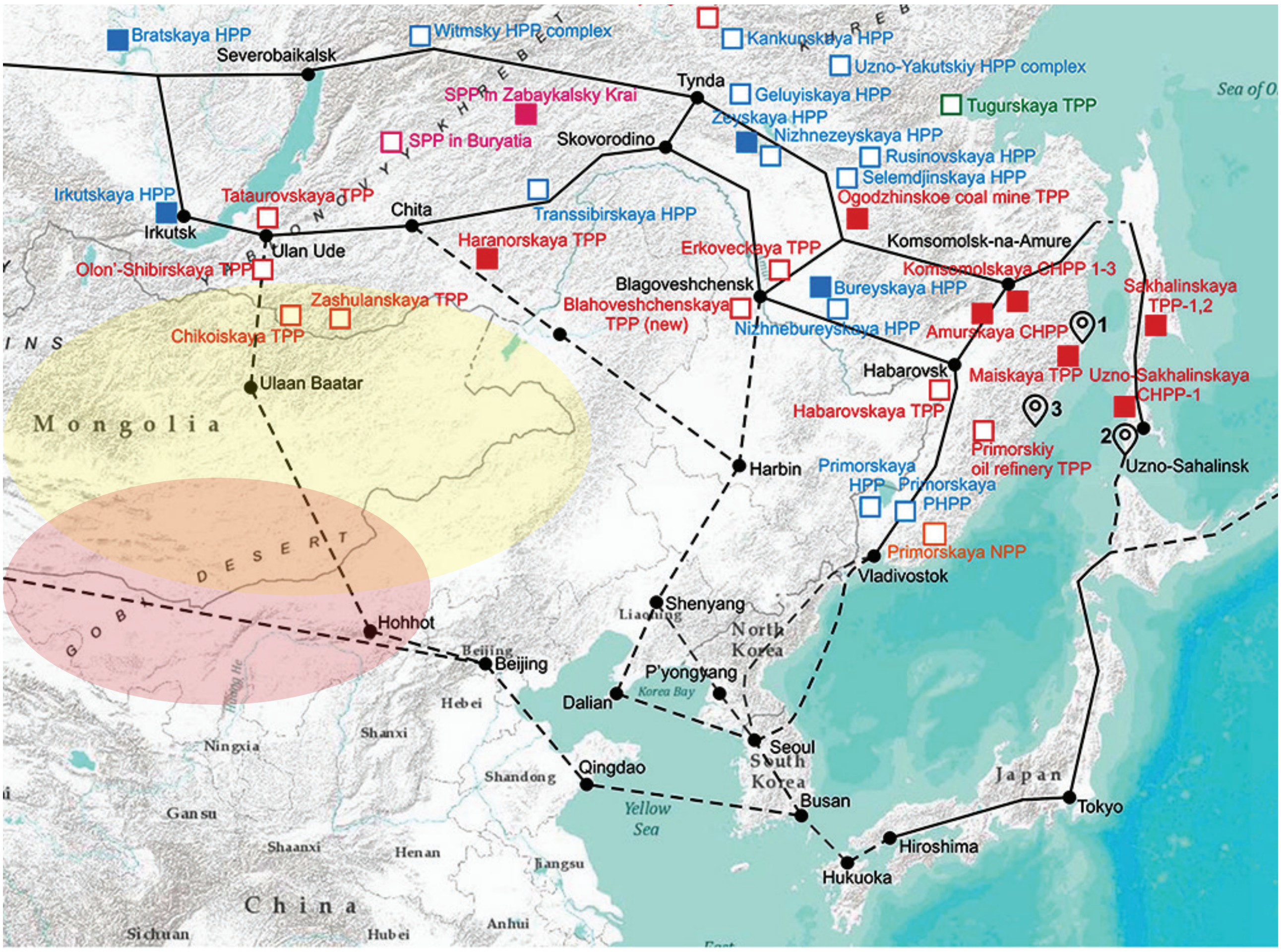

Fig. 6. General scheme of the projected Northeast Asian Super Grid. Map source: Skolkovo Institute of Science and Technology.

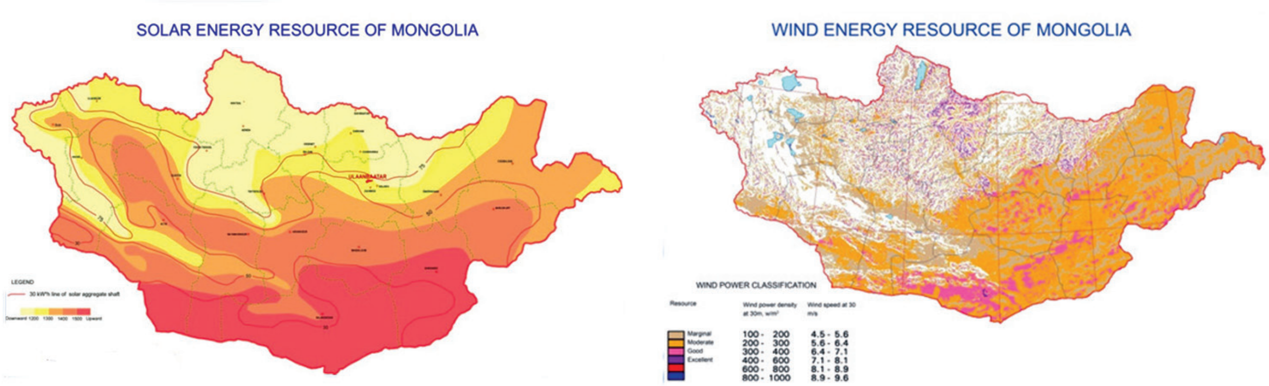

Fig. 7. Average annual solar and wind potential in the projected solar-wind Gobitec system. Source: http://eeam.energy.mn/

Table 7. General characteristics of electric power industry of Mongolia and Northeast Asia countries.

Indicator	PRC (2013)	Russia		Republic of Korea (2013)	Japan (2012)	Mongolia (2012)	DPRK (2012)
		Siberia* (2013)	Russian Far East* (2013)				
Area, m sq. km	9598	5115	6169	99	373	1565	121
Population, m people	1357.4	19.3	6.3	50.0	127.6	2.8	24.8
Electricity consumption, TWh	5322.3	205.3	31.61	474.9	991.6	5.2	1.2
Per capita consumption, kWh	3921	10637	5017	9498	7771	1857	734
Power generation, TWh	5347.4	197.4	35.2	517.1	1094.0	5.2	21.5
Installed capacity of power plants, GW	1247.4	49.3	9.1	91.0	287.3	1.02	7.22
Including thermal power plants:	796.4	25.0	5.7	56.3	188.9	0.97	2.96
On coal	758.1	24.2	5.2	24.5	50.9	0.88	2.76
On gas and fuel oil	38.3	0.8	0.5	31.8	138.0	0.09	0.2
HPP	280.0	24.3	3.3	6.5	48.9	0.03	4.26
NPP	14.6	-	-	20.7	46.1	-	-
Renewable energy sources	86.8	-	-	3.5	3.4	0.01	-

*Power production and consumption, and installed capacities are given for Interconnected Power Systems of Siberia and the Russian Far East, respectively

conventional and renewable, and at the same time it suffers from electric power shortage that keeps growing against the background of continuous power consumption increase (from 7% to 10% annually) [20]. Unfortunately, appropriate measures to bridge this gap have not been taken. For instance, power import from neighboring countries in 2017 reached 1420 million kWh, its major share being the power flow through the Mongolia-Russia cross-border transmission line. The existing energy cooperation with the neighboring countries is as a rule limited to power import. It is obvious that this principle of cooperation is inefficient in the context of cooperation between electric power systems of neighboring countries, to say nothing about cooperation in creation and development of the Northeast Asian Super Grid.

3. Specific aspects of Northeast Asian Super Grid and Prospects for Mongolia

Currently, there are several 110-220 kV cross-border transmission lines operating in the Northeast Asia with a transfer capability of 100-150 MW. Existing transmission lines between Russia and Mongolia, Russia and China, China and Democratic People's Republic of Korea (DPRK), and China and Mongolia can also be referred to such cross-border transmission lines [13 - 15]. An export

500 kV cross-border transmission line connecting Amur (RF) and Heihe (China) substations was put into operation in 2011; its transfer capability is 750 MW and it has a DC link [21, 22].

Studies on creation of interstate electric power systems are carried out by research institutions from Russia, the Republic of Korea, the People's Republic of China (PRC), Japan, Mongolia and from some other countries, as well as by Asian-Pacific Energy Research Center (APERC) in Tokyo (Japan). General characteristics of electric power industry of potential participants in the Asian Super Grid Project are given in Table 7.

Mongolia can become an important player in the energy space of Northeast Asia and increase its role in shaping and developing Northeast Asian Super Gird, provided the country has a comprehensive target-oriented energy policy and a scientifically grounded energy development concept. The implementation of this concept will open up the following opportunities for Mongolia:

1. Power from Mongolia will be supplied to the Northeast Asia regions that have a high demand for electricity due scarce energy resources;
2. The intermittency of renewable power generation will reduce and the efficiency of renewable energy sources will increase.
3. The nature of weakly developing Mongolia's electricity export and import will change qualitatively, as it will become an exporting-importing country rather than an importing country.

Technical and technological issues related to interconnection of regions by cross-border EHV (500 kV, 750 kV) and UHV (1150 kV) AC overhead transmission and cable lines, and DC ±400 kV, ±600 kV, ±800 kV transmission lines come to the forefront.

4. Formation of an Interstate Electricity Market

The above facts and level of the country development necessitate working out the national concept of Mongolia's participation in the large-scale project of the Northeast Asian Super Grid. For maintaining and expanding its electricity market and for entering the interstate electricity market in the near future, Mongolia needs to accomplish the following tasks:

1. Create incentives for foreign and domestic investors.
2. Develop and implement the projects on construction of new generating sources and transmission lines in cooperation with interested parties on the basis of Mongolia's energy development strategy.
3. Deploy solar and wind power plants with a capacity above 4000 MW, and new cross-border transmission lines in the sparsely populated areas of the desert.
4. Cooperate with the countries of Northeast Asia in the field of electric power industry. Enhance the efficiency of such cooperation by considering seasonal variations in loads in each country, time differences, and climatic features.

The creation of the Super Grid infrastructure primarily requires commitment and support of the neighboring countries and feasibility studies on power export-import.

According to [9, 11], the cross-border 220 kV transmission lines are currently operating in Mongolia for connection with the EPSs of Russia and China, which allows gaining the required experience of operating such lines. In the event that the existing interstate relations are developed and huge renewable energy resources of the Gobi Desert and coal reserves are involved, Mongolia can play a significant role in the formation and further development of interstate interconnections within the Northeast Asian Super Grid.

Table 8. World power production and consumption.

	Country	Generation, GWh	Population, thousand people	Per capita consumption kWh/capita
1	China	5649500	1376622	4103.89
2	USA	4297300	323394	13288.13
3	India	1208400	1288306	937.98
4	Russia	1064100	146545	7261.25
5	Japan	1061200	126980	8357.22
6	Germany	614000	81174	7564.00
7	Canada	615400	34850	17658.54
8	Brazil	582600	205738	2831.76
9	France	555700	64513	8613.77
10	Republic of Korea	517800	51431	10067.86
119	Mongolia	5541.7	3000	1847.23
215	NIUE	3	14	214.29
	World, total	23536500	7300000	3224.18

Japan comes second in the region after China in electric power generation and consumption and ranks first in Northeast Asia in nuclear power development. Due to limited domestic energy resources and import-oriented power supply, the electric power industry of the country has two objectives: to reduce the dependence on energy import and mitigate negative impact of thermal power plants on the environment. In this context, the interstate electric ties between neighboring countries and import of environmentally clean electric power from Russia and China could considerably improve the environmental situation in the country. Different projects of cross-border transmission lines between Japan and neighboring countries are proposed. They need feasibility studies for construction of overhead transmission and submarine cable lines.

The Republic of Korea has a highly developed electric power industry. This country is a leader among other Northeast Asia countries in per capita electric power production (Table 8). Structure of generating capacities in South Korea is similar to that in Japan. The country is highly interested in import of environmentally clean electricity from Russia and China.

Table 8 presents indicators of power production and consumption in the countries of Northeast Asia and the world versus similar figures for Mongolia. Of interest are the figures on specific per capita power consumption that are widely dispersed as regards the average level. Per capita power consumption is the highest in Canada, the USA, and South Korea. This indicator for Mongolia is below the mid-level. At the same time, it has a potential for enhancing this indicator owing to rich resources of conventional and renewable energy. Moreover, the country can enter the electricity market as an exporter.

5. Prospects for the Northeast Asian Super Grid

The studies [7, 10 – 15 et al.] show that the prospects for cooperation in the electric power sector in Northeast Asia largely depend on the projects of interstate electric ties and large-scale projects for the construction of the Northeast Asian Super Grid. There can be various forms of the cooperation: cross-border trade; electricity export; interconnection of national and local EPSs of neighboring countries for joint (or parallel) operation. There can also be different structures of generating capacities (ratio between power sources of different types), and engineering and technological solutions for the cross-border transmission lines (Table 9)

Power transmission from the wind-solar system in the Gobi Desert is another interesting option of interstate electrical ties in Northeast Asia (Table 9).

Russia offers options of constructing large-scale hydro power plants intended for long-distance electric power transmission. One of them is a 9050 MW HPP proposed to be constructed on the Lena River. The average multi-year

Table 9. Prospective interstate electrical ties between Northeast Asian countries.

Interstate electrical ties	Length, km	Voltage, kV	Transmission capacity, GW	Transmitted power, TWh/year	Tentative cost, bn USD
Russia-China					
Bratsk - Ulaanbaatar - Beijing	2250	±600	5-6	18	1.8
Bureya HPP - Harbin	700	±400	1.0	3	2.2
Large-scale electric power export projects	3400*	±600	10*	60*	18*
Erkovetskaya TPP – Shenyang	1300	±600	3.6	20	8.8
DC transmission line Ust-Ilimsk - Khabarovsk	5000	±750	10.0	40	16.5
Russia - Korean peninsula					
Vladivostok - Chongjin	370	±500	0.5	3	0.13
Vladivostok - Pyongyang - Seoul	1150	±500	4.0	7	4.8
South-Yakutia HPP - Shenyang - Seoul	2400	±750	5.0	20	10.5
Russia – Japan					
Sakhalin - Hokkaido - Honshu	1850/1400**	±600	4.3	24	9.6
Sakhalin - Hokkaido	500/50**	±500/±400	4.0	24	6.7
Asian Super Grid					
Gobitec - Mongolia, Russia, China, Korea, Japan	7300	±800	100	200	56.7

*Generalized indicators of the project
** Total length is in the numerator, submarine cable length is in the denominator

power generation is 7.8 TWh, cost of HPP construction is about USD 3.6 billion. There are plans to construct Mokskaya HPP on the Vitim River in Buryat Republic; its power will be transmitted to the power-deficient areas in the Russian Far East, Mongolia and China. The Bureya and Zeya HPPs operating within the Amur EPS can be referred to the export-oriented plants. Implementation of those proposals will ensure power supply to consumers in Siberia and the Russian Far East. Moreover, the above plants will certainly enable the maneuverable operation of cross-border transmission lines, and enhance the efficiency of the cross-border electric power systems.

Connection of the Mongolian EPS to the future Bratsk-Ulaanbaatar-Beijing project for export of surplus power from the Siberian interconnection will increase the efficiency of this project, and create good conditions for power export to the neighboring countries. A contract on mutually beneficial energy cooperation between RAO EES of Russia and State-Owned Network Corporation of China was concluded in 2005. According to this Contract, Russia was to export 60 trillion kWh annually to China [20]. Phase I of this project was completed by connecting the Russian Far East interconnection to Heihe network (Northeast province of China), which at present enables an annual supply of up to 3.5 billion kWh from the Russian Far East interconnection to the Northeast provinces of China.

Connection of the Russian Far East Interconnected System to the EPS of the Republic of Korea through the cross-border transmission line Vladivostok - Pyongyang-Seoul, 1150 km long, is expected to be the most cost-effective project among the projects named. The expected economic effect due to the interconnection of capacities and use of time zones will be USD 6-7 billion [7].

The Sakhalin - Hokkaido - Honshu project, the so-called "power bridge" whose idea emerged in the 1990s, is another interesting project of cross-border power transmission. Export-oriented thermal power plants (4 GW Solntsevskaya coal-fired power plant at Phase I and Vakhrushevskaya steam-gas power plant at Phase II) and a ±400 kV DC transmission line Sakhalin - Sapporo – Tokyo, covering the distance of 1600 km with two submarine cable lines across La Peruza Strait (50 km) and Tsugaru Strait (40 km), are planned to be constructed within this Project.

For participation in the creation of the Northeast Asian Super Grid, Mongolia should conduct a feasibility study on the project for construction of a wind-solar system in the Gobi Desert (Gobitec) with a view to exporting cheap electric power to China, the Republic of Korea, Japan, Russia, and take part in its implementation. This generates the need to construct DC (±600 kV) and AC (500 kV) transmission lines.

The use of the 100 GW wind-solar system in the Gobi Desert (Gobitec) will give an impetus to the formation of the Northeast Asian Super Grid, particularly, to some of its components: the Mongolian Ring: Gobitec-Mugden-Harbin-Kharanuur; the Sea-of-Japan Ring: Seoul-Pyongyang-Hokkaido-Honshu; the Big Ring: Bratsk-Urgalsk-Sakhalin-Tokyo-Shanghai-Beijing-Ulaanbaatar-Irkutsk. It is obvious that it will take a very long time to implement this super-project, but its effect will be enormous. For example, fuel saving alone will be USD 10.0 trillion a year.

IV. Conclusion

There are four stages in the creation and development of Mongolia's electric power industry, each with its specific features conditioned by the level of development and needs of the economy. Five electric power systems are currently in operation in Mongolia. They are interconnected but have no technical and technological prerequisites for operation within the Integrated Power System of Mongolia. With intensive development of industry, including mining industry and production of mineral resources, the power demand in the country grows dramatically. For meeting the growing power demand, Mongolia imports electric power from Russia and China. The imported electric power currently accounts for about 20% of its annual consumption.

An analysis of the current state of Mongolia's electric power industry shows that it faces some problems to be solved. These are incompletely used transfer capability of transmission lines due to lack of appropriate network equipment; comparatively high (up to 30%) power transmission losses; rather low efficiency of power plants (25-30%), etc. In order to increase the efficiency of EPSs, enhance their performances, and identify prospective innovative development of the electric power industry, it is necessary to undertake great research effort to study the unit commitment, structure of the systems, potentials for their technological advancement, feasibility of their interconnection into the Integrated power system, and substantiate the principles of its integration into the Northeast Asia energy space. This paper proposes conceptual models of restructuring Mongolia's electric power industry to meet the needs of its rapidly developing economy and allow the country to enter the electricity market of Northeast Asia.

Creation of an interstate power pool starts with construction of cross-border electrical lines ensuring joint operation of national or local EPSs. Normally, such lines are reverse, which makes it possible to gain many benefits constituting the synergy effect. For active participation of Mongolia in the creation and development of the Northeast Asian Super Grid, the future Shivee-Ovoo power plant should be considered as a candidate for integration into the interstate grid covering the Russian Far East, North and Northeast of China, Mongolia, South Korea and North Korea.

Mongolia is interested in active participation in the multilateral studies on the prospects for the development of the Northeast Asian Super Grid.

References

1. B. Bat-Erdene, S. Batmunkh, ., N. I. Voropai, V.A. Stennikov, "Some issues of Mongolia's energy industry development strategy." *Energy Policy*. 2016. Issue 6. pp. 95-105 (in Russian).
2. Kh. Enhzhargal, S. Batmunkh, V.A. Stennikov, "Prospective directions of the development of Mongolia's electric power system." *Energy Policy*. 2012. Issue 4. pp. 70-81 (in Russian).
3. G.N. Aleksandrov, "Operating conditions of overhead transmission lines: Textbook." Second edition. Training Energy Center. Saint Petersburg. 2006. 40 p. (in Russian).
4. 2014 Statistical Data for Energy Sector. Energy Control Committee of Mongolia. Mongolian Ministry of Energy. Ulaanbaatar. 2015. 69 p.
5. Kh. Enkhzhargal, S. Batmunkh, V.A. Stennikov, "Creation of the electric power systems of Mongolia on the basis of Shivee-Ovoo TPP." Bulletin of Irkutsk State Technical University. 2012. No. 5. pp. 173-181. (in Russian)
6. State Energy Policy for 2015-2030. Decree of Great Khural No. 63 of June 19, 2015. - Ulaanbaatar. 2015. - P. 4.
7. Yu. Kucherov, O. Kucherova, L. Kapoyi, Yu. Rudenko, "Reliability and efficiency of large-scale trans-national power system operation." Novosibirsk. Nauka. 1996. 386 p. (in Russian)
8. S. Batmunkh, V.A. Stennikov, B. Bat-Erdene, A. Erdenebaatar, "Mongolia's potential in international cooperation in the Asian energy space," E3S Web of Conferences 27, 01006 (2018), AEC 2017, https://doi.org/10/1051/e3sconf/20182701006.
9. Source: National Renewable Energy Center of Mongolia. www.nrec.mn
10. H. Bahar, J. Sauvage, "Cross-border trade in electricity and the development of renewables-based electric power: Lesson from Europe" // OECD Trade and Environment Working Papers. February 2013. OECD Publishing.
11. "Eastern vector in the energy strategy of Russia. Present-day state and prospects." Ed. by N.I.Voropai. Novosibirsk. Geo. 2011. 256 p. (in Russian).
12. S. Mano, B. Ovgov, Z. Samadov, "Gobitec and Asian Super Grid for renewable energies in Northeast Asia." 2014. 194 p.
13. http://www.encharter.org/fileadmin/user_upload/Publications/Gobitec and the Asian Super Grid 2014 ENG.pdf
14. Wind Energy Resource Atlas of Mongolia, National Renewable Energy Laboratory. NREL/TP-500-28972. USA. 2001.
15. J.Y. Yoon, D.W. Park, H.Y. Kim, "The pre-feasibility results of NEAREST between the RK, and the DPRK, and RF" //Proceeding of 6th International Conference — Asian Energy Cooperation: Forecast and Realities. Irkutsk. Russia. September 7-11. 2008. pp. 77 – 86.
16. W. Chandler, Ch. Shiping, H. Twin, L. Ruosida, W. Yanjia, "China's future generation. Assessing the maximum potential for renewable power sources in China to 2050." WWF Report, February 2014, 38 p.
17. Reference Book on Climate of Mongolian People's Republic. Vol. 1. Solar Energy Inventory of Mongolian People's Republic, the Institute of Meteorology and Hydrology. – Ulaanbaatar, Issued by SMS. 1984. 218 p.
18. Climate of Mongolia. Ulaanbaatar. Gosizdat. 1985. 458 p.
19. Brief overview of coal deposits, oil and shale oil fields in Mongolia. Oil and Mineral Resources Management Board. Ulaanbaatar, Geological Information Center. 2007. 25 p.
20. Uranium resources, production of Mongolia (RED BOOK), Uranium 2009: Resources, Production and Demand. Joint report by the OECD Nuclear Energy and International Atomic Energy Agency, 2010, S. Enkhbat et al. OECD. IAEA. p. 276-286.
21. Energy Sector Statistics, 2016. Annual Report of Energy Coordination Committee. Ulaanbaatar. 2017. 54 p.
22. S.V. Podkovalnikov, V.A. Saveliev, L. Yu. Chudinova, Prospects for electric power cooperation between Russia and Northeast Asia countries. External Economic Relations, 2015.No. 4. pp. 18-130.
23. Interconnection in APEC Region. Current Status & Future Potential. Tokyo, Asia Pacific Energy Research Center. 2000. 226 p

Reduced-Order Modeling of Pulverized Coal Staged Gasification: Influence of Primary and Secondary Fuel Proportion

Igor G. Donskoy[1,*], Denis A. Svishchev[1], Alexander F. Ryzhkov[2]

[1] Melentiev Energy Systems Institute of Siberian Branch of Russian Academy of Sciences, Irkutsk, Russian Federation
[2] Ural Federal University, Ekaterinburg , Russian Federation

***Abstract* — The paper is concerned with the numerical simulation of the coal gasification process in an entrained flow of high-temperature air-steam mixture. Due to the high initial temperature and the process staging, it is possible to obtain an efficient gasification process. The study aims to examine the stationary conditions of staged gasification process by using a mathematical model based on one-dimensional heat and mass transfer equations with combined submodels to describe physicochemical transformations. The simulation makes it possible to determine the boundaries of the transition from the "single-stage" to the "two-stage" gasification conditions and identify the most promising ones.**

***Index Terms* — coal, staged gasification, mathematical modeling, reduced order modeling.**

I. Introduction

Gasification of solid fuels for energy gas and chemicals production is one of the promising ways to improve the technological and environmental efficiency of fuel consumption [1]. Nowadays, gasification plants are successfully operating in a number of countries around the world, and new projects are being developed for their construction [2]. Among gasifiers for large power plants (more than 100 MWe), entrained flow reactors are widely used [3]. In the entrained flow conditions, reacting mixture is a suspension of fine solid particles or droplets in gaseous oxidizer.

Gasifier usually works as part of a complex power or/and process plant [4]. Therefore, its operating conditions and parameters are determined by the operation of the plant and the power system as a whole. In this regard, the important task is to develop numerical models enabling the efficiency evaluation for different gasifier operating conditions for the comprehensive optimization of such plants.

One of the trends in gasification technologies is to increase temperature of reaction core, which improves the equilibrium yield of the target combustible components, increasing the specific rate of chemical reactions, and ensures liquid slagging. Therefore, oxygen-enriched gasification agent is most widely used in the industrial processes. Oxygen production requires additional costs, therefore, in some processes, high temperature air is used [5, 6], or a staged supply of fuel and a recycling of unreacted fuel are used [7]. According to thermodynamic estimates, the efficiency of power plant with an air-blown gasifier can be close to the efficiency of a plant with oxygen-blown gasifier [8, 9].

In [9], the authors propose a new integrated coal gasification combined cycle power plant, in which both high-temperature heating of gasification agent and recirculation of unreacted fuel were used. The present paper is devoted to the study of stationary conditions of the gasifier in a similar scheme with different ratios between primary and secondary fuel.

II. Staged processes of pulverized coal gasification: application and modeling

The use of staged gasifiers is usually associated with the gas quenching by the utilization of process heat in endothermic chemical reactions to produce combustible products. Reduction in the temperature of the product gas allows, in general, decreasing thermodynamic losses of the process [10]. In addition, the organization of the staged gasification process simplifies the cooling of the product gas [11].

E-Gas gasifiers fed by water-fuel suspensions or emulsions are widely used in the chemical industry to produce syngas and hydrogen. In the first stage of the

* Corresponding author.
E-mail: donskoy.chem@mail.ru

http://dx.doi.org/10.25729/esr.2018.04.0003
Available online February 28, 2019.

process, the fuel droplets are burned in oxygen to produce a hot gas, and in the second stage secondary fuel is injected into this gas. Fuel evaporates and gasifies due to the heat obtained in the first stage. The Wabash River thermal power plant (260 MWe) uses the E-Gas gasifier to produce fuel gas [3, 12].

The Mitsubishi Heavy Industries (MHI, later MHPS) gasifier is implemented at the Nakoso station (250 MWe) [3, 7, 13]. The fuel here is coal dust, and the primary gasification agent is air. The first stage, as in the E-Gas process, is burning of primary fuel to produce hot gas. The second stage is also the gasification of the secondary fuel in the hot combustion products. However, due to the high nitrogen content, a significant amount of coke residue is produced. Thus, the coke-ash residue is directed back to the first stage, where it is burned along with raw fuel.

The EAGLE (Energy Application for Gas, Liquid and Electricity) gasifier was developed by J-Power. The fuel conversion process in this gasifier is based on the organization of swirled flows within the reactor, when the combustion and reduction stages occur in counter-current streams within a single reactor unit. This process is presented by the pilot plant Wakamatsu (8 MW) [3].

China is actively working on the development of new gasifiers, including the staged ones: TPRI, HNCERI, etc. [14–17].

There are many papers devoted to the development of mathematical models for the staged processes of pulverized coal gasification. In some of them, the authors make attempts at CFD-modeling, which is explained by the importance of proper flow organization in the reaction zone. Thermochemical equilibrium models are often used to evaluate the operation of a gasifier as part of complex technological schemes [8, 18, 19]. The CFD-models of the E-Gas gasifier were studied and used in [20-25]; MHI gasifier models are presented in [25-32]; EAGLE gasifier models are presented in [33, 34]. The CFD-models of staged processes in laboratory and pilot units were proposed in [35–38]. The main problems of using these modelsare computational efforts and appropriate choice of empirical coefficients corresponding to submodels of turbulence and radiation transfer in dispersed flows.

The authors of [17, 39, 40] propose simplified models of staged processes, which are sets of connected one-dimensional and zero-dimensional reactors. Such models (Reduced Order Models, or ROMs) allow variants calculations and the process behavior evaluation in a wide range of conditions for a reasonable time. The present paper also uses a simplified mathematical model of a staged gasifier, which allows a sufficiently detailed study of the influence of individual factors on the gasification process characteristics with smaller computational requirements.

III. Initial data and model description

Gasification process in a staged reactor can be represented as follows (see Fig. 1 and [7, 9]):

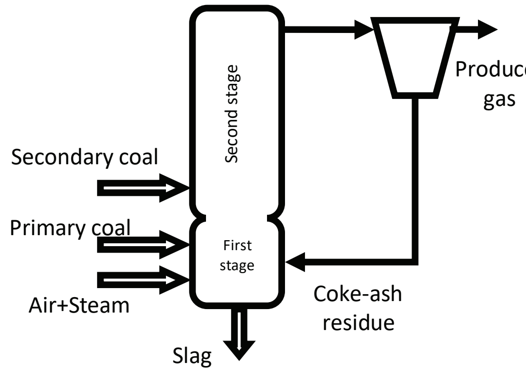

Fig. 1. Scheme of entrained-flow two-stage gasifier.

high-temperature air and steam with primary fuel are supplied to the first stage along with a coke-ash residue, which is formed in the process. Nitrogen is used as a transport media for fuel supply. Combustion occurs in the first stage, and temperature is supposed to be sufficiently high to ensure liquid slag removal. The obtained high-temperature gas enters the second stage together with the stream of secondary fuel, where its allothermic gasification occurs (for the products of the first stage are predominantly CO2 and H2O). Unreacted coke is returned to the first stage of the process. Thus, one of the important process parameters is the primary fuel proportion (i.e. primary fuel consumption divided by overall fuel consumption). This value determines the combustion stage efficiency, i.e. the first stage equivalence ratio, ?1 (equivalence ratio is defined as a ratio of actual oxygen to fuel ratio to the stoichiometric ratio). The combustion stage efficiency in turn determines gasification stage efficiency. Thus, there is a feedback that could result in specific features in the entire gasification process.

The fuel in the calculations is the Kuznetsky coal, grade D. The composition and properties of the fuel are given in Table. 1. The total length of the reaction zone is 12 m, the first stage is about 3 m; the diameter of the reactor is 3 m along the entire length. The pressure in the reactor is considered constant and equal to 3 MPa. Overall fuel consumption is constant and is equal to 70 t/h.

Preliminary thermodynamic calculations showed that the equilibrium gasification process has optimal characteristics for the yield of combustible gas under the conditions given in Table 2. For these conditions, we made calculations to find the options for implementing

Table 1. Kuznetsky coal characteristics.

Fuel characteristics	Values and units
W^r	2.9%
A^d	23.7%
C^{daf}	78.79%
H^{daf}	5.97%
N^{daf}	2.16%
S^{daf}	0.97%
O^{daf}	12.11%
V^{daf}	29.9%
d_p, μm	100

Table 2. Equilibrium parameters of kuznetsky coal air-blown gasification under 900°C

Variable	Unit	Value
Equivalence ratio, α	-	0.33
Steam ratio	mol(H_2O)/mol(C)	0.2
Cold gas efficiency	%	85.7
Producer gas composition % vol.		
CO		28.3
H_2		19.5
H_2O		2.1
CO_2		3.9
N_2		45.8

the limiting equilibrium characteristics of the gasification process.

The mathematical model used in this study was discussed in our previous papers [41–43]. This is a system of spatially one-dimensional equations of heat and mass transfer with a combined kinetic-thermodynamic submodel for solving the problem of chemical transformations. The authors previously used similar models in [39, 44–48] to estimate the characteristics of the gasification process.

The model is based on the heat balance of coal particles and the gas film adjacent to them. The following assumptions are made about the course of the gasification process [41, 42]:

1) the drying rate is limited by external mass transfer of particle with ambient gases;
2) the pyrolysis rate is proportional to the content of volatiles in the particle and depends on temperature according to the Arrhenius law;
3) the gasification rate is determined from the well-known equation of the diffusion-kinetic theory of carbon combustion.

The heat balance equation for a coal particle is written as follows:

$$c_p \frac{d\left(m_p T_p\right)}{d\tau} = \varepsilon\sigma S\left(T_w^4 - T_p^4\right) + \alpha_T S\left(T_g - T_p\right) - Q_w + Q_r.$$

Here c_p is the specific heat of the fuel, $J\ kg^{-1}\ K^{-1}$; mp is current particle mass, kg; T_p – particle temperature, K; ε is the degree of the particle blackness; σ is the Stefan-Boltzmann constant, W (m^{-2} K^{-4}); S is a particle surface area, m2; T_w is ambient temperature, K; α is convective heat transfer coefficient, W/m^{-2} K^{-1}); Q_w is heat of moisture evaporation, W; Q_r is heat of chemical reactions, W.

Drying rate is calculated by the formula:

$$j_w = K_w S\left(C_{H_2O}^{eq} - C_{H_2O}\right)$$

Here j_w is the flow of moisture, kg s^{-1}; K_w is drying rate constant, m/s; C_{H_2O} is the concentration of water vapor, kg m^{-3}.

The coefficient of convective heat and mass transfer for a particle in a stream is calculated by the formula:

$$\mathrm{Nu} = \mathrm{Sh} = 2 + 0.16\,\mathrm{Re}_p^{2/3}$$

Here Nu is the Nusselt number; Sh is the Sherwood number; Re_p is the Reynolds number for the velocity of the carrier flow and current particle size.

The pyrolysis rate is described by the first-order kinetic equation:

$$\frac{dm_V}{d\tau} = -k_V^0 \exp\left(-\frac{E_V}{RT}\right) m_V$$

Here m_v is the mass of volatiles in the particle, kg; k^0_v – pre-exponential coefficient, s^{-1}; E_V is the activation energy of the pyrolysis stage, J/mol; R is the universal gas costant, J mol^{-1} K^{-1}. The volatiles in the model are represented by a mechanical mixture of chemical elements,. After exiting the fuel particle, volatiles achieve their molecular forms according to the conditions of chemical equilibrium.

The reaction rate of the fuel with gaseous oxidizing agents is recorded as follows:

$$\frac{dm_C}{d\tau} = -k_{eff} S C_{ox}$$

Here m_C is the mass of fuel, kg; k_{eff} is effective rate constant for heterogeneous reaction, m/s; S is a fuel surface area, m^2; C_{ox} is the oxidizer concentration, kg m^{-3}.

The effective rate constant is expressed in terms of the kinetic and mass transfer coefficients (assuming that the kinetic order of the reaction with respect to the oxidant is one) as follows [49]:

$$k_{eff} = \frac{k_C k_d}{k_C + k_d}$$

Here k_C is the kinetic rate constant for a heterogeneous reaction, m/s; k_d is the mass transfer coefficient of the particle with the flow, m/s.

The kinetic rate constant for a heterogeneous reaction depends on temperature exponentially:

$$k_C = k_C^0 \exp\left(-\frac{E_a}{RT}\right)$$

Here k^0_C is the preexponential coefficient, m/s; E_a is activation energy, J/mol.

Overall change in particle mass is written as follows:

$$\frac{dm_p}{d\tau} = -j_w + \frac{dm_V}{d\tau} + \frac{dm_C}{d\tau}$$

Chemical kinetics of reactions in the gas phase is not considered. It is assumed that substances entering the gas phase pass into a state of equilibrium. Thus, chemical transformations are described using a thermodynamic model with macrokinetic constraints on the rate of heterogeneous transformations. This approach is applicable to high-temperature processes in which the rates of gas-phase processes are quite high compared to the rates of heterophase processes [50].

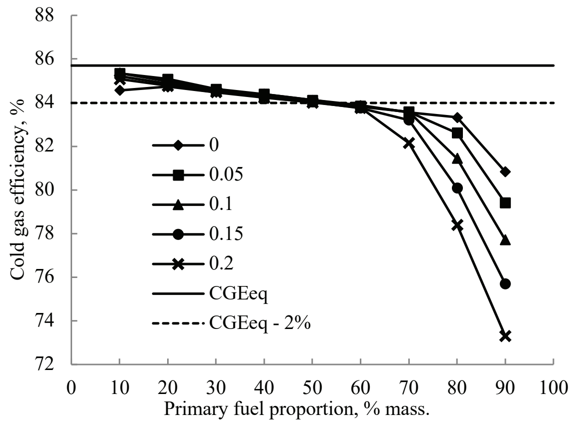

Fig. 2. Cold gas efficiency versus primary fuel and secondary steam proportions, mol(H2O)/mol(C). Dashed lines are equilibrium cold gas efficiency and 2% less values.

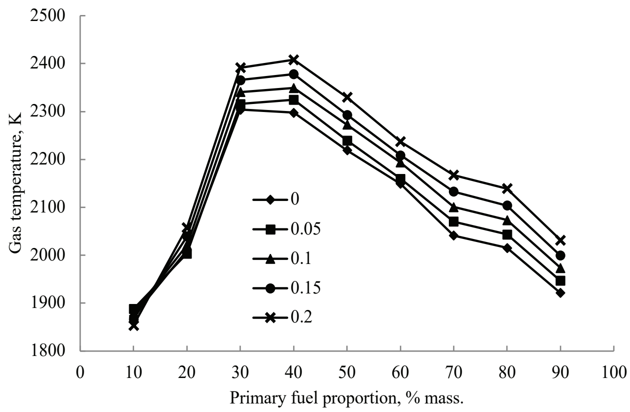

Fig. 3. The first stage output temperature versus primary fuel proportion and secondary steam proportion, mol(H2O)/mol(C).

In the model, the equations of complex heat transfer (convective and radiant) between fuel particles, reactor wall and the gas phase are solved. The wall is considered to be adiabatic. This circumstance additionally simplifies the calculations, since it allows neglecting the specific features of the heat exchange with the wall and with the cooling jacket. In a more accurate formulation, however, it is necessary to take into account the heat transfer inside the reactor wall, ash melting and thermal conditions of slag films [51, 52].

Since, as mentioned above, the transfer processes and chemical reaction are closely related, it is necessary to solve the equations of diffusion kinetics and heat transfer. In the present work, these equations are solved separately at different steps of iterative procedure. The following iterative algorithm is proposed to calculate 1) chemical transformations of fuel particles in the gas stream; 2) transfer of heat released as a result of chemical transformations. Each time chemical transformations are calculated with a refined temperature profile, then the temperature profile is adjusted to chemical transformations [53, 54].

The calculation of the staged process as a whole is carried out as follows. The algorithm is based on the repeated application of fuel particle model in a changing thermal field. This model allows us to calculate the processes in the oxidation and reduction zones separately: when combustion reactor is calculated, the output gas stream is directed to the reduction zone.

The consumption of primary fuel is fixed in each calculation. However, the total fuel consumption in the first stage varies between iterations, since the output of the coke-ash residue is not controlled. This value is set in the calculation progress. The algorithm stop condition is a small change in the total fuel consumption in the first stage: the fuel consumption in the first reactor in two successive iterations changes by less than 5%.

The feedback in the system of reactors can lead to a significant change in its behavior (as compared to the one-step process). At low degrees of secondary fuel conversion, the resulting coke-ash residue is cooled and then recycled. It leads to an increase in heat loss and to a decrease in the degree of fuel conversion in the first stage. In this

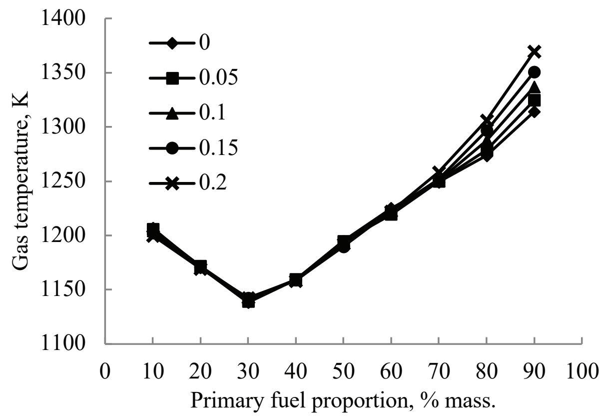

Fig. 4. The second stage output temperature versus primary fuel proportion and secondary steam proportion , mol(H2O)/mol(C).

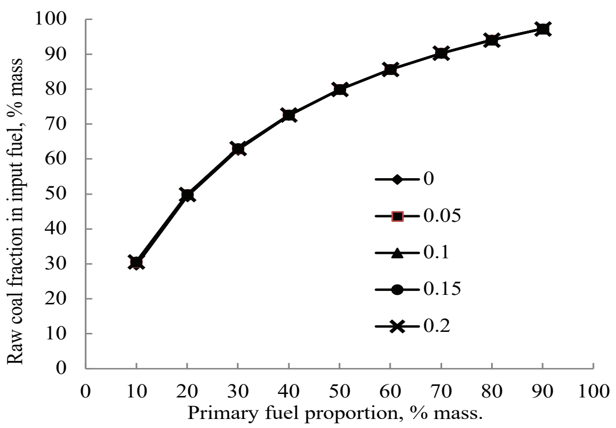

Fig. 5. The raw fuel fraction versus primary fuel and secondary steam proportions , mol(H2O)/mol(C).

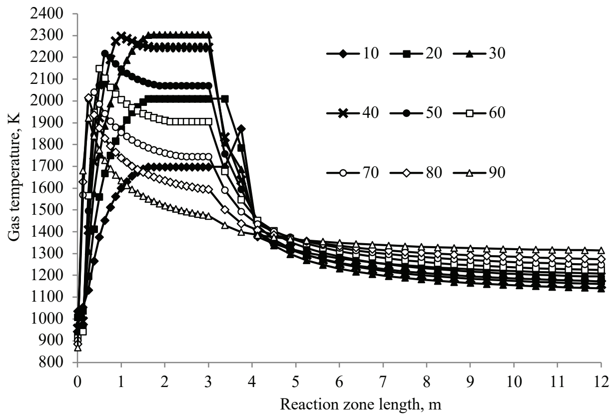

Fig. 6. Temperature distribution along reactor versus primary fuel proportion .

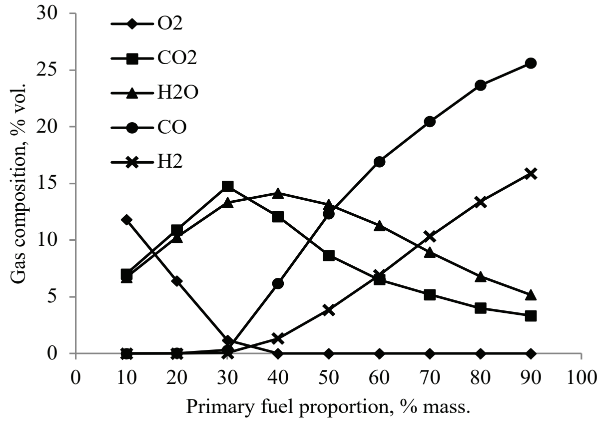

Fig. 7. The first stage output gas composition versus primary fuel proportion .

case, however, its quantity does not increase, since the calculation assumes that all the solid residue from the first stage output is carried away with the liquid slag. Actually, such operation of reactors will be ineffective. It should also be noted that, under the conditions of a stable staged gasification process, combustion temperature is to be sufficiently high to ensure liquid slag removal (otherwise, the ash will be recycled together with the coke-ash residue of the gasification stage, which is undesirable).

The model of a staged gasifier was verified in [41] for a pilot reactor with a capacity of 2 t/day. The calculations showed good agreement with the experimental data on gas composition.

IV. Results and discussion

Two fuel flows and two steam flows are considered with respect to the gasification process stages. Primary fuel and primary steam feed the first stage. Secondary fuel and secondary steam correspond to the second stage. Distribution of fuel and steam between stages is described by different proportions. The influence of these two parameters was studied numerically. Overall steam and fuel consumption is fixed. The secondary steam consumption is varied from 0 to 0.2 mol/mol(C) (the primary steam consumption is determined by the difference from 0.2 to 0 correspondingly). Primary fuel proportion varies from 10% to 90%, secondary fuel proportion changes from 90% to 10%, respectively. The results of the calculations are presented below.

Efficiency of gasification process is usually described by cold gas efficiency (CGE, ratio of producer gas heating value to solid fuel heating value). As it can be seen from Fig. 2, the cold gas efficiency is close to the equilibrium value (CGEeq) in a wide range of primary fuel ratios (up to about 50%), its further increase leads to a decrease in the cold gas efficiency due to a decrease in combustion reactor temperature (Fig. 3). At the same time, the temperature of the second stage product gas (see Fig. 4) is very sensitive to the primary fuel proportion: with its growth, the gas temperature gradually increases close to the equilibrium value (1373 K). Deviations are associated with an imbalance in reagent consumption. The low temperature of the product gas with a small primary fuel proportion is associated with heat loss due to coke-ash residue cooling. As can be seen from Fig. 5, the fraction of raw coal in a mixture with recirculating coke-ash residue could be about

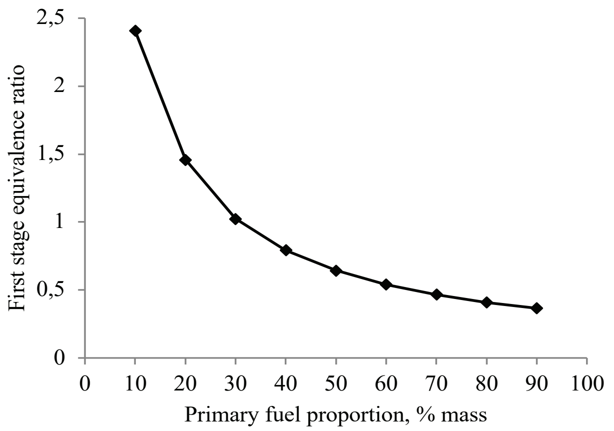

Fig. 8. The first stage equivalence ratio versus primary fuel proportion.

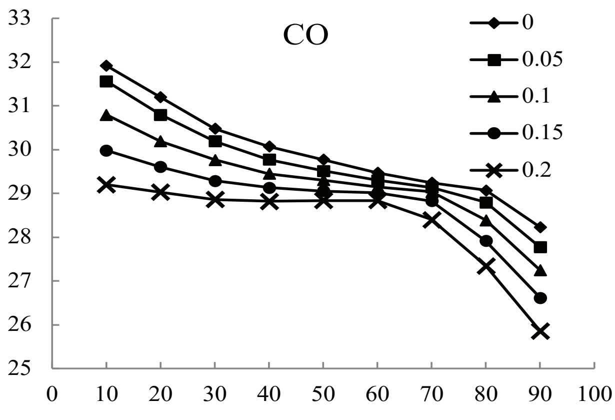

Fig. 9. The CO volume fraction in produced gas versus primary fuel and secondary steam proportions.

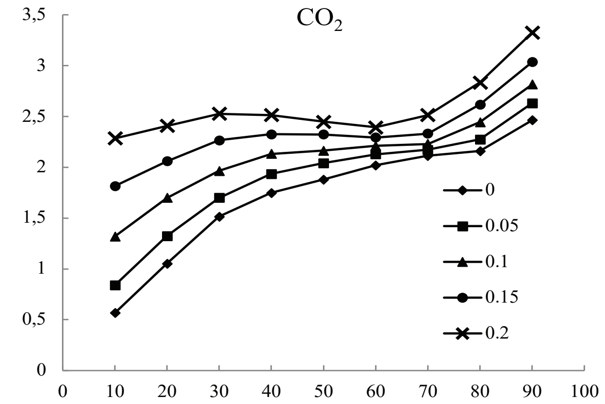

Fig. 10. The CO_2 volume fraction in produced gas versus primary fuel and secondary steam proportions.

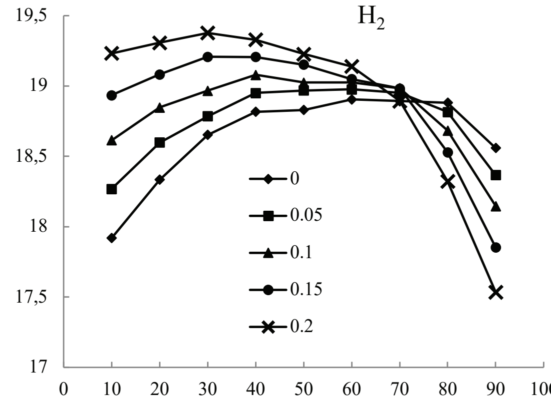

Fig. 11. of The H_2 volume fraction in produced gas versus primary fuel and secondary steam proportions.

30%. Since the model uses the assumption that the coke-ash residue is cooled during transport, and the slag is removed at the temperature of the combustion reactor, considerable heat loss occurs. Therefore, to maintain the desired level of the product gas temperature , it is necessary to deviate from the equilibrium estimate of the parameters of the optimal conditions (for example, towards an increase in the oxygen-fuel ratio).

An interesting effect is the extremum value of gas temperature: the maximum temperature of the first stage and the minimum output temperature is achieved with a primary fuel proportion of ~30%. This is due to the full use of air : with a low primary fuel proportion , its complete combustion occurs. With an increase in the primary fuel proportion above 30-40%, carbon gasification with carbon dioxide and water vapor begins already in the first stage, thus, the peak temperature decreases. On the other hand, the primary fuel underburning increases, which leads to an increase in the effective excess of oxidant (this is associated with an increase in the temperature of the product gas and a decrease in cold gas efficiency with a high primary fuel proportion).

The effect of the transition from the two-stage to the single-stage reactor operation can be observed in Fig.

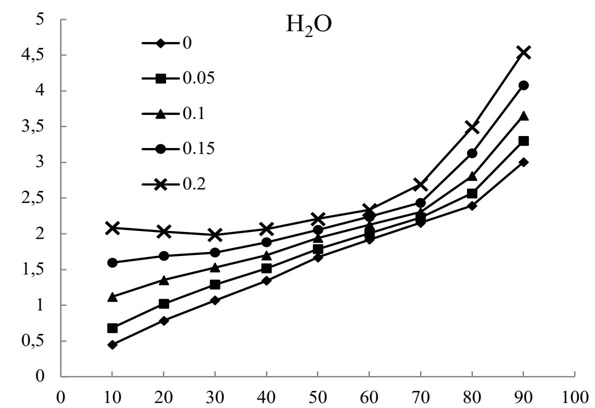

Fig. 12. The H_2O volume fraction in produced gas versus primary fuel and secondary steam proportions.

6 (the curves were obtained for the conditions without secondary steam, however, the same picture is observed for other distributions of steam by stage). An abrupt change in temperature over a length of 3 m is associated with the transition of gas from one stage to another: in this case, the gas is cooled by heating and drying the secondary fuel. Then, heterogeneous chemical reactions begin: under small primary fuel proportions , the presence of residual oxygen leads to the development of exothermic reactions, and temperature profile can have a drop.

With a primary fuel proportion above 20–30%, there is no molecular oxygen in the products of the first stage. Therefore, the temperature curves are monotone, becoming the profile of a single-stage process with a high primary fuel ratio. This is evidenced by the course of changes in the intermediate gas composition and the first-stage oxidizer proportion α_1, as shown in Figs. 7-8 (calculations are carried out without secondary steam). With a high primary fuel proportion , the first stage produces the main quantity of combustible gases. Thus, with a primary fuel proportion of less than 30–40%, the operating conditions are characterized by an obvious two-stage temperature profile, and with a higher primary fuel proportion , the process gradually approaches the usual single-stage gasification process.

It is worth noting that the fraction of raw coal in the mixture with coke-ash residue entering the first stage (Fig. 5) remains almost constant when the proportion of the primary and secondary steam changes. Apparently, this characteristic of the process is determined primarily by the overall stoichiometry for the system of two reactors.

different behavior is observed before and after the primary fuel proportion of 60-70%. As already mentioned, above these values, a significant amount of underburning begins to form in the first stage, which leads to the present picture. This boundary can serve as the upper limit of the primary fuel proportion when choosing the operating conditions of a staged gasifier. The estimates obtained using one-dimensional model can be used as source data for CFD calculations [55]. According to the results of

3D-modeling, the efficiency of the gasification process with a primary fuel proportion of 30% is 84.9%. This value is in good agreement with the results of this model (84.5%). Further areas of research will be associated with the search for new ways to control the staged gasification processes. To this end, it is necessary to investigate the effect of heat and material flows between the stages and within them. The calculations show that an increase in the fraction of recycled coke-ash residue is a negative factor in general, therefore, this value should be minimized.

However, There can be various options of the process organization , that could shift boundaries of the efficient conditions (compared with those obtained in present work). For example, implementation of the additional stages: additional supply of gasification agent and fuel (including separation of the raw coal and coke-ash residue inputs), as well as the use of hot recycling systems for the coke-ash residue.

V. Conclusion

Alteration in the proportion of primary and secondary fuels in a two-stage pulverized gasification process leads to a successive change from the conditions with a staged sharp temperature profile (with a primary fuel proportion of 10-40%) to the conditions with a smoother profile that are typical of one-stage processes.

The calculated cold gas efficiency of the gasification process is quite close to the equilibrium (85.7%) in the range of the primary fuel proportion of 10-50%, the higher this proportion the lower the efficiency due to the formation of a significant amount of unburnt coke-ash residue. The use of secondary steam is ineffective in all the conditions considered. An analysis of the results makes it possible to choose the conditions in which the first stage implements the most complete fuel combustion: these conditions are primary candidates to be tested as optimal ones.

Further study can be focused on a new staged gasification process, including additional reagent supply sections (for example, an additional section for steam blast, separation of raw fuel and coke-ash residue, etc.)

Acknowledgements

The study is performed with partial support of the Russian Science Foundation (project No. 14-19-00524, Ural Federal University) and Siberian Branch of the Russian Academy of Sciences (Fundamental Research program, scientific project III.17.1.2, registration number AAAA-A17-117030310448-0, Melentiev Energy Systems Institute.)

References

[1] A.M. Cormos, C. Dinca and C.C. Cormos, “Multi-fuel multi-product operation of IGCC power plants with carbon capture and storage (CCS),” *App. Therm. Eng.*, vol. 7, pp. 20-27, 2015. DOI: 10.1016/j.applthermaleng.2013.12.080

[2] G. G. Olkhovskii, “New projects for CCGTs with coal gasification (Review),” *Therm. Eng.*, vol. 63, no. 10, pp. 679-689, 2016. DOI: 10.1134/S0040601516100074

[3] I. Barnes, “Recent operating experience and improvement of commercial IGCC,” IEA Clean Coal Centre, London, UK, 2013.

[4] A.M. Kler, E.A. Tyurina, A.S. Mednikov, “A plant for methanol and electricity production: Technical-economic analysis,” *Energy*, vol. 165B, pp. 890-899, 2018. DOI: 10.1016/j.energy.2018.09.179

[5] C. C. P. Pian and K. Yoshikawa, “Development of a high-temperature air-blown gasification system,” *Biores. Tech.*, vol. 79, pp. 231-241, 2001. DOI: 10.1016/S0960-8524(01)00054-2

[6] P. F. Li, J. C. Mi, B. B. Dally, F. F. Wang, L. Wang, Z. H. Liu, S. Chen and C. G. Zheng, “Progress and recent trend in MILD combustion,” *Science China. Tech. Sci.*, vol. 54, no. 2, pp. 255-269, 2011. DOI: 10.1007/s11431-010-4257-0

[7] T. Hashimoto, K. Sakamoto, K. Ota, T. Iwahashi, Y. Kitagawa and K. Yokohama, “Development of coal gasification system for producing chemical synthesis source gas,” *Mitsubishi Heavy Ind. Tech. Rev.*, vol. 47, no. 4, pp. 27-32, 2010.

[8] A. Guiffrida, M. C. Romano and G. Lozza, “Thermodynamic analysis of air-blown gasification for IGCC applications,” *App. Energy*, vol. 88, pp. 3949-3958, 2011. DOI:10.1016/j.apenergy.2011.04.009

[9] A. F. Ryzhkov, S. I. Gordeev and T. F. Bogatova, “Selecting the process arrangement for preparing the gas turbine working fluid for an integrated gasification combined-cycle power plant,” *Therm. Eng.*, vol. 62, no. 11, pp. 796-801, 2015. DOI: 10.1134/S0040601515110075

[10] S. K. Som and A. Datta, “Thermodynamic irreversibilities and exergy balance in combustion processes,” *Prog. Energy Comb. Sci.*, vol. 34, pp. 351-376, 2008. DOI: 10.1016/j.pecs.2007.09.001

[11] Q. Zhu, “High temperature syngas coolers,” IEA Clean Coal Centre, London, UK, Report CCC/257, 2015.

[12] Integrated gasification combined cycle (IGCC) technologies, T. Wang and G. Stiegel, eds. Woodhead Publ., 2017. DOI: 10.1016/B978-0-08-100167-7.00001-9

[13] G. Guan, “Clean coal technologies in Japan: A review,” *Chinese J. Chem. Eng.*, vol. 25, no. 6, pp. 689-697, 2017. DOI: 10.1016/j.cjche.2016.12.008

[14] Z. Huang, J. Zhang and G. Yue, “Status of domestic gasification technology in China,” *Front. Energy Power Eng. China*, vol. 3, no. 3, pp. 330-336, 2009. DOI 10.1007/s11708-009-0021-1

[15] S. Xu, Y. Ren, B. Wang, Y. Xu, L. Chen, X. Wang and T. Xiao, “Development of a novel 2-stage entrained flow coal dry powder gasifier,” *App. Energy*, vol. 113, pp.

318-323, 2014. DOI: 10.1016/j.apenergy.2013.07.045

[16] A. F. Ryzhkov, T. F. Bogatova, Zeng Lingyan and P. V. Osipov, "Development of entrained-flow gasification technologies in the Asia-Pacific region (review)," *Therm. Eng*., vol. 63, no. 11, pp. 791-801, 2016. DOI:10.1134/S0040601516110069

[17] B. Zhang, Z. Ren and S. Shi, "Development of reduced order model for HNCERI gasifier," in *Clean Coal Technology and Sustainable Development*, G. Yue and S. Li, eds., Springer, 2016, pp. 597-601. DOI 10.1007/978-981-10-2023-0_81

[18] M. Grabner and B. Meyer, "Performance and exergy analysis of the current developments in coal gasification technology," *Fuel*, vol. 116, pp. 910-920, 2014. DOI: 10.1016/j.fuel.2013.02.045

[19] A. Ryzhkov, T. Bogatova and S. Gordeev, "Technological solutions for an advanced IGCC plant," *Fuel*, vol. 214, pp. 63-72, 2018. DOI: 10.1016/j.fuel.2017.10.099

[20] A. Silaen and T. Wang, "Effect of turbulence and devolatilization models on coal gasification simulation in an entrained-flow gasifier," *Int. J. Heat Mass Trans*., vol. 53, pp. 2074-2091, 2010. DOI:10.1016/j.ijheatmasstransfer.2009.12.047

[21] A. Slezak, J. M. Kuhlman, L.J. Shadle, J. Spenik and S. Shi, "CFD-simulation of entrained-flow coal gasification: Coal particle density/size fraction effects", *Powder Tech*., vol. 203, pp. 98-108, 2010. DOI:10.1016/j.powtec.2010.03.029

[22] Y.-T. Luan, Y.-P. Chyou and T. Wang, "Numerical analysis of gasification performance via finite-rate model in a cross-type two-stage gasifier," *Int. J. Heat Mass Trans*., vol. 57, pp. 558-566, 2013. DOI: 10.1016/j.ijheatmasstransfer.2012.10.026

[23] H. J. Jeong, D. K. Seo and J. Hwang, "CFD modeling for coal size effect on coal gasification in a two-stage commercial entrained-bed gasifier with an improved char gasification model," *App. Energy*, vol. 123, pp. 29-36, 2014. DOI: 10.1016/j.apenergy.2014.02.026

[24] A. Rakhshi and T. Witowski, "A framework for devolatilization breakdown in entrained flow gasification modeling," *Fuel*, vol. 187, pp. 173-179, 2017. DOI: 10.1016/j.fuel.2016.09.036

[25] M. Kumar, "Entrained flow gasification: Current status and numerical simulation," in: *Coal and biomass gasification. Recent advances and future challenges*, S. De, A. K. Agarwal, V. S. Moholkar and B. Thallada, eds. Singapore: Springer, 2018. pp. 281-306. DOI: 10.1007/978-981-10-7335-9_11

[26] C. Chen, M. Horio and T. Kojima, "Use of numerical modeling in the design and scale-up of entrained flow coal gasifiers," *Fuel*, vol. 80, no. 10, pp. 1513-1523, 2001. DOI: 10.1016/S0016-2361(01)00013-8

[27] H. Liu, C. Chen and T. Kojima, "Theoretical Simulation of Entrained Flow IGCC Gasifiers: Effect of Mixture Fraction Fluctuation on Reaction Owing to Turbulent Flow," *Energy Fuels*, vol. 16, no. 5, pp. 1280-1286, 2002. DOI: 10.1021/ef0200626

[28] W. Vicente, S. Ochoa, J. Aguillon and E. Barrios, "An Eulerian model for the simulation of an entrained flow coal gasifier," *App. Therm. Eng.*, vol. 23, no. 15, pp. 1993-2008, 2003. DOI: 10.1016/S1359-4311(03)00149-2

[29] M. Kumar and A. F. Ghoniem, "Application of a validated gasification model to determine the impact of coal particle grinding size on carbon conversion," *Fuel*, vol. 108, pp. 565-577, 2013. DOI: 10.1016/j.fuel.2013.02.009

[30] H. Watanabe, K. Tanno, H. Umetsu and S. Umemoto, "Modeling and simulation of coal gasification on an entrained flow coal gasifier with a recycled CO2 injection," *Fuel*, vol 142, pp. 250-259, 2015. DOI: 10.1016/j.fuel.2014.11.012

[31] H. Watanabe, S. Ahn and K. Tanno, "Numerical investigation of effects of CO2 recirculation in an oxy-fuel IGCC on gasification characteristics of a two-stage entrained flow coal gasifier," *Energy*, vol. 118, pp. 181-189, 2017. DOI: 10.1016/j.energy.2016.12.031

[32] M. S. Alam, A. T. Wijayanta, K. Nakaso and J. Fukai, "Study on coal gasification with soot formation in two-stage entrained-flow gasifier," *Int. J. Energy Environ. Eng*., vol. 6, pp. 255-265, 2015. DOI: 10.1007/s40095-015-0173-1

[33] V. Kuznetsov, M. Chernetskiy and A. Ryzhkov "Study of the two-stage gasification process of pulverized coal at the hydrodynamic flow separation," *J. Phys. Conf. Ser*., vol. 754, 2016. DOI:10.1088/1742-6596/754/11/112007

[34] V. Kuznetsov, M. Chernetskiy, N. Abaimov and A. Ryzhkov, "Study of the two-stage gasification process of pulverized coal with a combined countercurrent and concurrent flow system," *MATEC Web Conf*., vol. 115, 2017. DOI: 10.1051/matecconf/201711503008

[35] M. Sijeric and K. Hanjalic, "Application of computer simulation in a design study of a new concept of pulverized coal gasification. Part II. Model of coal reactions and discussion of results," *Combust. Sci. Tech.*, vol. 97, pp. 351-375, 1994. DOI: 10.1080/00102209408935385

[36] H. Watanabe and M. Otaka, "Numerical simulation of coal gasification in entrained flow coal gasifier," *Fuel*, vol. 85, pp. 1935-1943, 2006. DOI:10.1016/j.fuel.2006.02.002

[37] N. A. Abaimov, E. B. Butakov, A. P. Burdukov and A. F. Ryzhkov, "Investigation of two-stage air-blown and air-steam-blown entrained-flow coal gasification," *J. Phys. Conf. Ser*., vol. 899, 2017. DOI: 10.1088/1742-6596/899/9/092001

[38] N. A. Abaimov and A. F. Ryzhkov, "Development of advanced air-blown entrained-flow two-stage bituminous coal IGCC gasifier," *EPJ Web Conf*, vol.

159, 2017. DOI: 10.1051/epjconf/201715900001

[39] R. F. D. Monaghan and A. F. Ghoniem, "A dynamic reduced order model for simulating entrained flow gasifiers. Part II: Model validation and sensivity analysis," *Fuel*, vol. 94, pp. 280-297, 2012. DOI: 10.1016/j.fuel.2011.08.046

[40] H. Ishi, T. Hayashi, H. Tada, K. Yokohama, R. Takashima and J. Hayashi, "Critical assessment of oxy-fuel integrated coal gasification combined cycles," *App. Energy*, vol. 233-234, pp. 156-169, 2019. DOI: 10.1016/j.apenergy.2018.10.021

[41] I. G. Donskoy, D. A. Svishchev, V. A. Shamansky and A. N. Kozlov, "Mathematical modeling of the staged pulverized coal gasification process," *Sci. Bull. NSTU.*, vol. 58, no. 1, pp. 231-245, 2015. DOI: 10.17212/1814-1196-2015-1-231-245

[42] I. G. Donskoi, "Mathematical modeling of the reaction zone of a Shell-Prenflo gasifier with the use of the models of sequential equilibrium." *Solid Fuel Chem.*, vol. 50, no. 3, pp. 191-196, 2016. DOI: 10.3103/S0361521916030034

[43] I. G. Donskoy, V. A. Shamansky, A. N. Kozlov and D. A. Svishchev, "Coal gasification process simulations using combined kinetic-thermodynamic models in one-dimensional approximation," *Combust. Theor. Model.*, vol. 21, no. 3, pp. 529-559, 2017. DOI: 10.1080/13647830.2016.1259505

[44] S.S. Hla, D.G. Roberts and D.J. Harris, "A numerical model for understanding the behaviour of coals in an entrained-flow gasifier," *Fuel Proc. Tech.*, vol. 134, pp. 424-440, 2015. DOI: 10.1016/j.fuproc.2014.12.053

[45] Y. Ju and C.-H. Lee, "Evaluation of the energy efficiency of the shell coal gasification process by coal type," *Energy Convers. Manag.*, vol. 143, pp. 123-136, 2017. DOI: 10.1016/j.enconman.2017.03.082

[46] M. H. Sahraei, M. A. Duchesne, R. W. Hughes and L. A. Ricardez-Sandoval, "Dynamic reduced order modeling of an entrained-flow slagging gasifier using a new recirculation ratio correlation," *Fuel*, vol. 196, pp. 520-531, 2017. DOI: 10.1016/j.fuel.2017.01.079

[47] B. Zhang, Z. Ren, S. Shi, S. Yan and F. Fang, "Numerical analysis of gasification and emission characteristics of a two-stage entrained flow gasifier," *Chem. Eng. Sci.*, vol. 152, pp. 227-238, 2016.DOI: 10.1016/j.ces.2016.06.021

[48] M. Hwang, E. Song and J. Song, "One-dimensional modeling of an entrained coal gasification process using kinetic parameters," *Energies*, vol. 9, 2016. DOI:10.3390/en9020099

[49] D. A. Frank-Kamenetskii, *Diffusion and Heat Exchange in Chemical Kinetics*, USA: Princeton Univ. Press, 2015.

[50] A. V. Messerle, V. E. Messerle and A. B. Ustimenko, "Plasma thermochemical preparation for combustion of pulverized coal," *High Temp*,. vol. 55, no. 3, pp. 352-360, 2017. DOI: 10.1134/S0018151X17030142

[51] J. Kim, H. Oh, S. Lee and Y.-S. Yoon, "Advanced One-Dimensional Entrained-Flow Gasifier Model Considering Melting Phenomenon of Ash," *Energies*, vol. 11, no. 4, 2018. DOI: 10.3390/en11041015

[52] D. Safronov, T. Forster, D. Schwitalla, P. Nikriyuk, S. Guhl, A. Richter and B. Meyer, "Numerical study on entrained-flow gasification performance using combined slag model and experimental characterization of slag properties," *Fuel Proc. Tech.*, vol. 161, pp. 62-75, 2017. DOI: 10.1016/j.fuproc.2017.03.007

[53] V. I. Kovenksii, "Method of calculating the bed combustion of a solid fuel coke residue," *Theor. Found. Chem. Eng.*, vol. 46, no. 2, pp. 180-192, 2012. DOI: 10.1134/S004057951202005418.

[54] Patankar S.V. *Numerical heat transfer and fluid flow*, NY: Taylor&Francis, 1980.

[55] A. F. Ryzhkov, N. A. Abaimov, I. G. Donskoy and D. A. Svishchev, "Modernization of Air-Blown Entrained-Flow Gasifier of Integrated Gasification Combined Cycle Plant," *Combust. Explos. Shock Waves*, vol. 54, no. 3, pp. 337-344, 2018. DOI: 10.1134/S0010508218030103

Igor Gennadyevich Donskoy
Candidate of Since 2017 he has been seniour researcher in Laboratory of Thermodynamics of Melentiev Energy Systems Institute (Irkutsk). His research interests include mathematical modelling, fuel processing, thermal engineering.

Denis Alekseevich Svishchev
is a researcher in Laboratory of Thermodynamics of Melentiev Energy Systems Institute (Irkutsk). His research interests include thermophysical experiment, fuel processing, biomass energy.

Aleksandr Filippovich Ryzhkov
Doctor of. Science, is full professor of Thermal Power Plants Chair, Power Engineering Institute of Ural Federal University (Ekaterinburg). His research interest include integrated gasification combined cycle plants, heat and mass transfer, computational fluid dynamics.

Comprehensive studies on reliability of jointly operating fuel and electric power systems

Tatyana Dzyubina, Gennady Kovalev

Melentiev Energy Systems Institute of Siberian Branch of Russian Academy of Sciences, Irkutsk, Russia

Abstract **— The paper places an emphasis on the fact that many publications on complex reliability assessment of electric power and fuel systems do not always substantiate the application of various methods. We address the "system", "nodal", and "estimation" approaches to assess the reliability of electric power systems, given reliable fuel supply to power plants. These approaches are accompanied by an analysis of their correspondence to the objectives and goals of the study, as well as an analysis of the validity of their application in terms of the obtained result accuracy, research time, complexity of search for and preparation of the input data and forms of their representation in a model. All the approaches were tested in case studies. The nodal and system approaches were tested on a conventional power system, while the estimation approach was tested on design diagrams of the gas and electric power systems of the Northwestern Federal District of the Russian Federation.**

Index Terms **— fuel system, electricity system, complex research, power plant fuel supply, reliability indices.**

I. Nomenclature

$p(Q)$ – series of the fuel system operable state probability distributions.

i – power plant index.

p_i^F – fuel supply probability (supply coefficient) of the ith power plant.

p_i^G – operable state probability of each generator of the ith power plant.

p_i^{GF} – operable state probability of each generator of the ith power plant, considering the supply coefficient.

$P_n(m)$ – probability that m units of n are in operable state with the total power $\sum_{i=1}^{m} P_i$

n – the total number of units.

p, q – probabilities of operable and non-operable states of each of n units, .

$P^{F(G,L)}$ – unit capacity of a fuel system component (F), generator (G), or load (L) in an electricity system.

$P_i^{F(G,L,Gd,R)}$, $p_i^{F(G,L,Gd,R)}$ –outputs of the fuel system (F), available capacity (G), or load (L) in an electric power system, generalized (Gd) and resultant (R) outputs necessary to supply the load (megawatts) and related probabilities.

Q_i^F – output of the fuel system in tons of coal equivalent (tce) per year.

p'_i, q'_i – mean and root-mean-square deviation of the fuel system actual output (available capacity or load).

P', P'' – corrected probabilities of failure-free operation and idle time of units at power plants.

– upper and lower boundaries of the nodal reliability index of electricity supply to consumers - probabilities of electricity supply, given fuel system reliability.

p_i^{GSS}, p_i^{EPS} – nodal probabilities for shortage-free operation of gas and electric power systems.

II. Introduction

A comprehensive study of the electric power system adequacy suggests an assessment of whether or not the system (EPS) is provided with all kinds of resources, particularly with primary energy resources, i.e. fuel (gas, coal, fuel oil, etc.) for thermal power plants, water in reservoirs for hydroelectric power plants, and nuclear material for nuclear power plants.

Natural gas is the most relevant fuel of all the fuel types for thermal power plants due to its environmental compatibility, efficiency and availability. In some regional power systems, the coal share in the total amount of fuel currently accounts for 70-90% [1]. According to forecasts,

* Corresponding author.
E-mail: tvleo@isem.irk.ru

http://dx.doi.org/10.25729/esr.2018.04.0004
Available online February 28, 2019.

in the Russian Federation, after 2030, the electricity generated from gas is expected to increase by 1.9 times [2], and in 2040 the share of gas in the world energy balance will reach 24% [3]. It is worth noting that gas, unlike other types of fuel, cannot be stored at power plants. Another point affecting the reliability of power systems is the liberalization of electricity markets. For example, market "refusals" to deliver fuel affect the operation of electric power system [4].

In this regard, it became necessary to study the reliability of integrated operation of gas systems (GSs) and electric power systems (EPSs).

The issues of integration (joint operation) of the electricity, gas and heat systems are addressed in [5-14]. The studies presented in [5-8] focus on the models [5, 7, 8] and methods [6] for solving problems of optimal energy flow for integrated electricity and natural gas systems for one or several time periods [7, 8]. In [9], the authors propose a distributed control system for such systems.

In [10], the authors present an integrated model to co-optimize the expansion of electrical energy storage, in combination with electrical and natural gas infrastructures to reliably supply electric loads at the least cost.

The proposed model is formulated as a two-stage stochastic optimization problem, in which investment decisions are made in the first stage, followed by a variety of operating conditions under different potential random scenarios.

The authors of [11] propose a mixed-integer linear programming approach to security-constrained co-optimization of expansion planning of natural gas and electricity transmission systems. This approach simultaneously considers N-1 contingency in both natural gas system and electric power system.

Attention is drawn to the increased risk of emergency situations in the natural gas system, which threaten the security of the entire integrated energy system. A disadvantage of the study is limited consideration of unforeseen events by the level of N-1 contingency.

A broader consideration is given in [12, 13], where the authors discuss the operation of an integrated energy system consisting of electricity, gas and heat systems. The study in [12] addresses a unified fault identification and location method using big data analysis. Here, the concept of "fault" does not include the concept of "partial failure" as in the theory of reliability. In [13], the authors focus on the impact of a gas pipeline emergency on fuel supply to electricity and heat sources. They also raise, to some extent, the issues of reliability (security) of the integrated energy system. The study presented in [14] is similar in scope. It focuses on the influence of gas system on adequacy of an electric power system.

In Russia, there have been no studies on reliability of jointly operating gas and electricity systems.

A comprehensive analysis of the electric power system adequacy, given the reliability of a system of fuel delivery to power plants can be made by two methods [14]:

1) first, we assess the reliability of fuel system and then the consequences of its failures for the power system adequacy are taken into account;

2) the joint operation of gas and electric power systems is considered by simulating simultaneous failures in both systems based on stochastic modeling.

We have proposed and tested a system approach according to which the reliability of gas system and the adequacy of electric power system of the Northwest Federal District are analyzed [15–17]. The nodal approach was also mentioned here, although no studies on it were conducted.

In the studies based on the system approach, an all-round analysis of the reliability of jointly operating gas and electric power systems was carried out by the first method, i.e. in the beginning, the operation of gas system was modeled and its reliability was assessed, and then the operation of the power system was modeled, given the consequences of the gas system failures. For these purposes, we used the mathematical models to analyze the reliability of complex gas systems [18] and electric power systems [19].

The publications devoted to the assessment of power system adequacy in terms of reliability of gas systems, i.e. reliable gas delivery to gas-fired power plants, do not always explain the appropriateness of applying a particular method from the standpoint of the accuracy in presenting the technical and economic properties of the studied objects in the computational model [15–17]. Therefore, the novelty of this study lies in considering the methods with an analysis of their correspondence to the research objectives and aims, as well as with an analysis of their appropriateness in terms of time consumption to calculate reliability, complexity of input data preparation, availability of the necessary data and forms of their representation in a model. Special emphasis is put on partial failures [20, 21].

Additionally, we propose a wider problem statement: to address fuel supply to the plants operating not only on gas, but also on any other fuel (coal, fuel oil, etc.), i.e., we analyze the reliability of a fuel system (FS) in general and its effect on the electricity supply reliability. We have also put forward an estimation method to scrupulously consider the nodal and system approaches.

We have performed a comparative analysis of several methods to calculate the reliability of electricity system, taking account of the fuel system reliability.

The most universal representation of random values is their function or a distribution series in the most detailed form (with a sufficiently great number of steps). Therefore, all the models examined in this study are compared with this standard representation.

The paper focuses on various models and approaches ("nodal" (Section III), "systems" (Section IV) and "estimation" (Section V)) to allow for reliability when calculating and analyzing the adequacy of energy systems, and the methods for their evaluation.

III. Nodal approach

In the nodal approach, the reliability of fuel system is taken into account in the calculation of electric power system adequacy by considering the reliability depending on the equipment failure rate for the system directly supplying fuel to a certain EPS node.

The reliability analysis of fuel system is performed on the assumption that it operates independently of electric power system (sometimes, this is not true, but this issue is not addressed here). By analyzing the fuel system reliability, we find a series of probability distribution of its operable states, *p(Q)*. The latter is used to determine the main reliability indices of the system, including the probability of meeting consumer demand for fuel, or shortage-free supply, and the mean of actual output. Knowing them, it is possible to analyze the reliability of joint operation of energy system components. This can be done using two methods.

Method 1: The standard calculation suggests multiplication of the initial distribution series of operable state of the generating equipment of power plant operating on a certain fuel by the *p(Q)* series corresponding to it.

Method 2: With the supply coefficient used for estimation, we determine the fuel delivery probability for each i^{th} power plant (supply coefficient) p_i^F. In this case, the operable state probability of each generator p_i^G of the i^{th} power plant is calculated by the formula

$$p_i^{GF} = p_i^G \cdot p_i^F$$

This formula is used to build a corrected initial series by electricity generation to analyze the adequacy of EPS node, considering the fuel system reliability, i.e., the corrected values are applied in further calculations of the EPS reliability.

The results of the calculation by the nodal method were compared by a simplified test case yet considering all the essential factors affecting the integral reliability of power supply to consumers.

To calculate the distribution series for the fuel and electric power systems random states, we used the scheme of independent trails based on Bernoulli distribution [22]

$$P_n(m) = C_n^m p^m q^{n-m} \quad C_n^m = \frac{n!}{m!\,(n-m)!}$$

$$0! = 1;\ n! = 1 \cdot 2 \cdot \ldots \cdot n, \tag{1}$$

where $q = 1 - p$; $m = 0, 1, 2, \ldots, n$.

In this notation: P_n(m) is the probability that *m* units of *n* are in the operable state with the corresponding total power $\sum_{i=1}^{m} P_i$; *p*, *q* are probabilities of operable and non-operable states of each of *n* units, $p+q=1$; P_i is the unit capacity.

These distribution series can also be represented as a result of processing the statistical (reported) data on functioning of the corresponding equipment.

Table I. Fuel system distribution series.

No	Q_i^F, Mln TCE/YR	P_i^F, MW	p_i^F
1	0	0	$0.1 \cdot 10^{-9}$
2	7.656	100	$0.9 \cdot 10^{-8}$
3	15.312	200	$0.3645 \cdot 10^{-6}$
4	22.968	300	$0.8748 \cdot 10^{-5}$
5	30.624	400	$0.13778 \cdot 10^{-3}$
6	38.28	500	$0.5931 \cdot 10^{-2}$
7	45.936	600	$0.8787 \cdot 10^{-3}$
8	53.592	700	$0.574 \cdot 10^{-1}$
9	61.248	800	0.1937
10	68.904	900	0.3874
11	76.56	1000	0.3487

Note: The calculation correctness is confirmed by meeting the normalizing condition, i.e. the sum of probabilities of events equals 1.0.

Let us consider a fuel system represented by ten objects with an output of 100 MW each and with a 0.9 operable state probability of each object, i.e. $P^F = 100$, $n = 10$, $P^F = 0.9$, $q^F = 0.1$. Table 1 demonstrates the fuel supply random state distribution series calculated by the Bernoulli distribution (1). The system output is given as Q_i^F (tons of coal equivalent per year) and as P_i^F (megawatts).

The mean and the standard deviation of the actual fuel system output , are respectively equal to

$$M[P^F] = 852.32 \text{ MW};\ \sigma[P^F] = 300.92 \text{ MW}.$$

Table 2 presents the available capacity distribution series for the power plants comprising nine units with a 100 MW capacity, and with a 0.85 operable state probability, i.e.

$$P^G = 100,\ n = 9,\ P^G = 0{,}85,\ q^G = 0{,}15.$$

The mean and the standard deviation of the available capacity, respectively, equal

$$M[P^G] = 765.055 \text{ MW};\ \sigma[P^G] = 106.94 \text{ MW}.$$

Table 3 presents the distribution series of the load to be supplied. This series is regarded to be given.

The mean and the standard deviation of load are respectively equal to

$$M[P^L] = 477 \text{ MW},\ \sigma[P^L] = 229.28 \text{ MW}.$$

The connection diagram of the studied object is sequential in terms of reliability, therefore it can be

Table 2. Power plant available capacity distribution series.

No	P_i^G, MW	p_i^G
1	0	$0.3842 \cdot 10^{-7}$
2	100	$0.196 \cdot 10^{-5}$
3	200	$0.444 \cdot 10^{-4}$
4	300	$0.5876 \cdot 10^{-3}$
5	400	$0.4994 \cdot 10^{-2}$
6	500	$0.283 \cdot 10^{-1}$
7	600	0.10692
8	700	0.25969
9	800	0.3679
10	900	0.23163

Note: The normalizing condition is met: $\Sigma p_i = 1.0$.

Table 3. Load distribution series

No	P_i^G, MW	p_i^G
1	100	0.105
2	200	0.11
3	300	0.115
4	400	0.12
5	500	0.125
6	600	0.13
7	700	0.145
8	800	0.15

Note: The normalizing condition is met: $\Sigma p_i = 1.0$.

presented as follows (Fig. 1).

Fuel system → Electric power system → Load

Fig. 1. Diagram of fuel system connection to electric power system and to load.

Normally, the power supply reliability is determined for a uniquely set output of each of the systems included in the diagram (fuel system, electric power system, load), and for the probability of providing this efficiency. Here, consideration is given to the distribution series for various outputs and the probabilities related to them, which corresponds better to real operation conditions of the systems, because this is how the electric power system partial failures and the load undersupply are considered.

The fuel system available capacity is assumed to be larger than the power system available capacity, considering the redundancy (1000>900>800) required.

Based on the data from Fig. 1 and Tables 1 and 2, we should obtain a generalized fuel system and electricity system series and multiply it by the load series. The resultant series can be used to determine the power supply reliability indices for the investigated scheme.

The generalized distribution series characterizes possibilities for the joint operation of fuel and electricity systems, considering their individual reliability of operation.

The formation of the generalized distribution series requires a technological analysis of the complex object at issue. Naturally, the main link here is electricity system.

Table 4. Load distribution series

No	P_i^{Gd}, MW	p_i^{Gd}
1	0	$0/382955\cdot10^{-7}$
2	100	$0/194855\cdot10^{-5}$
3	200	$0/445049\cdot10^{-4}$
4	300	$0.593439\cdot10^{-3}$
5	400	$0.663965\cdot10^{-2}$
6	500	$0.298266\cdot10^{-1}$
7	600	0.11212877
8	700	0.2916282
9	800	0.3877872
10	900	0.1713499

Note: The normalizing condition is met: $\Sigma p_i = 1.0$.

Table 5. Load supply distribution series

No	P_i^{Gd}, MW	p_i^{Gd}
1	0	0.0918451
2	100	0.105
3	200	0.1099997
4	300	0.1149946
5	400	0.1199232
6	500	0.1243209
7	600	0.1255264
8	700	0.1238744
9	800	0.0845157

Note: The normalizing condition is met: $\Sigma p_i = 1.0$.

Therefore, when composing (multiplying) the distribution series for the outputs of fuel and electric power systems, the generalized output values are taken from the relation $P^{Gd} = \min(P^{Gd}, P^L)$, i.e. the minimum values are selected according to the scheme in Fig. 1.

The results of this analysis are used to form the final generalized series presented in Table 4.

The multiplication of the generalized distribution series for the outputs of joint operation of fuel and electricity systems (Tab. 4) with the load distribution series (Tab. 3) provides the resultant distribution series for this load supply (Tab. 5). This series allows obtaining exact ("standard") reliability indices. The values of the output used to supply the load are determined according to the technological features of a system from the $P^R = \min(P^{Gd}, P^L)$ relation. The probabilities of each of the load supply random states show the extent to which this load is provided by the system, Fig. 1.

According to Table 5, the variable load is supplied with a probability of 0.9081549 equal to the sum of probabilities of supplying all the loads. Consequently, a denial in supply will occur at probability

$$P_1^R = 0.0918451 = 1.0 - 0.9081549 \qquad (2)$$

Below is the calculation using the fuel supply coefficient p^F of each generator in the system and the operable state probability p^G with the values assumed in the previous calculation ($p^G = 0.85$; $p^F = 0.9$). We assume that given the fuel supply to generators, their operable state probability has the value

$$p^{GF} = p^G \cdot p^F = 0.85 \cdot 0.9 = 0.765$$

Table 6. Available generating capacity, distribution series

No	P_i^{GF}, MW	p_i^{GF}
1	0	$0.21\cdot10^{-5}$
2	100	$0.612\cdot10^{-4}$
3	200	$0.82319\cdot10^{-3}$
4	300	$0.633294\cdot10^{-2}$
5	400	$0.309238\cdot10^{-1}$
6	500	0.10067804
7	600	0.21849862
8	700	0.30483716
9	800	0.2480856
10	900	0.0897331

Note: The normalizing condition is met: $\Sigma p_i = 1.0$.

To calculate the distribution series for random values of the available generating capacity, we used the Bernoulli distribution (1). Table 6 presents the generalized series.

The multiplication of the series presented in Table 6 by the load series (Tab. 3) provides the resultant load supply distribution series (Table 7).

As seen from Table 7, the load is supplied with a probability of 0.9999979 equal to the sum of probabilities of supplying all the non-zero loads. Therefore, a denial in supply will occur at probability

$$P_1^R = 0.0000021 = 1.0 - 0.9999979 \quad (3)$$

Comparing the results based on Table 5 (standard distribution series, expression (2)) and Table 7 (distribution series based on fuel supply coefficient, expression (3)), we can conclude that there is an essential error, when the technique presented in Table 6 is used. Therefore, this technique can hardly be recommended, despite the simplification in calculations.

Even less exact results will be obtained, if, the means of the outputs of the indicated electric system components are used instead of the distribution series for the states of fuel system, electric power system and load. Thus, the means for the systems outputs calculated from the data in Tables 1, 2, and 3 equal

$$M[P^F] = 852.32 \text{ MW}; M[P^G] = 765.055 \text{ MW};$$
$$M[P^L] = 477 \text{ MW}.$$

The presented means allow us to conclude that the load will be supplied absolutely reliably at a probability of 1.0. However, this is not true. Even for our test case, the obtained standard deviation values provide a variance of random values such that even at their minimal values, the load will be supplied unreliably.

Based on the conducted study, we can conclude that, to calculate the reliability of EPS load supply, the calculations should rely on the technological features of the addressed systems, the block diagram of their connections, and avoid (for the calculation effort reduction) various ways to unreasonably simplify the initial scheme, its parameters, and calculation techniques.

IV. System approach

In the system approach, the calculation of the adequacy of electricity system nodes takes into account the fuel system reliability calculated for the entire fuel system, i.e. firstly, we estimate the reliability of a fuel system (the probabilities of shortage-free fuel supply to consumers are calculated, which implies estimating the reliability of fuel delivery to power plants operating on a given fuel).

When analyzing the reliability of the electricity supply to consumers in electric power system, the fuel system reliability can be taken into account by two methods.

Method 1. Correction of the generating equipment failure rate [15, 16].

The reliability indices calculated for fuel supply to consumers by node p_i^F are taken into account before calculating the generating capacity distribution series. First, we recalculate the failure rates of the generating equipment q_i^G for power plants of the given node i that operate on a given fuel.To this end, we calculate the probabilities of failure-free operation of the equipment of power plants operating on a given fuel, $p_i^G = 1 - q_i^G$. These probabilities are then multiplied by the corresponding fuel system nodal reliability indices p_i^F, i.e. $p_i' = p_i^G \cdot p_i^F$. Further, the corrected equipment failure rates for the power plants $q'_i = 1 - p_i'$ are calculated, and, based on them, the distribution series of generating capacity, or of operable state of units at power plants are calculated.

Method 2. Correction of the generating capacity distribution series.

The reliability indices calculated for the fuel supply to consumers by node i (probabilities of shortage-free fuel supply to consumers, p_i^F) are taken into account after calculating the distribution series of generating capacity or operable state of the units at power plants, by multiplying the calculated series by the corresponding series $(1 - p_i^F p_i^F)$.

Thus, by using these two methods, we obtain the input data for a mathematical model to estimate the EPS adequacy, given the reliability of fuel supply to these power plants.

In the system approach, the methods were compared to consider the fuel system reliability for a conventional power system: the system contains 5 units, (n = 5), each with a capacity of 800 MW and with the same failure rate = 0.03. The probability of the fuel system shortage-free operation equals $p^F = 0.9$.

According to Method 1 (correction of the generating equipment failure rate), we recalculate the power plant

Table 7. Load supply distribution series, considering table 6

No	P_i^R, MW	p_i^R
1	0	$0.21 \cdot 10^{-5}$
2	100	0.10505
3	200	0.110636
4	300	0.119138
5	400	0.136139
6	500	0.163017
7	600	0.176407
8	700	0.13891
9	800	0.05066673

Note: The normalizing condition is met: $\Sigma p_i = 1.0$.

Table 8. Distribution series for generating equipment operable state, considering fuel system operation, method 1.

No	Number of units in operation	Capacity P^1, MW	Probability, p_i^1
1	0	0	$0.3303837 \cdot 10^{-4}$
2	1	800	$0.\ 113553 \cdot 10^{-2}$
3	2	1600	$0,\ 156113 \cdot 10^{-1}$
4	3	2400	0.10731247
5	4	3200	0.36883379
6	5	4000	0.50707386

Note: The normalizing condition is met: $\Sigma p_i = 1.0$.

Table 9. Distribution series of the generating equipment operable state, disregarding fuel system operation.

No	Number of units in operation	Capacity P^1, MW	Probability, p_i^1
1	0	0	$0.243{\cdot}10^{-7}$
2	1	800	$0.39285{\cdot}10^{-5}$
3	2	1600	$0.254043{\cdot}10^{-3}$
4	3	2400	$0.8214057{\cdot}10^{-2}$
5	4	3200	0.1327939215
6	5	4000	0.8587340257

Note: The normalizing condition is met: $\Sigma p_i = 1.0$.

Table 10. Distribution series for the generating equipment operable state, considering fuel system operation, method 2.

No	Number of units in operation	Capacity P^2, MW	Probability, p_i^2
1	0	0	0,1
2	1	800	$0{,}353565{\cdot}10^{-5}$
3	2	1600	$0{,}228639{\cdot}10^{-3}$
4	3	2400	$0{,}7392651{\cdot}10^{-2}$
5	4	3200	0,119514529
6	5	4000	0,772860623

Note: The normalizing condition is met: $\Sigma p_i = 1.0$.

generating equipment failure rate, given the fuel system reliability. For this purpose, we calculate the initial and the corrected probabilities for the failure-free operation

$$p^G = 1 - q^G\ 1 - 0.03;$$
$$p' = p^G \cdot p^F = 0.97{\cdot}0.9 = 0.873$$

The corrected equipment failure rate will equal

$$q' = 1 - p' = 1 - 0.873 = 0.127$$

Let us calculate a new distribution series of the power plant operable state with the corrected equipment failure rate by the Bernoulli distribution (1). Table 8 presents the obtained distribution series for the generating equipment operable state, considering the probability of the fuel system shortage-free operation.

Based on this distribution series, we calculated the mean and the standard deviation for the actual output: $M[P^1] = 3492$ MW, and $\sigma[P^1] =$ MW, respectively.

According to Method 2 (correction of the generating capacity distribution series), we calculate the distribution series of the power plant operable state, based on the scheme of independent trials with the Bernoulli distribution (1).

Then, $n = 5$, $q = 0.03$, $p = 1 - q = 0.97$, $m = 0, 1, 2, \ldots, 5$. Table 9 presents the calculated distribution series for the generating equipment operable state.

Based on the distribution series, we calculated the mean and the standard deviation of the actual output: $M[P^2] = 3492$ MW and $\sigma[P^2] = 1199.46$ MW, respectively.

A comparison of the calculation results for the two methods of considering the fuel system reliability to estimate the electricity system adequacy (Tables 8 and 10) indicates that the first method (that takes into account the system specificity more precisely) demonstrates the real (although smaller) reliability, than the second, simplified method. The means of the outcomes are equal; the standard deviations are less in the first case, which indicates to a greater data homogeneity. We can conclude that the first method, considering the process technology, is more preferable.

V. Estimation approach

To estimate the interval of the power system nodal adequacy indices, namely, the lower and upper boundaries of the probability for shortage-free power supply to consumers, we, first, analyze the fuel system reliability. Thus, we calculate the reliability indices for fuel supply to consumers at all nodes , namely, the probability of shortage-free fuel supply to consumers p_i^F, $i = \overline{1, I}$, where I is the number of estimated consumer-nodes in the system. Similarly, we can calculate the EPS nodal reliability indices, i.e., the probabilities of the shortage-free power supply to consumers at an absolute reliability of fuel system (or disregarding the unreliable fuel system operation) – p_i^G. Then, the probability of power supply to consumers,

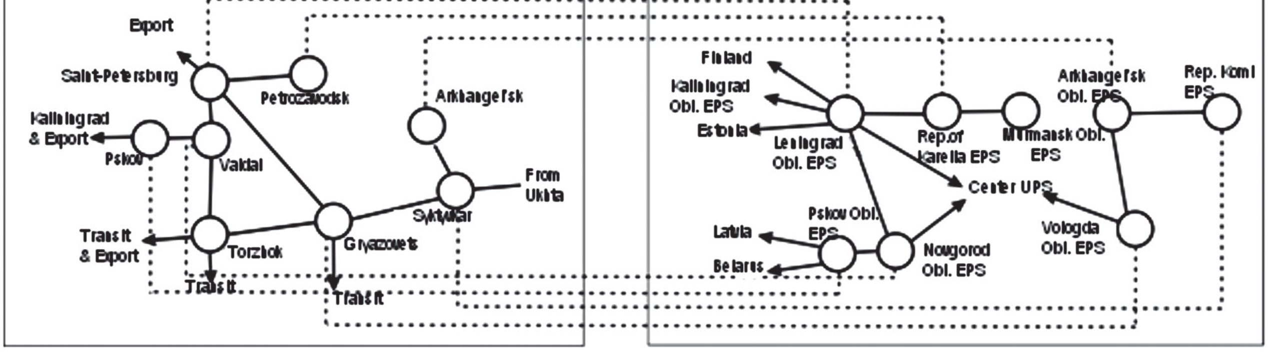

Fig. 2. Design diagrams for the NWFD gas system (a) and electric power system (b) with functional connections.

Table 11. Reliability indices of gas system in NWFD.

No	Node	Probability of shortage-free gas supply to consumers
1	Petrozavodsk	0.935208
2	Syktyvkar	0.997083
3	Arkhangelsk	0.997083
4	Gryazovets	0.994958
5	Saint-Petersburg	0.969208
6	Valdai	0.994958
7	Pskov	0.977292
8	Torzhok	0.994958

Note: The normalizing condition is met: $\Sigma p_i = 1.0$.

Table 12. Nwfd eps adequacy indices.

No	Node	Probability for shortage-free operation power consumers p_i^{EPS}	
		Disregarding Gas system reliability ($p_i^{GSS}=1$)	Considering gas system reliability (system approach)
1	Republic of Karelia EPS	0.992859	0.987581
2	Komi Republic EPS	0.998984	0.998982
3	Arkhangelsk Region EPS	0.999944	0.999944
4	Vologda Region EPS	0.999999	0.999999
5	Leningrad Region EPS	0.999944	0.999944
6	Novgorod Region EPS	0.999944	0.999944
7	Pskov Region EPS	0.998555	0.997259
8	Murmansk Region EPS	0.997770	0.997763

given reliability of fuel system p_i^{GF}, is calculated as $p_i^{GF} = p_i^G \cdot p_i^F = P_i'$ This value can be considered as the lower boundary P_i' of the nodal reliability index of the power supply to consumers p_i^{GF}. Indeed, the EPS nodal reliability index, given the fuel system operation, will be above the lower boundary due to the manifestation of the system mutual-aid effect in the EPS. The upper boundary of the nodal index will be at $p_i^F = 1$, i.e., we believe that the fuel system is absolutely reliable, or its reliability is not considered in the analysis of the EPS reliability, $p_i^{GF} = 1\, p_i^F = P_i'$. Obviously, the probability of power supply to consumers, given the fuel system reliability, will be within a range from the lower boundary P_i' to the upper boundary P_i'', i.e. $P_i' \le p_i^{GF} \le P_i''$.

The interval estimation of the EPS nodal adequacy indices was tested for the energy system of the Northwestern Federal District (NWFD) [15, 17]. The fuel system is represented by a gas transmission system. The NWFD power system was selected because the share of the NWFD power system generating capacity using gas as a primary energy resource accounts for about 70% of the total generating capacity [23].

Fig. 2 presents the design diagrams of the NWFD gas and electric power systems. The dashed line marks the functional connections of the given systems.

To estimate the reliability of gas and electric power systems, we developed and used the mathematical models [15, 18, 19]. Based on the reliability estimation for the NWFD gas system, we obtained the reliability indices of gas supply to consumers by node. Table 11 presents the probabilities of meeting the consumer demand for gas or shortage-free gas supply [16].

We also estimated the NWFD power system reliability, both with and without consideration of the reliability of gas supply to power plants, and calculated the probabilities of shortage-free power supply to consumers (p_i^{EPS}) by node

Table 13. NWFD eps adequacy indices

No	Nodes in systems			Probabilities of shortage-free power supply to consumers		
	Gas system	p_i^{GSS} (from Table 11)	EPS	disregarding gas system reliability ($p_i^{GSS}=1$), $P_i'' = p_i^{EPS}$ (upper boundary)	considering gas system reliability (nodal approach) $P_i' = p_i^{GSS} \bullet p_i^{EPS}$ (lower boundary)	considering gas system reliability (system approach)
1	Petrozavodsk	0.935208	Republic of Karelia EPS	0.992859	0.92852968	0.987581
2	Syktyvkar	0.997083	Komi Republic EPS	0.998984	0.996069964	0.998982
3	Arkhangelsk	0.997083	Arkhangelsk Oblast EPS	0.999944	0.997027163	0.999944
4	Gryazovets	0.994958	Vologda Oblast EPS	0.999999	0.994957005	0.999999
5	Saint-Petersburg	0.969208	Leningrad Oblast EPS	0.999944	0.969153724	0.999944
6	Valdai	0.994958	Novgorod Oblast EPS	0.999944	0.994902282	0.999944
7	Pskov	0.977292	Pskov Oblast EPS	0.998555	0.975879813	0.997259
8	Torzhok	0.994958	Murmansk Oblast EPS[1]	0.997770	0.997770	0.997763

[1] No connection to gas system

[16]. Table 12 presents the results.

To calculate the lower boundary of the nodal reliability indices for power supply to NWFD consumers, we superimposed the fuel system nodes on electricity system nodes. Table 13 presents the results. Thus, for example, the lower boundary for the Republic of Karelia EPS node (which corresponds to the Petrozavodsk node in the fuel system scheme) was obtained as follows:

$$P_i' = p_i^{GSS} \cdot p_i^{EPS} = 0.935208 \cdot 0.992759 = 0.92852968$$

An analysis of the calculation results confirms the theoretical assumption that the probability of power supply to consumers (considering the gas system reliability), calculated as $P_i' = p_i^{GSS} \cdot p_i^{EPS}$, is the lower boundary of the nodal reliability index for power supply to consumers (the next-to-last column in Table 13).

The nodal EPS reliability indices (considering the gas system operation) calculated according to the system approach (the last column in Table 13), appeared above the lower boundary due to the mutual-aid system effect of the power system operation.

The nodal and system approaches calculate the EPS reliability based on the point or discrete reliability index obtained as one certain number, which can lead to errors when making a decision. The estimation approach provides an interval estimation of the index, which is more objective and reduces calculation errors to minimum.

VI. Conclusions

1. We have proposed several methodological approaches (nodal, system, and estimation) to estimate the adequacy of an energy system, considering the reliability of fuel systems, i.e. reliable supply of a given fuel to power plants.

2. All the approaches were tested in case studies. The nodal and the system approaches were tested using a conventional electric power system. The estimation approach was tested using the design diagrams of gas and electric power systems of the Northwestern Federal District.

3. The reliability of energy system load supply should be calculated with respect to the technological features of the systems at issue and the block diagram of their connections.

References

[1] Energy strategy of Russia until 2030. Decree № 1715 of RF Government, 2009. (In Russian)

[2] V. Bushuev, V. Kalamanov "World energy–2050." (White paper). Energia, Moscow, 2011, 360 p. (In Russian)

[3] World energy outlook. International Energy Agency, 2015.

[4] S. Pikin, A. Shkolnikov "Emergency in Perm: impact on the market," Gosgortehnadzor of RF. http: www. gosnadzor.ru [Online]. Available: 26 March 2017. (In Russian)

[5] A. Seungwon, Qing, L. and Gedra, T. W. "Natural gas and electricity optimal power flow," Transmission and Distribution Conference and Exposition, 2003 IEEE PES, 7-12 Sept. 2003, Vol. 1, pp. 138-143.

[6] C. Liu, M. Shahidehpour, and J. Wang, "Coordinated scheduling of electricity and natural gas infrastructures with a transient model for natural gas flow," *Chaos an Interdisciplinary Journal of Nonlinear Science*, Vol. 21, pp. 025102, 2011.

[7] M. Chaudry, N. Jenkins, and G. Strbac, "Multi-time period combined gas and electricity network optimization," *Electric Power Systems Research*, 78, pp. 1265-1279, 2008.

[8] S. Clegg, P. Mancarella, "Integrated electrical and gas network modelling for assessment of different power-and-heat options," *Power Systems Computation Conference* (PSCC), 2014, 18-22, pp. 1-7, Aug. 2014.

[9] M. Arnold, R.R. Negenborn, G. Andersson, B. De Schutter, "Distributed control applied to combined electricity and natural gas infrastructures," Infrastructure Systems and Services: Building Networks for a Brighter Future (INFRA), 2008 First International Conference, pp. 1-6, 10-12 Nov, 2008.

[10] Bining Zhao, J. Antonio Conejo, Ramteen Sioshansi "Using electrical energy storage to mitigate natural gas-supply shortages," IEEE Trans. Power Syst., vol. 33, № 6, pp. 7076-7086, Nov. 2018.

[11] Yao Zhang. Yuan Hu, Jin Ma and Zhaohong Bie "A mixed-integer linear programming approach to security-constrained co=optimization expansion planning of natural gas and electricity transmission systems," *IEEE Trans. Power Syst.*, vol. 33, № 6, pp. 6369-6378, Nov. 2018.

[12] Junjie Zhong, Yong Li, Yijia Cao, Denis Sidorov, Daniil Panasetsky "A Uniform Fault Identification and Positioning Method of Integrated Energy System," Energy Systems Research, vol. 1, № 3, pp. 1-9, 2018.

[13] N. Voropai, V.A. Stennikov, S.M. Senderov, E. Barakhtenko, O. Voitov, A. Ustinov "Modeling of Integrated Energy Supply Systems: Main Principles, Model, and Applications," *Journal of Energy Engineering*. Vol. 143, Issue 5 (October 2017). DOI: 10.1061/(ASCE)EY.1943-7897.0000443

[14] C. Correa-Posada, C. Sanchez-Martin "Security-constrained optimal power and natural-gas flow," IEEE Transactions on Power Systems, vol. 29, № 4, July 2014, DOI: 10.1109/TPWRS.2014.2299714.

[15] G.F. Kovalev, D.S. Krupenev, and T.V. Dzyubina "Comprehensive approach to estimation of power system balance reliability, considering reliable gas supply to power plants," *Vestnik IrGTU* (Irkutsk State Technical University Bulletin), №. 9, pp. 140-145,

Sep. 2015. (in Russian)

[16] G.F. Kovalev, D.S. Krupenev and T.V. Dzyubina “Relation between the gas supply to power plants and reliable functioning of a power system,” *Vestnik IrGTU* (Irkutsk State Technical University Bulletin), №. 10, pp. 195-200, Nov. 2015. (in Russian)

[17] Dmitry Krupenev, Gennady Kovalev, Tatyana Dzyubina. “Assessment of Electric Power System Adequacy Considering Reliability of Gas Supply to Power Plants,” *Energy Systems Research*, vol. 1, № 1, pp. 21-28, 2018.

[18] N. Ilkevich, T. Dzyubina, Z. Kalinina “Multilevel modeling of gas supply system expansion,” Novosibirsk: Nauka, 2014, 217 p. (in Russian)

[19] G.F. Kovalev, L.M. Lebedeva, “Reliability of electric power systems,” Ed. by N.I. Voropai. Novosibirsk: Nauka, 2015, 224 p.

[20] Reliability of energy systems: collection of recommended terms. Moscow: IATs “Energia” (ENERGY Information-Analytical Center), 2007, 192 p. (in Russian)

[21] K. Uhlen, D. Cirio, L. Haarla, “IEA ENARD: International collaboration on development in transmission system R&D,” CIGRE 43th Session, pub. C4305, Paris, 2010.

[22] Venttsel' E.S. “Probability Theory,” Moscow: Vysshaya Shkola (Higher School) Publishers, 2002, 565 p. (P. 4.1, pp. 58-60) (in Russian)

[23] The scheme and program for the development of Russia’s Unified energy system for 2014–2020. Order of the Ministry of Energy of Russia of August 1, № 495, 2014. (In Russia)

Gennady Kovalev graduated from Kalinin Polytechnic Institute. He is leading researcher of ESI SB RAS, Doctor of Engineering, Professor. His scientific interests include reliability of electric power systems (EPS), optimization of EPS reliability in the stages of design and expansion planning, diagnostics of power equipment.

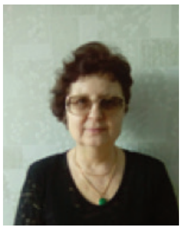

Tatyana Dzyubina graduated from Irkutsk Polytechnic Institute. She has worked at ESI SB RAS, since 1976. She is a senior researcher, PhD in engineering. Her scientific interests are connected with mathematical modeling of reliability of large energy systems, the issues of calculation of natural gas prices and tariffs.

East Asia as an object for Russia-Mongolia energy cooperation

Sergei P. Popov*, Darya V. Maksakova

Melentiev Energy Systems Institute of Siberian Branch of Russian Academy of Sciences, Irkutsk, Russia

***Abstract* — The paper analyses the role of the Asia Pacific Region and East Asia, in particular, for both Russia and Mongolia as energy exporters. A quantitative assessment of coal, oil and natural gas markets demand of East Asia countries is made. The assessment relies on our outlook, and the outlooks of Russian and foreign organizations. The prospective directions of energy cooperation between Russia and Mongolia, which allow harnessing the resource, geographical and economic potential of the two countries and expanding energy cooperation with the other countries in East Asia, are proposed.**

***Index Terms* — East Asia, energy cooperation, Mongolia, resources, Russia.**

I. Introduction

Primary energy demand projection up to the middle of this century is made for all the countries in East Asia. Regional coal, oil and natural gas market volumes are estimated. The main directions of advancing cooperation between Russia and Mongolia, as primary energy exporters within the region, toward East Asia countries are highlighted.

A. Asia Pacific Region, Northeast Asia and East Asia: economic and geographical definition

The Asia Pacific Region (APR) is not a clearly defined economic and geographic object. Initially, it included the USA, Canada and the countries bordering the west section of the Pacific Ocean, from Japan to Singapore to Australia and New Zealand. The geography of cooperation expanded when Latin American countries joined. At the end of the XX century, twenty-one countries around the Pacific Ocean established the Asia-Pacific Economic Cooperation (APEC), the regional international organization with the main objective to promote economic integration on the grounds of free trade.

The Northeast Asia region (NEA) is generally assumed in Russian and foreign economic literature as part of Eurasia that includes six countries: Mongolia, the People’s Republic of China (PRC) (including Special Administrative Regions Hong Kong and Macao as well as Taiwan Province), the Democratic People's Republic of Korea (DPRK), the Republic of Korea (RoK), Japan and the Russian Federation (Russia). Sometimes Taiwan Province is called “country” outside of the APEC context to underline its high level of political and economic independence from the central government of PRC. To avoid political controversy within the cooperation process in the APEC region all above mentioned economic and geographic objects are called “economies“, since Taiwan and Hong Kong by themselves are full APEC members. Here the term “East Asia” means all Northeast Asia countries except Russia.

East Asia (EA) countries, other than Mongolia, provide gas, electricity, and coal markets for Russian and Mongolian exports. In this respect,the energy markets are “objects” of the multilateral cooperation within the EA region. Russia-Mongolia energy cooperation towards such energy markets could be coordinated or independent. On the other hand, Mongolia, being one of EA countries, could be considered as an object for bilateral Russia - Mongolia energy cooperation by itself. Here the first approach is considered to be major driver for Russia – Mongolia collaboration as energy exporters, while energy complementarity issues arise as drivers for bilateral energy cooperation.

II. The current status of Russia and Mongolia energy cooperation with the East Asia countries

Energy sector meets the requirement for energy services from a country’s economy and population. Additionally, it plays an important role in the GDP growth, government

* Corresponding author.
E-mail: popovsp@isem.irk.ru

http://dx.doi.org/10.25729/esr.2018.04.0005
Available online February 28, 2019.

Table 1. Resource potential of Mongolia, Siberia and the Russian Far East.

Indicator	Unit	Russia		Mongolia
		Siberia	Far East	
Coal reserves	Gt	153.8	20.2	21.5
Conventional oil reserves	– “ –	3.5	1.0	0.206
Natural gas reserves	trillion m^3	6.1	3.0	-
Hydropower technical potential	TW·h	757	684	9
Wind energy technical potential	GW	900	1200	1100
Solar energy technical potential	– “ –	1100	1400	1500

Source: [1].

Table 2. Energy export from Mongolia in 2017.

Importer	Coal		Crude oil		Electricity		Total energy export, billion USD
	million doll.	Mt	million doll.	Mt	million doll.	GW·h	
APR	**2 236**	**34.1**	**362**	**1.0**	**0.3**	**23**	**2.6**
Russia	-	-	-	-	0.3	23	..
EA	**2 236**	**34.1**	**362**	**1.0**	-	-	**2.6**
China	2 212	34.0	362	1.0	-	-	2.6
Taiwan	6	..	-	-	-	-	..
Japan	18	0.1	-	-	-	-	..
World	**2 236**	**34.1**	**362**	**1.0**	**0,3**	**23**	**2.6**

Source: calculated based on [2].

budget revenues, social development and the interaction with other countries when energy resources trading is taking place. In other words, energy sector ensures economic growth, being one of the major drivers for socioeconomic and political development. The role of energy sector in Mongolia and Russia is particularly important: the share of resource export in Mongolian GDP in 2017 is 23 %; the same indicator for Russia is 13 %. These figures are calculated on the basis of foreign trade statistics and the World Bank GDP statistics.

Huge resource potential (Table 1) and the features of geographical location of the two countries predetermine their role in international trade, especially in the APR and East Asia, as the suppliers of energy resources and the providers of related energy services.

Energy export accounts for 42 % of Mongolian total export; 86 % of it is coal export (Table 2). China is a monopolistic importer of Mongolian oil and almost a monopolistic importer of Mongolian coal. Import prices for Mongolian coal are the lowest for China. Besides, China provides transit services for Mongolian coal [3].

There are several power transmission lines between Russia and Mongolia, including Selenduma-Darhan transmission line to the Central Energy System of Mongolia [4], while 76 % of electricity comes from China (Table 3). In total, Mongolia imports up to 20 % of electricity consumed [5].

Petroleum products import makes up the biggest part (85%) of energy imports, and almost all of the petroleum products are imported from Russia (96%). The first Mongolian refinery in Altanshiree (Dornogovi Province in south-eastern Mongolia) with crude oil throughput of 1.5 million ton per year is planned to be put in operation in 2022 [6]. After this important turning point, Mongolia can substantially reduce petroleum product import from Russia by abandoning crude oil export to China.

East Asia is also an important region for Russia, as it is an export market for Russian coal, oil, petroleum products and LNG (Table 4). In 2017, being part of the APR, East Asia countries, including Mongolia, imported 92 % of Russian coal exported to the APR, which in turn represented 44 % of total coal export from Russia. That year the share of East Asia countries in Russian oil export to the APR was 97 %, which accounted for 25 % of Russian total crude oil export. The similar indicators for Russia's export of petroleum products were 46 % and 15 %, respectively.

While 100 % of pipeline gas goes in western direction – to Europe, Transcaucasia countries, and Turkey, almost 99 % of Russian LNG is exported to the EA region. After the commissioning of the Power of Siberia gas trunk line later this year, the East Asia region, represented by China, will become the importer of Russian pipeline gas too. In addition, new LNG projects on the Russian Arctic will expand the already established LNG export to EA, and provide exports to the USA and Europe.

Nevertheless, the cooperation between Russia and East Asia countries should not be limited by the role of Russia as energy resources supplier. The prospective directions for multilateral energy cooperation enhancement are the diversification of supply routes, energy transition issues, energy services export and energy-related machinery production.

Table 3. Energy import to Mongolia in 2017.

Exporter	Petroleum products		Electricity		LNG		Total energy import, million USD
	million USD	kt	million USD	GW·h	million USD	kt	
APR	**835**	**1509**	**137**	**1574**	**14**	**29**	**986**
Russia	777	1455	27	380	11	28	815
EA	**51**	**52**	**110**	**1194**	**2**	**1**	**164**
China	29	31	110	1194	-	-	140
RoK	21	21	-	-	2	1	23
Japan	1	-	-	-	-	-	1
World	**843**	**1514**	**137**	**1574**	**14**	**29**	**994**

Source: calculated from [2].

Table 4. Energy export from Russia in 2017.

Energy carrier	Unit	World	APR	EA
Coal	Mt	181.4	80.6	74.0
Crude oil	Mt	252.6	64.2	62.1
Petroleum products	Mt	148.4	31.3	14.4
Natural gas (pipeline)	billion m³	212.9	-	-
Natural gas (LNG)	Mt	11.0	10.9	10.9

Source: calculated based on [2, 7].

III. Quantitative assessment of energy markets of the East Asia countries

In 2017, global primary energy consumption accounted for 19.3 billion tce, with a 2.2 % year on year growth rate. The East Asia countries, holding 22 % of the World's population, provided 25 % of the World's GDP in purchasing parity power (PPP) terms, and consumed 30 % of primary energy. From the perspective of energy exporting countries, the most important characteristic is their niche on the energy markets. In 2017, EA countries imported 42 % of coal, 32 % of oil and 28 % of natural gas sold at the international markets. The dependence of Japan, RoK and Taiwan on energy imports is absolute in the case of coal, crude oil, and uranium, and almost absolute in the case of natural gas. Such a huge market is attractive to the countries with large and excessive energy resources. EA energy market includes China as the first World's economy in PPP terms, which is characterized by sharply growing shortage of domestic oil, gas, uranium and even coal. Moreover, even if the switch from fossil energy to renewable energy sources in the energy mix is fast enough, there is still a room for import of "clean energy" and energy services. This import could be based on solar and wind energy in the southern regions of Mongolia, the hydropower resources of Siberia and the Far East, and wind energy along the Arctic and Pacific coasts of Russia, to EA countries.

China is the undisputed leader of primary energy consumption in the EA region and in the World, accounting for 23.2 % of the World's energy consumption in 2017. Japan is the second in the EA region after China with 3.1 %. Along with the DPRK,Japan has demonstrated a decline in total energy consumption since 2000. The RoK is the next largest consumer of primary energy in East Asia, representing 2.6 % of the World's energy consumption in 2017. The share of the DPRK and Mongolia is negligible, as their total primary energy consumption accounts for approximately 0.12 % of the World's one.

The structure of primary energy consumption in EA countries differs significantly from the global one. The World's primary energy consumption in 2017 demonstrates the share of crude oil, coal and natural gas for more than 34 %, 28 %, and almost 23 %, correspondingly (Table 5). The share of fossil fuels in the East Asia region was 25 % for crude oil, 53 % for coal, and just 9 % for natural gas.

The positions for Russia and EA countries on energy markets are characterized by their complementarity. While East Asia is the World's largest regional energy importer, Russia is the World's largest single energy exporter (Fig. 1). In order to estimate future energy markets in the East

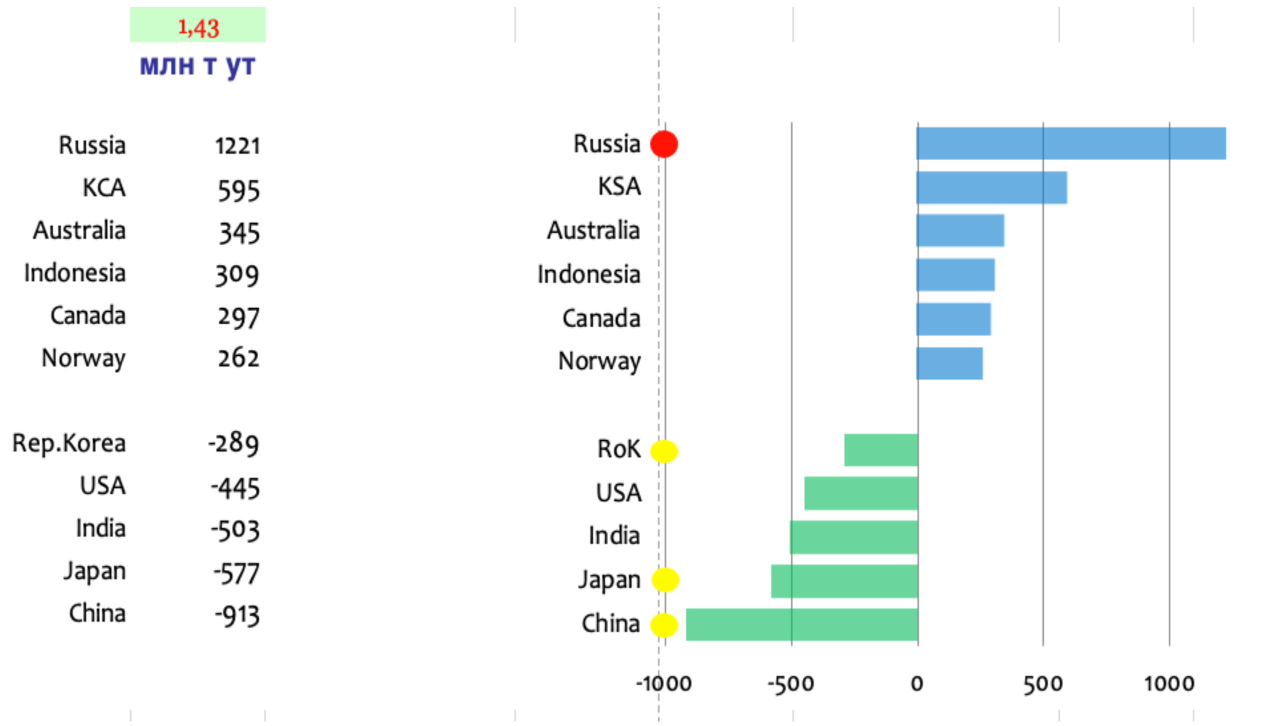

Fig. 1. World's largest energy exporters and importers in 2017, MTCE. Source: calculated based on [9].

Asia countries, the studies focused on energy consumption outlooks in these countries up to 2050 were carried out by the Melentiev Energy Systems Institute (MESI) SB RAS. The studies also took into account similar outlooks presented by a number of reputable international organizations, companies, and research centres that are accessible in the public domain. Within the expert community, the most recognized organizations are the International Institute for Applied Systems Analysis (IIASA), the International Energy Agency (IEA), and the Energy Information Administration of the US Department of Energy (EIA). In recent years, they were joined by the Institute of Energy Economics of Japan (IEEE), which focuses on the Asian region. Some large oil and gas companies, such as Shell and British Petroleum (BP), also have begun to provide qualitative outlook information on the open access basis as a supplement to the scenario description of their internal researches on long-term energy market outlooks. From the global studies, of special interest is the Global energy outlook developed jointly by the Energy Research Institute of the Russian Academy of Sciences (ERI RAS) and the Analytical Centre under the Government of the Russian Federation from 2012 to 2016. This particular outlook includes an in-depth analysis of the future Russian energy systems development.

A comparative analysis of five outlooks compiled by a number of well-known organizations, research centres and companies has been made. Two of them were published in 2018, the outlook by EIA was published in 2017, the others - in 2016. Table 6 demonstrates Total Primary Energy Supply (TPES) and the estimates of oil, coal and gas imports for East Asia countries corresponding to the baseline scenarios of the outlooks under consideration. Since the IEA's 2018 outlook was not available, the outlook for 2016 was analyzed. The ERI RAS outlook was not updated after 2016. None of the outlooks considered Mongolia and DPRK, thus they were not presented in Table 6. As the Table shows, the results for Japan, RoK and Taiwan are not consistent and logical.

The MESI SB RAS has been carrying out studies on the long-term energy demand and supply for all the countries of East Asia for a number of years. The major purpose of such studies, among other things, is to estimate the potential demand of East Asian energy market for energy resources from Russia [10]. The MESI methodology for long-term projections up to 2050 is based on the holistic approach to the energy system analysis – from technological to social and economic factors, from final energy consumption to primary energy production [11]. This approach starts from the assessments of final energy demand, based on elasticity of the specific useful energy consumption of aggregated economic sectors and end-use industries in terms of GDP (in constant prices). Then, as a result of the model-based optimization process, the structure for energy transformation sector is assessed. The assessment process incorporates the outcomes of institutional research at the

Table 5. Primary energy consumption structure in 2017, %.

Country, region	Crude oil	Coal	Natural gas	Nuclear energy	Hydropower	Other renewables
Russia	22	13	52	7	6	..
Asia-Pacific Region	29	48	12	2	6	3
East Asia	25	53	9	3	7	3
China	19	60	7	2	8	3
Hong Kong	71	20	9	-	-	..
Taiwan	43	34	17	4	1	1
Japan	41	26	22	1	4	5
RoK	44	29	14	11	..	1
North America	40	13	29	8	6	4
Central and South America	46	5	21	1	23	5
Europe and Eurasia	32	15	32	9	6	6
Near and Middle East	47	1	51	..	1	..
Africa	44	21	27	1	6	1
World, total	34	28	23	4	7	4

Source: calculated based on [8].

national level in order to provide the constraints within the models. Such constraints are supposed to reflect the "most probable" energy policy provisions for each East Asia country.

In 2018, energy consumption was estimated by the MESI SB RAS for all the six countries of East Asia, considering the so-called "reference" scenario, and the "gas" scenario made additionally for Mongolia. The base year assigned for the outlook was 2013, with sequential reference years 2025, 2035 and 2050. Then further analysis was made to provide energy market assessments.

Due to its scale and impact on energy markets development, China is the most interesting object, considering the prospects of the global and regional energy demand. The major drivers for China's energy policy, after the need for energy services, are the economics of coal supply and the impact of air pollution on social development. The coal supply economics relates to the depletion of highly profitable resources and rising cost of labour, combined with fierce competition at the metallurgical coal market due to the industrial stagnation – the decline of pig-iron production, or the processes that involve iron ore as an input. As the recent analysis made by the CRU consulting company indicates: "In China, we believe the authorities will continue to deliver a managed slowdown in economic activity. And that will lead to gradual slowing in the construction and auto sectors. Economic growth in China may slow to 6% in 2019.

Hot metal production will fall steadily in contrast with stable crude steel production, because of an increase in EAF-based production and greater scrap consumption in the BF-BOF steelmaking. Meanwhile, hot metal production

Table 6. Outlooks of total primary energy supply and import of coal, crude oil and natural gas for east asia countries.

Outlook	China	Taiwan	RoK	Japan
Total Primary Energy Supply, Mtce				
IEA (2016 | "current policies"), 2040.	6446	n.a.	n.a.	565
EIA (2017 | "reference"), 2050	6543	n.a.	652	659
ERI RAS (2016 | "basic"), 2040	5839	n.a.	n.a.	n.a.
IEEJ (2018 | "reference"), 2050	5533	150	410	524
BP (2018), 2040	6170	n.a.	n.a.	n.a.
Energy Import Estimations				
coal, Mt				
IEA (2016 | "new policies"), 2040	36	n.a.	n.a.	149
EIA (2017 | "reference"), 2040	112	n.a.	231	154
IEEJ (2018 | "reference"), 2050	23	55	125	137
crude oil, Mt				
IEA (2016 | "new policies"), 2040	571	n.a.	n.a.	101
EIA (2017 | "reference"), 2050	619	n.a.	154	151
IEEJ (2018 | "reference"), 2050	569	36	98	107
ERI RAS (2016 | " basic "), 2040	568	n.a.	104	98
natural gas, bcm				
IEA (2016 | "new policies"), 2040	268	n.a.	n.a.	95
EIA (2017 | "reference"), 2050	265	n.a.	85	116
IEEJ (2018 | "reference"), 2050	234	33	80	99
ERI RAS (2016 | " basic "), 2040	193	n.a.	47	94

Source: Calculated based on [12,13,14,15,16].

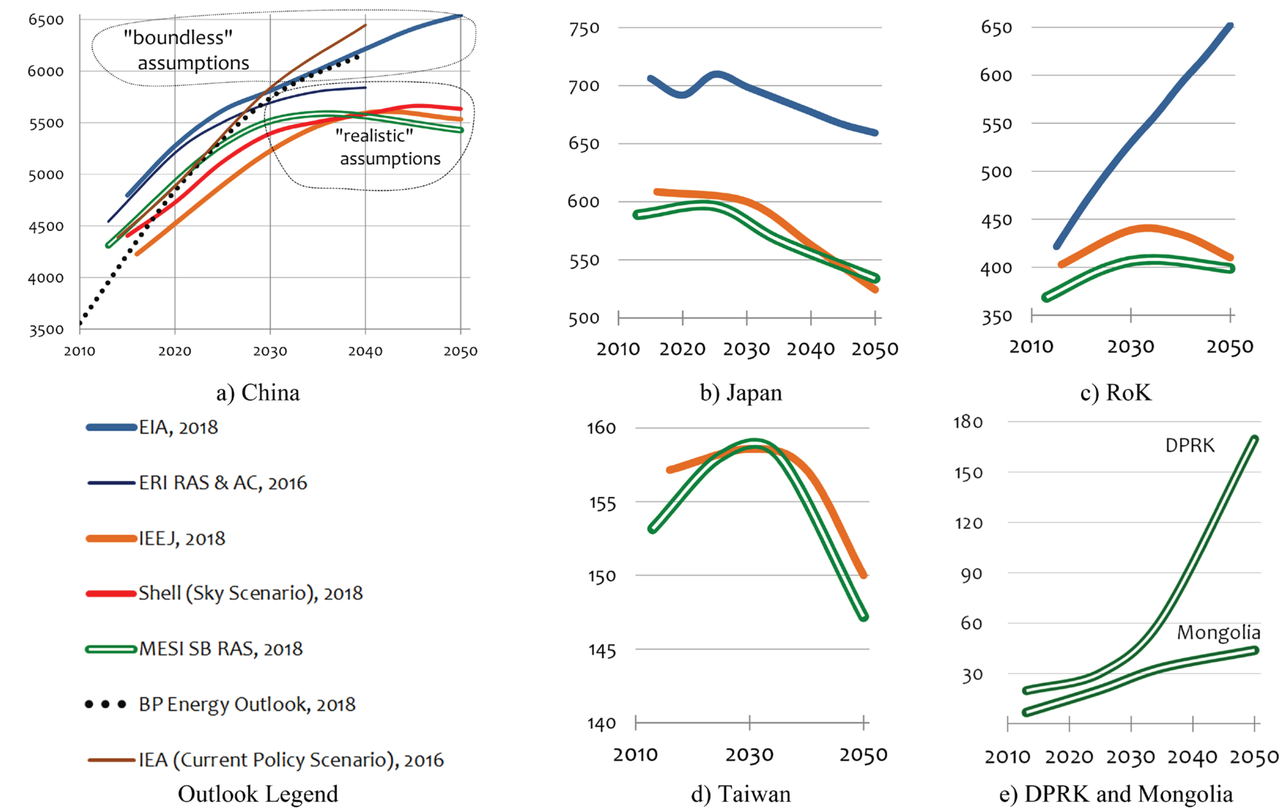

Fig. 2. Total Energy Supply Outlooks for comparison of East Asia economies, MTCE.

will rise elsewhere with rising crude steel production. As a result, the demand for key bulk steelmaking raw materials including iron ore, metallurgical coke and metallurgical coal is forecast to go down in China but pick up elsewhere.

Although China has eliminated some coke capacity over the past several years, domestic coke demand contraction will enable China to continue to be a key coke exporter globally. While Chinese coke demand is predicted to fall, the quality requirement will be higher, meaning that demand for high quality coal will be stable at the expense of demand reduction in weak coal. This will lead China to be a more critical metallurgical coal importer in the global trade market, as domestic coal quality will deteriorate over time." [17]

The impact of air pollution on energy choice in China is rather complex, while rooted in obvious reason that is poor management of air pollutions caused by burning coal for industrial purposes, electricity and heat generation within the industrialized agglomerations.

As shown in Fig. 2a for China, two groups of reference scenarios are distinguished, conventionally corresponding to the "boundless" and "realistic" assumptions on primary energy demand growth. The first group includes the EIA and BP outlooks published in the years 2017 and 2018, as well as the IEA "current policy scenario" (available since year 2016). The second group includes the IEEJ's basic scenario, the Shell's Sky scenario, and our reference scenario, all of them dated by the year 2018.

An intermediate option that lies between the described two outlook groups with a clear trend to stabilization of TPES, belongs to the last of known Joint research by the Energy Research Institute of the Russian Academy of Sciences and the Analytical Centre at the Government of the Russian Federation, published in 2016. It seems that the EIA's and BP's projections tend toward overestimation of future demand, despite the upcoming fundamental shift in the global economic development. Interestingly, such rearrangements within the globalization paradigm are currently actively pursued by tandem of the United States and the United Kingdom.

For Japan (Fig. 2b), despite the general decline of TPES, it is an inexplicable "drop" in the next 2-3 years, followed by a short-term growth and then a new steady decline, as the EIA's outlook suggests. In contrast, the IEEJ's outlook seems to be much more reasonable and logical. The most striking difference, in terms of the approaches to projections for East Asia industrialized countries by the researchers from the USA and Japan, is demonstrated by the RoK TPES projection in Fig. 2c. The EIA shows a simple case for the unbundled "growth over the roof", while IEEJ outlook indicates a coming peak after the 2030th, followed by a decline.

The IEEJ and MESI SB RAS projections for Taiwan TPES, which follow the trend established by Japan, RoK, and China, are presented in Fig. 2d.

This is the first time, the long-term projections for

Table 7. Crude oil balance for East Asia, Mt.

Balance	Year			
	2017*	2025	2035	2050
Demand, total	959	720-780	670-710	600-700
incl: China	589	430-460	410-420	360-400
Japan	162	150-160	120-130	95-110
RoK	162	100-110	90-100	80-95
Taiwan	43	40-45	40-45	35-45
DPRK	0,7	2-5	8-12	25-40
Mongolia	-	0-1	0-2	0-3
Production, total	197	155-190	140-190	115-140
incl: China	194	140-160	130-170	110-130
Import, total	770	570-620	530-600	490-570
incl: China	420	280-300	270-290	250-280
Japan	158	150-160	120-130	95-110
RoK	149	100-110	90-100	80-95
Taiwan	43	40-45	40-45	35-45
DPRK**	0,7	2-5	8-12	25-40
Mongolia**	-	0-1	0-2	0-3

Source: * – [9]; ** - [2].

TPES of DPRK and Mongolia (Fig. 2e) have been in the public domain. In actuality, they are the improved versions of the MESI SB RAS projections first made in 2015. The major improvements include much higher economic growth rate for the DPRK and the introduction of a natural gas supply option for both countries. For the DPRK, such an option assumes future tight economic cooperation on the Korean Peninsula. For Mongolia, the option for natural gas supply leads to the new "gas" scenario in addition to the compulsory "reference" coal-based scenario.

The main difference between the projections for energy system development in the DPRK and Mongolia is related to the size of economies and the population of the two countries. Mongolia is an agrarian economy with rapidly developing export-oriented mining sector and prospects for large-scale development of export-oriented, environmentally friendly renewable energy production. The DPRK is on the threshold of the domestic market's rapid growth and the country's reindustrialization. The assumption for the DPRK reindustrialization is based on positive assessment for the emerging cooperation with the RoK on their common path to Korea's reunification.

a. General assessment of the EA energy markets

The outlook assumptions are based on the established pricing mechanisms for crude oil and coal. While crude oil is imported to the region at prices determined by spot markets (including the whole set of derivative instruments), coal contracts are fixed-term, following crude oil prices. The pricing of natural gas in East Asia by 2050 will be based on gas-to-gas competition mechanism and determined by the exchange trade instruments.

China is expected to be the largest regional importer for all types of energy, particularly of natural gas. In 2050, China's share in total coal imports to the region can reach 60%, oil – 45-50%, and gas import – 60-65%. The energy transformation paradigm is actively pursuing the shift of the primary energy demand structure towards more gas and renewables instead of oil and coal, as well as the growing impact of the rising energy efficiency through the whole energy supply chain. It appears quite unusual to see such outlooks with sliding oil and coal demand.

It is worth reminding that for the MESI SB RAS energy outlook, the base year is 2013, which means that the holistic energy balance tables and actual trends for energy system development for the years 2014-2017 were missing from the analysis. However, energy development has proved to be very important for the last five years, as it is in line with the very start of the "new energy paradigm" and institutional changes at the international oil and gas markets. One of the lessons learned is that long-term outlook in a short run could have controversial implications, if the latest trends are missed. This is one, but important, explanation for some odd comparisons between factual data for the year 2017 (2016 in the case of coal balance) and assessments for the year 2025. The second explanation is statistical failures. Even for such respected statistical sources as BP's World Energy Statistics and Enerdata's Global Energy Statistical Yearbook, the difference for RoK oil demand in 2017 is more than 39 million tons, or 32 % [8, 9].

b. An assessment of the crude oil market for the East Asian countries

In 2017, East Asian countries imported 48 % of oil sold in the world crude oil market (Table 7). The likely decline in crude oil consumption is associated with the very core of the “energy transition” paradigm, which is characterized by the requirement to reduce consumption of so-called “carbon” primary energy, such as coal, crude oil, and even natural gas. In addition, oil demand will decline due to the switch from petroleum products to natural gas, electricity and hydrogen in transportation and construction.

c. An assessment of the coal market for the East Asia countries

The Asia-Pacific region is the world's largest coal market. This is explained by both the scale of demand, and the practical lack of own coal production in Japan, Taiwan and RoK. In the long term, the coal market will be highly competitive both for steam and metallurgical grades of coal. However, in ten years only Mongolia will maintain, or even improve its export capacity. It is supposed that coal export from DPRK will change to net import long before 2050 in order to feed emerging domestic power generation, (Table 8).

d. An assessment of the natural gas market for East Asia countries

The natural gas market in East Asia countries will be characterized as one of the fastest growing among other energy markets. China, Japan and RoK will be the major regional natural gas consumers. The Chinese segment of the regional market has the greatest potential for development in the next twenty to thirty years (Table 9). The Chinese gas market will have complex technological structure of gas production, import and national transportation system, complemented by sophisticated pricing instruments.

A new gas-related energy market is likely to emerge at the junction of “green energy” trade, power grid services and load management for Japan, RoK, Taiwan and China, including Hong Kong. This is a large-scale market of hydrogen produced on the basis of renewable energy. Economic estimations for new market can be made along with an analysis of real hydrogen infrastructure development at the national scale. Such an activity is currently underway in Japan, which is associated with the preparation of this country for the Tokyo Olympic Games in 2020.

The DPRK’s skyrocketing demand for natural gas will be observed after 2035 after the economic situation on the Korean peninsula improves in general, and its energy system gets mature. Supplemental gas pipeline from the Sakhalin Island will be instrumental for such development.

e. An assessment of electricity market for East Asia countries

The prospects for power interconnections development in the EA region were updated after the establishment of the Global Energy Interconnection Development Cooperation Organization (GEIDCO) in 2016. However, for more than twenty-five years a lot of research activities have been done to promote international power interconnections and even integration of the national electric power systems in

Table 8. Coal balance in East Asian countries, Mt.

Balance		Year			
		2016	2025	2035	2050
Demand, total		3816	3890-4150	3000-3300	2000-2150
incl:	China	3420	3550-3750	2700-2900	1700-1800
	Japan	187	140-160	110-125	90-100
	RoK	135	110-120	100-110	90-100
	DPRK	n.a.	25-30	30-50	60-80
	Taiwan	66	45-60	40-45	20-30
	Mongolia	8	20-25	35-40	35-40
Production, total		3093	3350-3670	2450-2780	1250-1600
incl:	China	3058	3300-3600	2400-2700	1200-1500
Import, total		666	520-650	540-630	585-685
incl:	China	289	220-300	280-330	350-400
	Japan	185	140-160	105-120	90-100
	RoK	126	110-125	95-105	85-100
	DPRK	(11)*	2-5	20-30	40-60
	Taiwan	66	45-60	40-45	20-25
	Mongolia	(24)*	(40-45)*	(50-80)*	(50-80)*

Note: * coal export.
Source: IEA data 2016 [18].

the NEA region. According to the recent estimations for interstate power pool in the NEA region, the total transfer capability of interstate transmission lines will reach tens of GW, and international electricity trade will be tens and hundreds of TWh [20], [21], [22], [23].

Bilateral electric power cooperation in East Asia has already been established between the continental countries (with the exception of RoK), while island's countries within the EA region are looking for the advantages it may provide. At present electric power from Russia is exported to China and Mongolia; and the latter is importing electric power from China. One of the greatest prospects for multilateral energy cooperation in East Asia is associated with the development of the so-called Gobitec, which is essentially a trilateral Russia-Mongolia-China power interconnection. The Gobitec project is expected to create a significant synergy of the use of Mongolian wind and solar resources, storage and peak-shaving capacities of the Siberian hydroelectric power plants, and thirst for clean energy in the Eastern and Northern Chinese provinces.

In addition, the idea to create a new electricity market for the unified Korean Peninsula has become more sensible and attractive. Such a market will require not only export of basic power load to the North of the Peninsula, but will also involve existing hydropower plants as system's storages, and will naturally integrate the national power systems in China, Russia, Mongolia, and Japan into a regional power pool.

However, the main obstacles in the East Asia region, outside the international power grid project economics, will be institutional issues, and energy security is one of the most important. The implications of the research study on power import possibilities to the Japanese electricity market [19] show few economic and institutional grounds for import from Russia to the northern Island Hokkaido.

IV. Cooperation between Russia and Mongolia

An analysis of the current state of the Mongolian energy system and the recent trends in the energy infrastructure development within the East Asia region made it possible to identify the following promising areas of energy cooperation between Mongolia and Russia, considering multilateral cooperation of these countries as net energy exporters:

1. Transit. Transit of Russian gas through Mongolia to China will not only reduce the costs by optimizing the supply logistics, but also provide conditions for Mongolia's switch to gas and the improvement of the country's fuel and energy balance by switching from coal to gas. The transit of Mongolian coal through Russia and its export through the ports of the Far East will allow diversification of markets and supply routes, which is important for Mongolia as a landlocked country. This approach seems rational given the long-term policy of the main importer of Mongolian coal, i.e. China, to reduce the share of coal in the total energy consumption. In this regard, an important cooperative effort for Russia and Mongolia will be the creation of international energy cooperation institutions in East Asia, to establish the legal and regulatory framework within this area. Currently, such a framework is being

Table 9. Gas balance in East Asian countries, bcm.

Balance		Year			
		2017*	2025	2035	2050
Demand, total		435	720-780	950-1050	1100-1300
incl:	China	238	480-510	680-730	880-910
	Japan	129	130-140	130-150	140-160
	RoK	48	70-80	85-95	90-100
	Taiwan	20	40-45	50-60	50-60
	DPRK	-	1-2	4-8	30-40
	Mongolia	-	-	-	-
Production, total		151	195-215	280-380	410-480
incl:	China	147	190-210	270-350	380-430
Import, total		288	540-590	650-730	760-840
incl:	LNG	255	420-480	550-650	620-750
	China	88	300-320	400-440	480-520
	Japan	117	130-140	120-130	120-130
	RoK	50	70-80	80-90	80-90
	Taiwan	20	40-45	50-60	50-60
	DPRK**	-	1-2	4-8	30-40
	Mongolia**	-	-	-	-

Source: *- [9]; ** - [2].

established in the region on a bilateral basis, while the creation of a single format of interaction at the regional level would significantly simplify trade in energy goods, energy equipment and services within the region and would facilitate multilateral cooperation.

2. "Green" energy. The rich resource potential of renewable energy and the urgent need for Mongolia's energy sector to shift from coal to cleaner energy resources are important prerequisites for the development of solar and wind energy in Mongolia and for the export of "clean" energy resources to other EA countries. A widely discussed project is the creation of the so-called "Asian super-ring", which will connect the power systems of Russia, countries of Central Asia and East Asia. In addition to the technical and economic aspects of such a project, the creation of an institutional framework for cooperation is also a prerequisite: the distribution of responsibility for the management of technical conditions, a common approach to the formation of tariffs, the rules of the "green certificates" trade for renewable energy, corresponding financing mechanisms, including "green bonds", etc.

3. Export of energy services and equipment from Russia to Mongolia. Russia and Mongolia have a rich experience in the energy cooperation, which goes beyond the trade in energy resources and includes joint implementation of projects for the extraction of minerals, Russia's participation in the construction of Mongolia's energy sector, Mongolian energy staff training, etc. The accumulated potential, as well as the established transport corridors and friendly relations between the countries at the political level, provide a solid basis for expanding the cooperation into such areas as uranium mining and the creation of oil refining industry in Mongolia.

4. Development of multilateral legal regimes. Russia and Mongolia, as well as the countries of the Korean Peninsula, the Maritime States of the Asia-Pacific region are interested in China's commitments to ensure the energy transit from Siberia and Mongolia to the ports of the Eastern coast of the country. Thus, transport costs when transiting through the Russian territory (up to 3-4 thousand km) can be reduced. Although Russia and Mongolia are competitors in the export of metallurgical coal to East Asia countries, in the event of China's refusal to provide access to its ports, Mongolia immediately becomes completely dependent on Russia's transit. There is a risk of diversification issue for Mongolian coal consumers due to China's monopsony in the case of refusal or inability of Mongolia to use access to seaports through the Russian territory.

V. Conclusions

Russia, Mongolia and DPRK are the only net energy-exporting countries in the East Asia region. Growing need of China, Japan, RoK and Taiwan to import coal, oil and gas is essential for these countries both for development of their economy and for improving technical and economic efficiency of their energy industries. As energy exporters, Russia and Mongolia have coinciding interests in regional energy markets and can be competitors at the same energy markets.

Based on the primary energy demand outlooks for all East Asia countries up to 2050, we have estimated the scale of regional markets for coal, oil and natural gas in East Asia.

The focus is made on the priority directions of Russia and Mongolia's joint efforts to develop energy cooperation with the rest of East Asia. A number of priority projects that require joint efforts from Russia and Mongolia in energy cooperation development in East Asia region are proposed:

1. The utilisation of Mongolia's services for transit of Russian pipeline gas to the Chinese central provinces, while enabling Mongolia's large-scale switch to gas as associated project;

2. The development of joint energy system with China, to allow significant synergy from the integration of solar and wind energy sources in Mongolia, large hydropower in eastern Russia, and coal generation within all participating countries, including CHP in winter season;

3. The study on the scope of hydrogen infrastructure development as a complementary segment of the International Power Grid in Northeast Asia, with primary purpose to improve security of energy supply in East Asia;

4. The integration of efforts of the energy research centres in the Northeast Asia countries to improve mutual understanding and increase trust by information exchange on energy policy issues.

Acknowledgments

The study was supported by RFBR, research project No. 18-510-94006

References

[1]. S. Batmunkh, B. Bat-Erdene, C. Ulam-Orgil, A. Erdenebaatar, "Roles of Mongolia in the Interstate Electric Power cooperation as of "Asian Super Grid" in Northeast Asia," *Automatics & software enginery*, no. 4, pp. 52–61, Dec. 2017.

[2]. Trade Map [Online]. Available: https://www.trademap.org/Index.aspx

[3]. Mongolian coal will be delivered in China sea port, March 24, 2017. [Online]. Available: http://news.mongolnow.com/24_03_a03.html, Accessed on: December 20, 2018.(in Russian)

[4]. Mongolia electricity import from Russia increased 5.4% compared to the previous year, February 16, 2017. [Online]. Available: https://tayga.info/132669, Accessed on: December 20, 2018. (in Russian)

[5]. Mongolian statistical information service [Online]. Available: https://www.1212.mn

[6]. B. Ariunbayar, "The ceremony of laying the foundation of a new refinery will take place on June 22," June 19, 2018. [Online]. Available:

https://montsame.mn/ru/read/163889, Accessed on December 20, 2018. (in Russian)

[7]. Natural Gas Exports of the Russian Federation, Sept. 25, 2018. [Online]. Available: http://www.cbr.ru/eng/statistics/default.aspx?PrtId=svs

[8]. BP Statistical Review of World Energy, June 2018. Pureprint Group Limited, UK. [Online]. Available: https://www.bp.com/en/global/corporate/energy-economics/statistical-review-of-world-energy.html, Accessed on: December 1, 2018.

[9]. Global Energy Statistical Yearbook 2018. [Online]. Available: https://yearbook.enerdata.net/

[10]. S.P. Popov, K.A. Korneev, E.V. Ershova "Long-term trends on energy markets of East Asia," *Proceedings of All-Russian Conference "Russian energy sector in 21st century. Innovative development and management"* [Online]. Available: https://bit.ly/2U91gSm (in Russian)

[11]. S.P. Popov, "Methodological approach to assessing the demand for Russian energy on the East Asia market," *7th Melentiev Readings*, ed. by A.A.Makarov, ERI RAS, Moscow, 2013,pp.116-127 (in Russian).

[12]. IEEJ Outlook 2019 —Energy transition and a thorny path for 3E challenges— Energy, Environment and Economy. [Online]. Available: https://eneken.ieej.or.jp/data/8122.pdf

[13]. Global and Russian Energy Outlook 2016. Edited by A. A. Makarov, L. M. Grigoriev, T. A. Mitrova. ERI RAS, ACRF, Moscow, 2016. 198 p.[Online]. Available: http://ac.gov.ru/files/publication/a/12767.pdf

[14]. International Energy Outlook 2017. US EIA. [Online]. Available: https://www.eia.gov/outlooks/archive/ieo17/

[15]. World Energy Outlook 2016. IEA.[Online]. Available: https://webstore.iea.org/download/direct/202?fileName=WEO2016.pdf

[16]. BP Energy Outlook 2018. [Online]. Available: https://www.bp.com/en/global/corporate/energy-economics/energy-outlook.html

[17]. Reflections from CRU China client seminar. CRU analysis. Available: https://www.crugroup.com/knowledge-and-insights/insights/2018/reflections-from-cru-china-client-seminar/

[18]. Statistics [Online]. Available: https://www.iea.org/statistics/?country=WORLD&year=2016&category=Key%20indicators&indicator=TPESbySource&mode=chart&dataTable=BALANCES

[19]. S. Popov, K. Korneev, "A "Green Option" for the Japanese Power Industry: Sakhalin-Hokkaido Interconnector," *Geopolitics of Energy*, vol. 39, no.5, pp. 12-16, Sept. 2017.

[20]. S.V. Podkovalnikov, V.A. Saveliev, L.Y. Chudinova, "Study on system energy-economic effectiveness of Northeast Asia electricity grid formation," *Proceedings of the Russian Academy of Sciences. Power Engineering*, no. 5, pp. 16-32, 2015.

[21]. S.V. Podkovalnikov, V.A. Saveliev, O.V. Khamisov, L. Yu. Chudinova, "Justification of Effectiveness of International Power Interconnections with Separation of Effects between Participants," *Automation and Remote Control*, no. 10, pp. 26-38, 2018.

[22]. T. Otsuki, Aishah Binti Mohd Isa, R.D. Samuelson, "Electric power grid interconnections in Northeast Asia: A quantitative analysis of opportunities and challenges," *Energy Policy,* vol. 89, pp. 311–329, Feb. 2016.

[23]. T. Otsuki, "Costs and benefits of large-scale deployment of wind turbines and solar PV in Mongolia for international power exports," *Renewable Energy*, vol. 108, pp. 321–335, Aug. 2017.

Sergei Popov graduated from the Cybernetics Department of Irkutsk Polytechnic Institute in 1982, specialising in Large Energy Systems. Since 1986, he has been with MESI SB RAS, where he got his PhD in 1993.
His research interests focus on export markets for the Northeast Asia economies undergoing energy transition, and energy cooperation options.

Daria V Maksakova received a Bachelor's degree in International Economics in 2016 and a Master of Finance degree in 2018 from Baikal State University. Now she is an engineer at MESI SB RAS. Her research interests lie in the sphere of Northeast Asia energy markets development and modelling.

Markov expert logical analysis for energy reserves probabilistic evaluation

Evgeny R. Stavrovsky*, Sergey A. Pryadko

Gubkin Russian State University of Oil and Gas (National Research University), Moscow, Russian Federation

***Abstract* — The paper focuses on the probabilistic evaluation of oil and gas resources with the models and methods of AHP/ANP analysis. The AHP/ANP models are shown to be the particular cases of finite Markov chains, i.e. discrete random processes with Markov property. An integrated method (Markov expert logical analysis (MELA)) is proposed. The method is based on the models, methods and algorithms of Markov chains theory. This basis will stimulate the progress in research on multi-criteria decision-making problems that arise in various spheres. The paper presents different methods using MELA to allow for the uncertainty of numeric and nonnumeric data on gas reserves as methods of transformation of expert estimations into the probability distributions. Typical logical schemes are proposed for multi-criteria comparison of analogous objects, to take account of possible errors in porosity evaluation and to estimate project life.**

***Index Terms* — Analytic Hierarchy Process (AHP); Analytic Network Process (ANP); Markov chains; evaluation of resources; Markov expert logical analysis (MELA); logical scheme; information uncertainty; Monte-Carlo method; project life; oil and gas resources probabilistic evaluation.**

I. Introduction

Probabilistic evaluation of geological oil and gas resources is an important objective of regional energy research. The hydrocarbon (HC) resources are evaluated by experts (geologists, geophysicists) on the basis of their judgments about petrology and process of reserve formation; generation, migration and dissipation of HC-fluid and other geological information, usually of hypothetical nature. In this case, there can be significant discrepancies in judgments by different experts. As this information is usually qualitative, it is normal to use the methods of expert logical analysis (ELA) that provide experts with universal language for analysis and agreement of final estimates.

Two main ELA methods [1,2] – analytic hierarchy process (AHP) and analytic network process (ANP) – allow us to probabilistically evaluate the porosity and permeability parameters of oil and gas reservoirs, from which it is easy to probabilistically evaluate the volume of the resources. The values of expert probabilities reflect expert's confidence in the correctness of the parameters evaluation.

II. AHP and ANP

The AHP and ANP suggest special logical schemes to organize the evaluation procedure (Figure 1).

The logical scheme of AHP (hierarchy) is characterized by the following special aspects:

all its elements are grouped in T+1 classes (levels of hierarchy) S_t, $t = 0,1,\dots,T$, so that in class S_0 one element 0 is included, showing the aim of investigation, in class S_T elements correspond to variants of decision-making ("alternatives"), elements of the other classes can have a certain meaning (actors, groups of criteria, criteria, factors and others);

links (indicated by arrows) exist only between the elements of neighboring levels. This means that elements of one level must be independent and they cannot influence each other.

In the models of analytical network these requirements are withdrawn. This means that logical schemes of ANP can be optional.

The second part of AHP and ANP consists of the methods of giving priorities (weight) $p_{ij}(t)$ to elements $i \in S_t$, $t = 0,1,\dots,T$, $\sum_j p_{ij} = 1$, which are stated in [2,3]

* Corresponding author.
E-mail: ers1938@rambler.ru

http://dx.doi.org/10.25729/esr.2018.04.0006
Available online February 28, 2019.

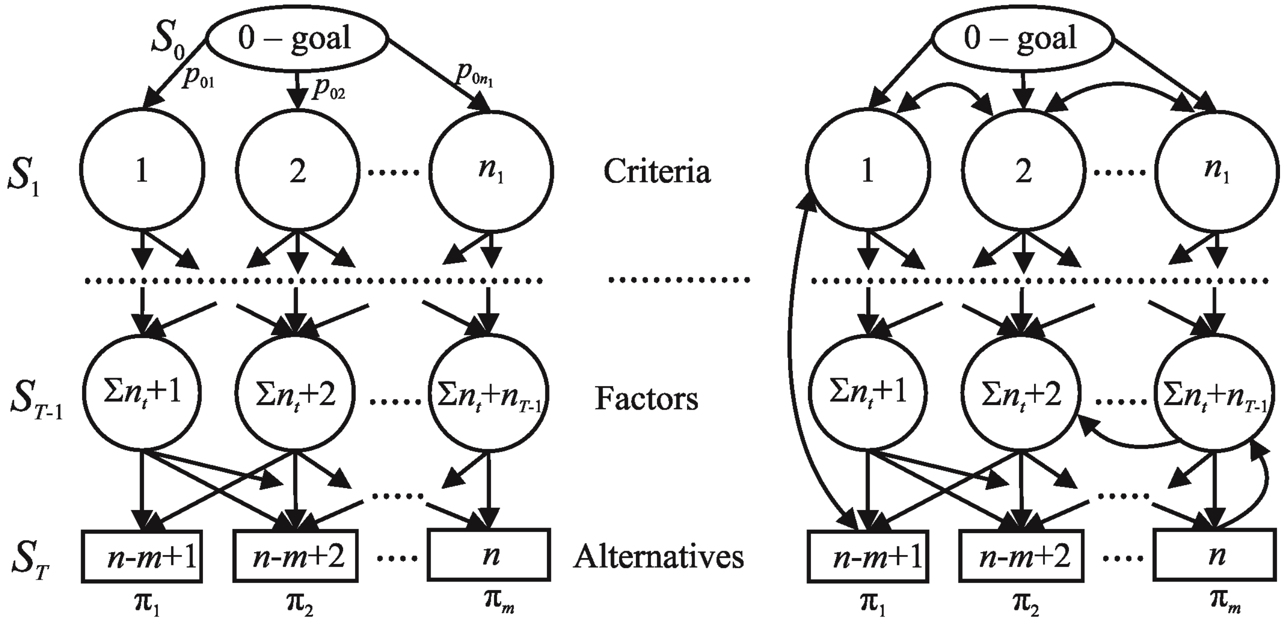

(a) logical scheme of AHP **(b) logical scheme of ANP**

Fig. 1. A general layout of logical schemes of AHP (a) and ANP (b).

These methods allow comparing the measured indicators as well as qualitative ones for calculating quantitative evaluations of preferable decisions (absolute priorities, weight).

The third part of AHP and ANP consists of calculating absolute priorities π_k of alternatives $k = 1,\ldots,m$ with logical scheme and of relative priorities $\{p_{ij}\}$, $i = 0,1,\ldots,n$.

Let us enumerate some important advantages of AHP:

- It makes it possible to effectively breakdown complicated schemes of analysis, which create favorable possibilities for dividing the complicated problems into a set of simple ones and combining their decisions;
- It controls logical conformity of expert's judgment, which allows avoiding logical errors in expert evaluations;
- It provides evaluation of priorities, resistant to small data variations.

The results of investigations with the AHP and ANP schemes (absolute priorities π_k of alternative $k = 1,\ldots,m$) are convenient to interpret as a share of total amount of votes during election, determined by logical scheme. In the decision making tasks, this allows ranging alternatives in correspondence with their importance. Another important interpretation lies in that π_k are expertprobabilities of accidental falling out of relative alternatives.

Neglect of the connections between elements can essentially influence the assessments of priorities. Therefore, the use of AHP, for example, under depending (correlated) criteria can lead to corrupted evaluations of priorities of alternatives. In this case, it is necessary to switch from AHP to the method of analytical networks, by reflecting all links in the logical scheme. In practice, this limits greatly the applicability of AHP.

III. Markov expert logical analysis

The authors of [3] state that any logical scheme of ANP after simple transformations (markovization) is isomorphic to the transition graph of some homogeneous Markov chain (MC) with unlimited "time". This isomorphism is assigned by the analogy of the main concepts of analytic networks (AN) [2, 3] and MC (Table 1).

Markov expert logical analysis (MELA) is an evident generalization of ANP, which requires fulfillment of the following stages:

1. Prepare logical scheme for considering the problem as a transition graph of Markov chain;
2. Choose the methods for evaluating relative priorities equivalent to probabilities of transitions between the MC states and form the transition matrix of probabilities;
3. Markovize analytical network by adding fictitious vertices and edges to AN so that the limit probabilities (or average limit probabilities for periodic chain) coincide with the distribution of ANP absolute priorities of alternatives;
4. Assign the initial values $p(0)$ of probabilities to all MC states;
5. Insert the data in the program and calculate the limit probabilities for all states of non-periodic MC (or the average probabilities of MC states for periodic one) that are considered as absolute priorities of logical

scheme of elements;

6. Control an agreement of expert judgments (correct them if some of them do not agree and repeat the calculations);
7. Interpret elements of decision in accordance with the sense of problem and correction of logical scheme, probabilities of transition and reevaluating relative and absolute priorities if necessary.

For the analytical network markovization, it is normally enough to make the following transformations of its graph G (Figure 2):

a. Build the condensation of graph G [4], point out all connected components in it, source components and sink components (Figure 2b);

b. Add fictitious vertex 0 ("common source"), fictitious vertex Z ("common sink") and fictitious edges connecting sinks with sources in graph G. Assign probabilities to edges, defined by the following simple rules:

Assign equal transient probabilities p_{0j} (equal to 1 in sum) to the edges $(0, j)$ coming into source blocks;

If i is the only vertex of sink block, assign transition probability $p_{iZ} = 1$ to edge (i, Z). In the event that the sink block contains several vertices, assign small probability $p_{iZ} = \delta$ to edge (i, Z), and divide probabilities p_{ij} of the other transitions from vertex i by $1 + \delta$;

- Assign the probability of transition $p_{Z0} = 1$ to the fictitious edge $(Z, 0)$.

It is obvious that such markovization makes the connected graph of analytical network strongly connected. This algorithm can be easily automated and the program will do all these operations by itself.

An analysis of the AN structure with the methods of the theory of graphs helps to reveal logical discrepancy and in some cases to significantly simplify the AN.

IV. Problems of hydrocarbon resources evaluation

The above-described method can be applied to probabilistic evaluation of initial V and extracted V_{ex} volumes of hydrocarbon (HC) resources. The main difficulties of such an evaluation are connected with the lack of reliable data on the shape and volume of the pore space Ω of reservoir and its properties: porosity m, gas α or oil α_o saturation, reservoir fluid composition, as well as pressure p and temperature T in the reservoir.

Let us consider gas reserves. Geometrical form of the pore space Ω, gas content and parameters α, m, p, T are not known precisely. In fact, they are assigned by geologists who base their estimations on the results of geophysical investigations and the data on lithological characteristics of reservoirs and the processes of hydrocarbon formation, migration, accumulation and dissipation in it.

It is common practice to substitute a reservoir with a homogeneous isotropic cylinder of the same volume with horizontal sole with an area S, taking $\Omega = hS\cos\varphi$, where h – average thickness of reservoir, φ – formation dip. For the volume of initial V and extracted V_{ex} gas reserves, the following formula are known:

$$V = C\alpha mhS\cos\varphi\frac{PT_0Z_0}{P_0TZ};\ V_{ex} \approx V\eta, \tag{1}$$

where η – average gas-recovery factor, P – average reservoir pressure, $Z = Z(P,T)$ – gas-compressibility factor (depends on gas composition), coefficient C takes into account units of measurements, and index 0 indicates standard value of magnitudes. It is reasonable to consider parameters α, m, h, S, P and η as random variables.

MELA can be used to take into account the uncertainty of both numeric and nonnumeric data on gas formation as a method for transformation of experts' estimations into the probability distribution series of evaluated magnitudes. We will consider two ways of building such distributions:

1. For insufficiently explored objects, this is the use of MELA to set discrete vector distributions $\{\pi_j, X_j\}$ (Figure 3). This method is based on comparison of a considered object with a set from n analog objects ("alternatives" in the MELA scheme). Here π_j is the probability that $X = X_j$ (weight of the j-th alternative), and $X_j = (x_{jk})$ is vector

Table 1. Analogy between AHP-ANP and Markov chains terms

Terms of T.Saati [1,2]	Standard terms of MC [4,5]
AN, logical scheme	Transition graph of MC
Element of analytical network	State of Markov chain
Component of analytical network	Subset of states of MC
Alternatives	States with numbers n-m+1,…, n
Influence of element i on element j	Transition from state i to state j
Relative priority of influence of element i on element j	Probability of transition from state i to state j
Absolute priority of element j	Limit probability of state j
Super-matrix of analytical network	Matrix of transition probabilities
Vector w of absolute priorities of the analytical network elements	Vector π of limit probabilities (or their Cesaro averages)
Component of structural graph	Component of connection
Source components	Subset of non-recurrent states
Sink components	Classes of adsorbing states
Structural graph	Graph condensation

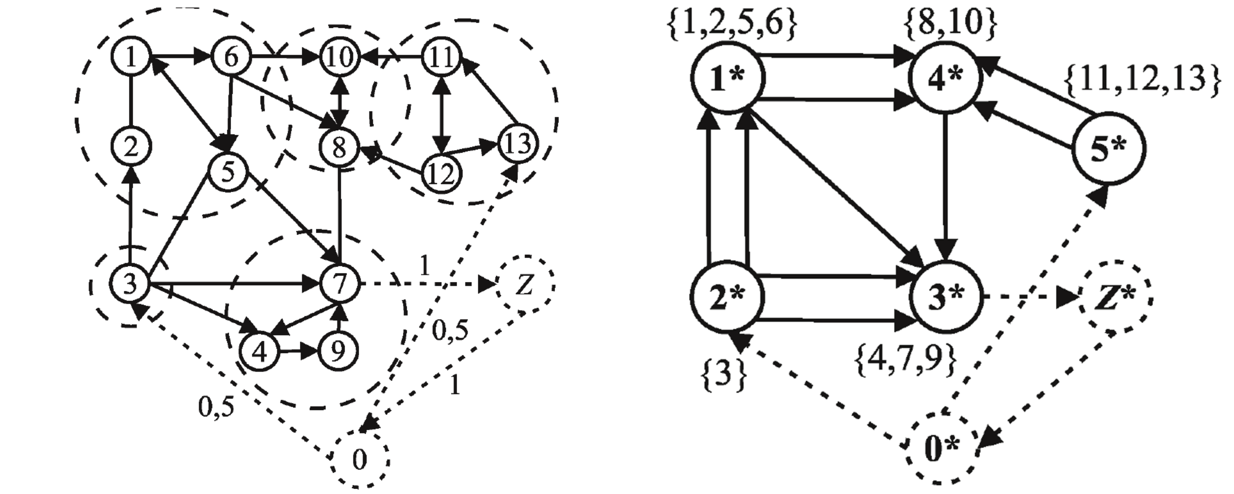

a. Graph G of analytic network and markovization b. Condensation of graph G and markovization

Figure 2. Markovization of analytic network

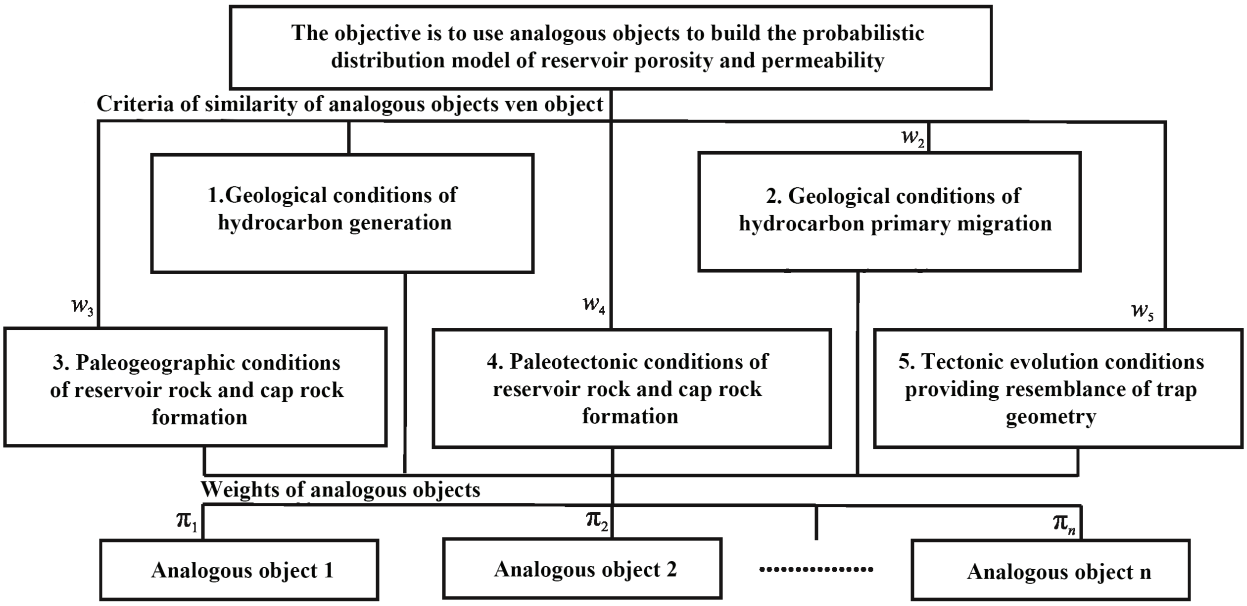

Figure 3. Logical scheme of multi-criteria comparison of analog objects to construct a probabilistic distribution model of reservoir parameters of the insufficiently explored object in question

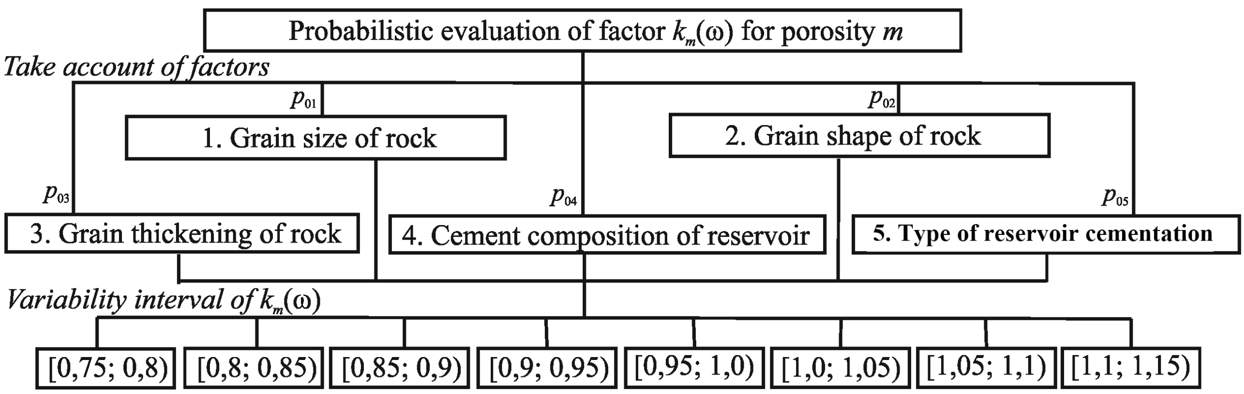

Figure 4. Typical MELA scheme for evaluation of factor km(ω) to allow for possible errors in porosity evaluation m (p_{0k} – weights of criteria)

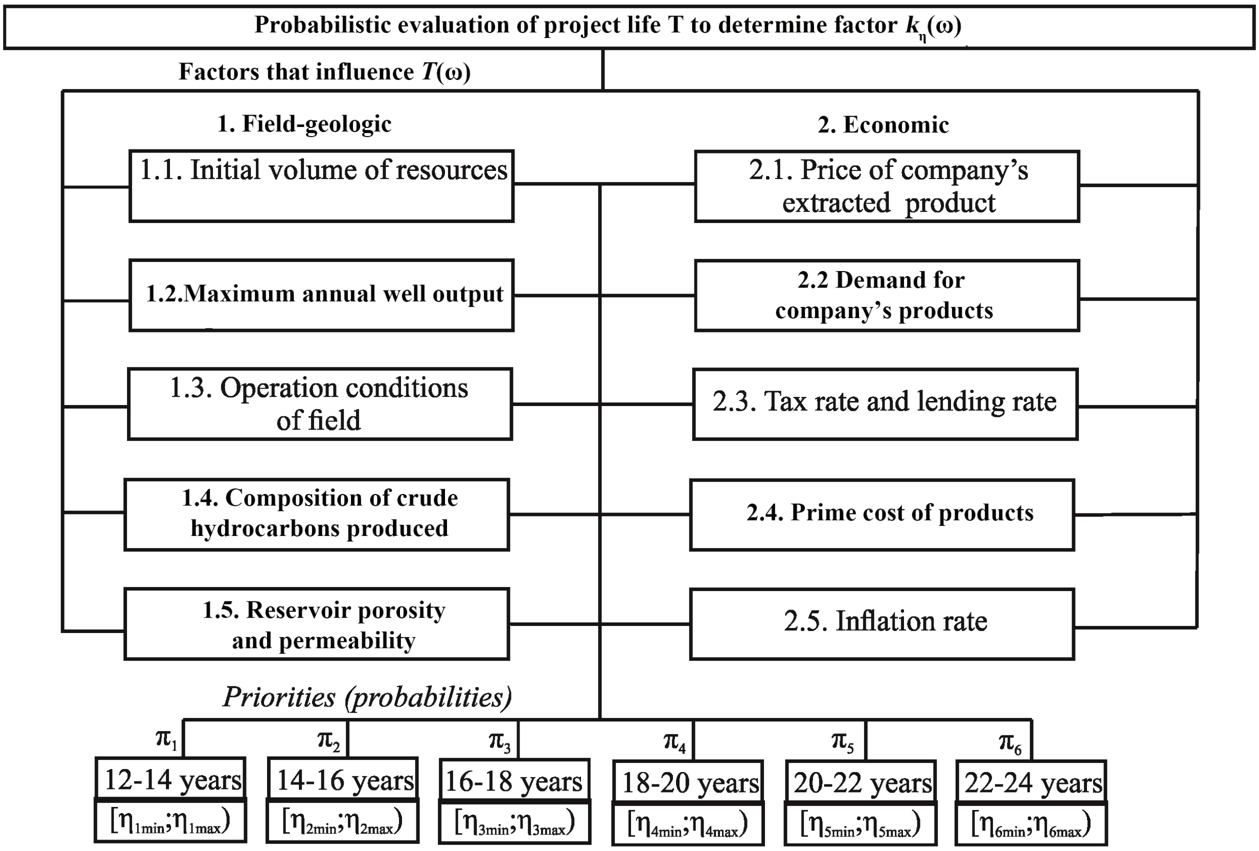

Figure 5. A typical MELA scheme for evaluation of project life and factor $k_\eta(\omega)$

of parameters of the j-th analog object, $j = 1,\ldots,n$. It is recommended to widen the list of analog objects;

2. For more studied objects, the MELA scheme is used to set the distribution $\{\pi_j, x_j\}$ of probability that parameter x belongs to the given intervals: where π_j – probability; x_j – average value of the *j-th* interval, $j = 1,\ldots,n$.

The logical scheme of AHP can be used to evaluate the proximity measure of analog objects to the insufficiently studied object (Figure 3). The weight coefficients w_i assess the importance of criteria indicating the proximity measures of formation conditions of a given object and analog objects. The closer the considered field to object j in terms of formation conditions, the larger the weight π_j of this analog object.

Figure 3. Logical scheme of multi-criteria comparison of analog objects to construct a probabilistic distribution model of reservoir parameters of the insufficiently explored object in question

The weights can be considered as expert assessments of probability of coincidence of porosity and permeability parameters of an object with those of an analogous object. The schemes of logic assessment can serve as data sources for building the probabilistic models of the object characteristics. The results of the evaluation specify the probabilities to vectors of parameters α, *m, h, S, P* :

Probability (weight), π_j: $\pi_1, \pi_2, \ldots, \pi_n$; Value of porosity and permeability parameters - vector dimension,

$$X_j: X_1 = (x_{1k}), X_2 = (x_{2k}), \ldots, X_n = (x_{nk}).$$

Thus, the unknown vector X of porosity and permeability parameters of this gas field can be predicted as the mean value by the formula:

$$X \approx \sum_{j=1}^{n} \pi_j X_j \, .$$

The second method suggests the following actions:

expert chooses the parameters in (1) to be considered as random variables. For each of them, we introduce a correction factor (random variable) $k_{.}(\omega)$ with corresponding index for the base value of the evaluated parameter $k(\omega)=1$ (ω – vector of random factors);

expert uses a typical MELA scheme or makes a logical MELA scheme for each factor $k(\omega)$ in (1), where alternatives are represented by sub-intervals of an interval of possible values $k(\omega)$;

MELA is used to calculate the empirical distribution $\{\pi_j, k_j\}$ of probabilities of factor $k(\omega)$ (k_j being the middle point of the *j-th* sub-interval);

factors $k(\omega)$ are assumed to be independent random variables, based on their empirical distributions the representative sample $\{V(\omega)\}$ of possible volume of reserves is generated with the Monte-Carlo method

[7]; the sample $\{V(\omega)\}$ is processed by the methods of nonparametric statistics [5].

Probabilistic evaluation of gas reserves in the field is determined by the formula:

$$V_{ex}(\omega) \approx V_{ex} k_{\alpha}(\omega)\, k_m(\omega)\, k_h(\omega)\, k_S(\omega)\, k_p(\omega)\, k_{\eta}(\omega) = k_V(\omega)\, V, \quad (2)$$

where $k_V(\omega)$ is a random factor for evaluating the volume of extracted gas reserves. Variable $k(\omega)$–1 indicates the value of a random error in the parameter with respect to its base value.

Fig. 4 demonstrates the MELA scheme for evaluation of $k_m(\omega)$. Expert has the right to correct it, add (delete) elements and links. Logical schemes for parameters $k_{\alpha}(\omega)$, $k_h(\omega)$, $k_S(\omega)$, $k_p(\omega)$, $k_{\eta}(\omega)$, included in $k_V(\omega)$, are built in the same way.

Fig. 4. Typical MELA scheme for evaluation of factor $k_m(\omega)$ to allow for possible errors in porosity evaluation m (p_{0k} – weights of criteria)

Correction $k_{\eta}(\omega)$ to the gas recovery factor (GRF) depends not only on geologic factors (characteristics of reservoirs, entrapment of gas with fallen condensate, etc.) but also on economic-geographical ones. The former factors are determined by conditions of formation of the reserves and geological characteristics of this region. The latter group can be divided into engineering-technological and economic factors requiring substantiation of GRF as a solution to the engineering-technological problem of determining the field development time. The first sub-group determines engineering-technological solutions for drilling and creation of a system for gas collection and preparation for transportation that should function during the whole life cycle of the field. The second sub-group is connected with the hypotheses about economic standard (unit costs of equipment and construction and installation work, operating costs, prices per unit, tax and lending rates, etc.).

The main factors of the first sub-group are the production horizon characteristics connected with the considered field (accumulation): type of reservoir, inhomogeneity and variability of massive material, tectonic features, deformation properties of massive material, type of accumulation, gas column, occurrence depth, characteristics of productive strata penetration, initial thermobaric conditions, recovery mechanism, reservoir gas content.

The gas recovery factor can be correctly evaluated only in the last stage of development. At the beginning of the development only its approximate evaluation is possible. The evaluation requires special stochastic optimization models with a criterion of maximum mean net present value [6]. Significant part of capital investment falls on reconstruction of the system for gas collection and preparation for transportation. These evaluations in the stage of decision making about the field exploration are approximate and require at least a simplified probabilistic risk analysis.

The GRF evaluation based on the materials of exploration drilling is made for the approval of reserves by State Commission of natural resources. The aim is to reveal the hydrocarbon volumes with a view to estimating capital investment in the system of production, transportation, processing, product distribution and determination of taxation basis. Normally, gas-dynamic calculations and GRF evaluation lack information, consequently, statistic data, analogies and expert evaluations are often used.

This forces the use of approximate evaluations by MELA based either on statistic data, or data from analogous objects, or judgments of geologists and economists. First two approaches are quite obvious (similar to the last examples) but they are usually not provided with necessary information. The third approach corresponds to the practice of GRF evaluation. Its scheme is presented in Figure 5.

The recovery factor is strongly correlated with the life of a project for exploration of a geological object, which should also be taken as random variable $T(\omega)$ (we consider here approximate evaluations of economic figures for geological objects of categories not higher than C_1). The above-listed factors (geologic-productive parameters, economic cost indicators and effects) influence the variable $T(\omega)$: factor $k_V(\omega)$ is evaluated by the Monte-Carlo method [7], which involves processing of a generated sample by the methods of nonparametric statistics [5].

The use of logical scheme does not reject the traditional calculations of supposed dynamics of techno-economic indicators of the project.

V. Conclusion

The evaluations of oil and gas resources in the early stages of choosing an object for exploration are based on geologists' concepts about structure and parameters of the fields, which is associated with high uncertainty and non-objectiveness of the evaluations. Generalization and application of modern methods for expert analysis of data and probabilistic models of planning exploration work allow us to numerically evaluate the influence of these factors on the field development indicators.

The evaluations made by geologists are based on detailed structural maps as well as on the notions of reserve formation history. It is necessary to connect, generalize and reconcile these notions with geophysical and field data. This is qualitative information and therefore AHP and ANP are recommended for evaluation, because they provide experts with universal language for analysis and agreement of their judgments.

AHP imposes strict restrictions on selection of a logical scheme and requires independence of elements of each level of hierarchy. Failure to meet these requirements may lead to significant errors in results. ANP is free of these restrictions but has no clear theoretical framework and needs a strict proof of computational algorithm.

The study indicates that AHP and ANP are special cases of homogeneous Markov chains, if we use the methods of markovization of the AHP/ANP logical schemes. This makes it possible to use Markov chains for analysis of logical schemes. The generalizations made constitute a theoretical basis for a new method of Markov expert logical analysis (MELA). This method enables multi-criteria decision making and multifactor analysis of data, by applying standard methods of Markov chains analysis.

Markov expert logical analysis, in particular, can be applied in probabilistic evaluation of resources in hydrocarbon fields. It determines the probability distributions for parameters of oil and gas reservoirs and recovery factor. The special schemes of MELA are recommended to find out the distribution series for resources, by evaluating similarities between the considered object and analogous objects. Thus, the probabilistic expert evaluation of parameters becomes a regulated procedure with formally controlled results.

References

[1] Saaty T. L. "The Analytic Hierarchy Process," McGraw-Hill, New York. 1980.

[2] Saaty T.L., Vargas L. G. "Decision Making with the Analytic Network Process," Springer, 1996.

[3] Saaty T. L., Özdemir, M. S. "The Encyclion: A Dictionary of Decisions with Dependence and Feedback based on the Analytic Network Process," RWS Publications, USA. 2005.

[4] Stavrovsky E. "AHP and ANP as Particular Cases of Markov Chains," E. Stavrovsky, M. Krasilnikova, S. Pryadko // IFAC Conference on Manufacturing Modeling, Management, and Control. Saint Petersburg, 2013, v.7, Part 1, pp. 531-536.

[5] Berzh K. "Theory of graphs and its applications," Moscow: Izdatelstvo inostrannoj litereturi, 1962. 319 p. (in Russian).

[6] Orlov A. I. "Practical statistics. M.: Ekzamen," 2004. 656 p. (in Russian).

[7] Stavrovsky E. Model of multistep stochastic design of systems "Short-cut gas field assets – gas line – consumer," Stavrovsky E., Fomin E., Shmyglya O. // Pipeline systems of energetics. Management of development and functioning. Novosibirsk: Nauka, 2004. P. 135-145. (in Russian).

[8] Sobol I. "Numerical methods of Monte-Carlo," Moscow: Nauka, 1973. 312 p. (in Russian).

Evgeny Romanovich Stavrovsky, Dr.Sc. in Engineering, Professor of Gubkin Russian State University of Oil and Gas (National Research University), Moscow, Russian Federation

Sergey Alexandrovich Pryadko, PhD in Engineering, Assistant professor of Gubkin Russian State University of Oil and Gas (National Research University), Moscow, Russian Federation

Determination of Phase Loads in the Primary Distribution Network Using Smart Meters

Irina I. Golub *, Evgeny V. Boloev, and Yana I. Kuzkina

Melentiev Energy Systems Institute of Siberian Branch of Russian Academy of Sciences, Irkutsk, Russia

***Abstract* — The paper presents an option for determination of phase loads in the primary distribution network using the results of state estimation of the secondary distribution network that are obtained by smart meter measurements installed at the load and generator nodes. The problem of state estimation in the secondary distribution network based on measurements of the active and reactive nodal powers and voltage magnitudes rather than by the Newton method traditionally used for this purpose is solved by a method of simple iterations. Efficiency of using the proposed approach for determination of phase loads of the primary distribution network for each hour of daily curve of nodal powers is illustrated by the example of a 32-node test network..**

***Index Terms* — distribution network, renewable generation, smart meter, state estimation, voltage control.**

I. Introduction

The major share of power losses and power transmission costs as well as power supply reliability costs are known to fall on distribution networks. This fact requires special attention to the distribution networks reliability and ways to enhance their efficiency.

Primary and secondary distribution networks are traditionally operated as opened ones, power flows in their feeders being directed from the primary distribution substation to the load nodes. A low-voltage secondary distribution network is modeled as a three-phase network with a zero wire; it can have single-, two- and three-phase loads, which leads to unbalance of currents and voltages both in the secondary and primary distribution networks.

A major trend in upgrading the traditional passive network is transition to an active intelligent network that integrates renewable energy sources, power storage units and active loads. Power flow directions in the active networks are changed during the day; load nodes may become generator ones, and voltage deviations may exceed permissible levels. First, we should understand that network behavior radically changes and then make a decision on its enhancement, improvement of its reliability and efficiency of its operation. The main way to ensure the flexible transition from a traditional passive network to an intelligent active one can be accurate and reliable state estimation (SE).

The state estimation methods are widely used in high and ultra-high voltage networks that are used for power transmission from power stations to distribution networks. Invention of synchronized phasor measurements played a major role in increasing the state estiamtion reliability. State estimation based on Phasor Measurement Units allows measurements of power transmitted to the primary medium-voltage distribution network, whereas loads of primary and secondary distribution networks cannot be measured.

Power meters in traditional distribution networks are as a rule installed on the medium-voltage side of primary substations only, while there is no data on the state of secondary distribution substations. There are methods that use such measurements for approximate estimation of load flows and power losses in the distribution network [1] but such measurements are rather scarce for state estimation even in the traditional networks, to say nothing about the active ones.

The average hourly loads determined based on measurements of power consumed and recorded in the reports of an Automatic System for Commercial Accounting of Power Consumption (ASCAPC) can be used for load flow calculation in the initial stage of transition to an active distribution network. The smaller the time interval between

* Corresponding author.
E-mail: golub@isem.irk.ru

http://dx.doi.org/10.25729/esr.2018.04.0007
Available online February 28, 2019.

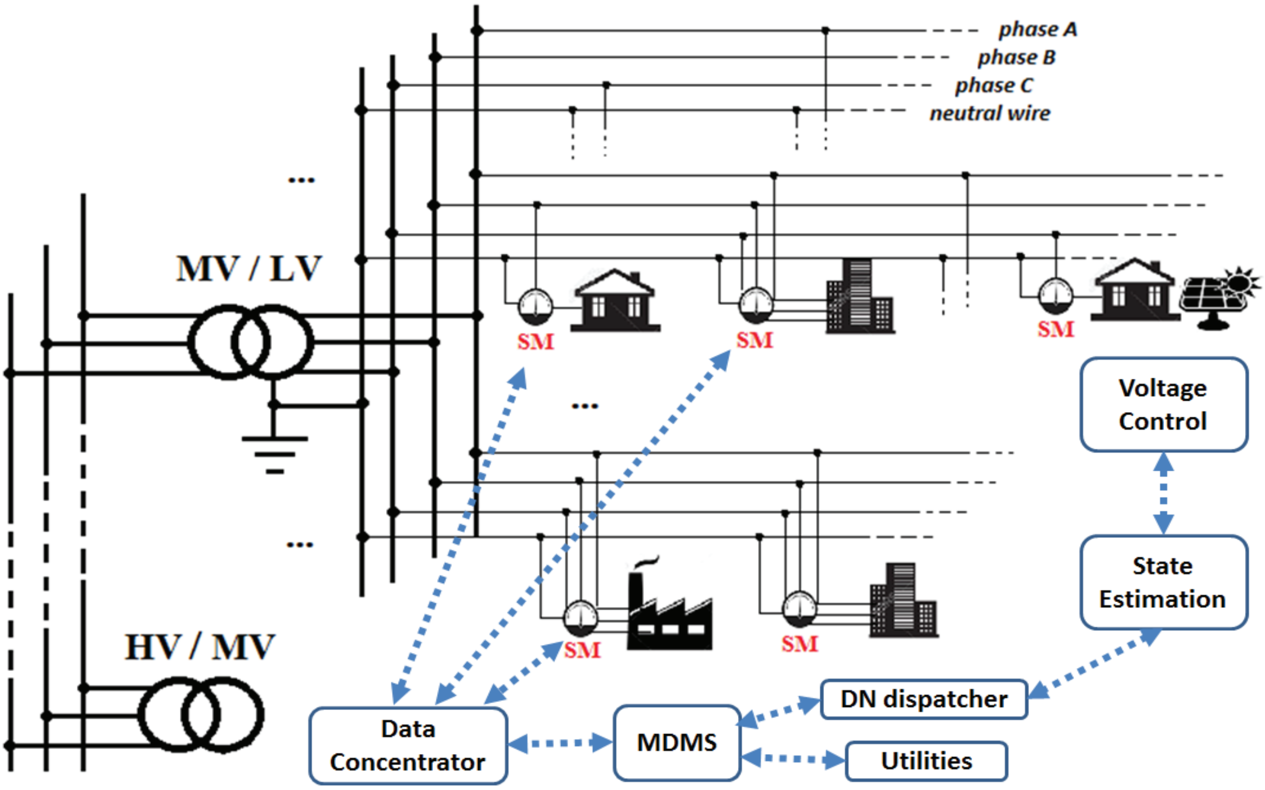

Fig. 1. Hierarchy of Advanced Metering Infrastructure for acquisition, transfer and processing of the Smart Meter recordings

measurements (subject to coincidence of time intervals for load determination), the higher the accuracy of load flow calculations using the ASCAPC data. It is also important to exclude errors in the data on connection of low-voltage feeders to transformer substations and in the data on the network topology that are obtained from special-purpose geographic systems. Information on connection of loads to feeder phases is of major importance and, as a rule, it requires special research. Load flow calculation based on average hourly loads can increase the accuracy of determining the nodal voltages and losses, but this accuracy is insufficient for state estiamtion.

The paper is arranged as follows.

Section II discusses the principles of building a system for collecting and processing measurements from smart meters, and the problem of clarifying information on the placement of meters in the phases of the distribution network.

Section III proposes an approach to significantly simplify the procedure for state estimation of the secondary distribution network. The approach is associated with solving a nonlinear system of measurement equations by simple iteration method.

Section IV analyzes the problem of placing smart meters to ensure the observability of all state variables in the distribution network or the observability of only voltage magnitudes.

Section V illustrates the effectiveness of the proposed approach for the state estimation and identification of phase loads and nodal voltages of the primary distribution network using a test network as an example.

II. Smart Meters and Modern Metering Infrastructure

The most complete and reliable data on the state of secondary distribution network can be obtained by the state estimation methods that use smart meters installed at load and/or generator nodes.

Meters of ELSTER Company [2] with 0.2S, 0.5S, 1 precision at 15-minute discreteness of metering are examples of smart meters. Similar meters are installed in the distribution networks of Europe. Ministry of Energy of Russia has developed a draft law stimulating the introduction of smart digital meters for power metering. Some Russian cities (Kaliningrad, Yaroslavl, and Tula) implement pilot projects on the use of smart meters [3, 4].

Advanced Metering Infrastructure (AMI) [5, 6] that unites an active distribution network, a communication network and a modern metering system is responsible for data transfer from a smart meter to the data acquisition and processing system, and back. Along with the consumed power, some smart meters can measure active and reactive power, active and reactive currents and voltage magnitudes at the nodes where they are installed [7].

Smart meter measurements processed by state estimation algorithms can be used for analysis of voltage and current admissibility, for calculation of power losses, and for assessment of the distribution network reliability.

Moreover, estimates of load flows in the secondary distribution network that at each phase come from the primary distribution network can be used for calculation of a three-phase load flow and/or state estimation of the primary distribution network.

A list of activities that need data on loads and load flows in the primary distribution network is rather extended. It includes power losses, reactive power control, optimization of capacitor banks allocation, network reconfiguration, load forecast, network enhancement, relay protection, and automation.

Fig. 1 presents an AMI hierarchy for the smart meter data collection and transfer to data concentrators at substations. The data are transmitted to Meter Data Management System (MDMS) for further processing of recordings on power consumed by utilities. The smart meter data are used by a distribution network dispatcher or by the state estimation algorithms.

Different media and communication means are used for the AMI arrangement [8]. Power Line Communication (PLC) technology became popular in both Europe and Russia. It ensures high-speed data transfer via power lines [9], has limited transfer capability and long response time to incoming smart meter messages.

ZigBee [10] and cloud technologies [11] are the most popular wireless technologies. In Kazakhstan and Belorussia, the cellular communication is used for communication between smart meters [4]. Wireless communication is less costly but distance and correctness of signals transmitted are limited, speed of data transfer is low, and ability to detect obstacles and bypass them is low. Moreover, wireless technologies can create noises for other devices. PLC is, as a rule, used for recordings transfer into data storage units located at primary distribution substations; communication between meters of one feeder is performed via wireless channels.

Before commencing the state estimation of the secondary distribution network as well as for meters used in the Automatic System for Commercial Accounting of Power Consumption (ASCAPC), we need data on the phase to which loads are connected and where smart meters are installed. A measurement experiment proposed in [12] is an efficient approach to phase identification in the distribution network. It consists in assessing mutual correlation of voltage profiles at two nodes of the network within a short period of time. The first one is a power supply node in the distribution network or the nearest node at every phase of which the voltage magnitudes are measured at certain time moments. The second node is represented by successive nodes with smart meters for voltage magnitude measurements taken simultaneously with the measurements in the phases of the first node. The phase of smart meter connection is determined based on the maximum values of cross-correlation coefficients.

The question if it possible to synchronize smart meter measurements has no answer. The authors of the first publications [13] are convinced that their synchronization is possible. Nevertheless, despite the existence of methods for synchronization of smart meter measurements, the authors of [14] recommend considering currently used smart meter measurements as non-synchronized ones and an interval of their transmission is advised to be taken equal to 15, 30 or 60 minutes. The authors of [15] propose compensating for the lack of smart meters synchronization at state estimation by increasing their error [15].

III. State estimation of the secondary distribution network

Let us analyze the possibility of using the smart meter measurements that include active $Z_P^{a,b,c}$ and reactive $Z_Q^{a,b,c}$ nodal capacities and voltage magnitudes $Z_U^{a,b,c}$ at phases *a, b, c* for state estimation of the secondary distribution network and the possibility of using the measurements of zero values of active and reactive nodal capacities (injections) at the transit nodes as additional ones. A secondary distribution network is modeled as a three-phase network disregarding cross-resistances between phase wires and shunt susceptance.

State variables phasor elements are real $u_i^{'a,b,c}$ and imaginary $u_i^{''a,b,c}$ components of phase voltage $u^{a,b,c} = u_i^{'a,b,c} + ju_i^{''a,b,c}$ at nodes $i = 1,..., n$ of the calculation model. Their real components that are equal to the measured voltage magnitudes are used as measured voltages. Admissibility of such substitution is determined by proximity of imaginary components of voltage in the secondary distribution network to zero, at the same time the imaginary voltage component at power supply node in the distribution network is fixed at a zero value.

A method of simple iterations is proposed to solve the non-linear system of measurement equations instead of the commonly used Newton iteration method based on linearization of measurement equations by their decomposition into Taylor series.

SE procedure in this method includes two steps repeated in an iterative manner. Values of nodal currents, here referred to as 'pseudo measurements' are determined at the first step of the first iteration using the measured values of active and reactive nodal powers and measurements of voltage magnitudes at node *i*, namely:

$$z_{Jai}^{a,b,c} - jz_{Jpi}^{a,b,c} = \left(z_{iP}^{a,b,c} - jz_{iQ}^{a,b,c}\right) \Big/ z_{U'i}^{a,b,c} \quad (1)$$

State variables are determined at the second step using pseudo measurements of currents with a real component of voltages, and their values are inserted in denominator of equation (2) at subsequent iterations:

$$z_{Jai}^{a,b,c} - jz_{Jpi}^{a,b,c} = \left(z_{iP}^{a,b,c} - jz_{iQ}^{a,b,c}\right) \Big/ \left(u_i'^{\,a,b,c} + j\,u_i''^{\,a,b,c}\right) \quad (2)$$

Iterations are terminated when maximum difference between state variables obtained at neighboring iterations does not exceed the calculation accuracy specified in advance. Linear equations of measurements that correspond to the phase values of active and reactive components of currents and a real voltage component measured at node i can be represented as:

$$\begin{pmatrix} g_i^{a,b,c} & b_i^{a,b,c} \\ -b_i^{a,b,c} & g_i^{a,b,c} \\ I^{a,b,c} & 0^{a,b,c} \end{pmatrix} \begin{pmatrix} u_i'^{a,b,c} \\ u_i''^{a,b,c} \end{pmatrix} = \begin{pmatrix} z_{Ja\,i}^{a,b,c} \\ z_{Jp\,i}^{a,b,c} \\ z_{U'i}^{a,b,c} \end{pmatrix} \quad (3)$$

where $g_i^{a,b,c}$ and $b_i^{a,b,c}$ are nodal conductance and susceptance matrices; $I^{a,b,c}$ and $0^{a,b,c}$ are identity and zero matrices, respectively.

System (3) in the general form can be written as:

$$H_z^{a,b,c} \cdot u^{a,b,c} = z_z^{a,b,c} \quad (4)$$

Similarly, equations of measurements of zero nodal currents at the transit node i will have the form:

$$H_0^{a,b,c} \cdot u^{a,b,c} = 0 \quad (5)$$

Let us represent the aggregation of equations (3) and (5) as:

$$H \cdot u = \begin{pmatrix} H_z^{a,b,c} \\ H_0^{a,b,c} \end{pmatrix} \cdot u^{a,b,c} = \begin{pmatrix} z_z^{a,b,c} \\ 0 \end{pmatrix} = \overline{z} \quad (6)$$

System (6) has a unique solution if the number of equations in it equals the number of variables (a basic system of measurements), and a rank of matrix H referred to as observability matrix [16, 17] equals the number of state variables. For smoothing the effect of errors in some measurements on the estimation of state variables, the measurement equations are multiplied by weight coefficients $R^{-1/2}$

$$R^{-1/2} H \cdot u = R^{-1/2} \overline{z} \quad (7)$$

where R is dispersion of measurement errors.

Such weighing has no effect on the solution to the basic measurement system. The necessary condition of the weighing efficiency is measurements redundancy that ensures the absence of critical measurements whose loss leads to the loss of observability. With redundant measurements, the matrix $R^{-1/2}H$ becomes re-defined as the number of rows in it exceeds the number of columns. There is no classic solution to the re-defined systems (7) but we can obtain a solution vector u that would allow minimization of the distance between vectors of the right-hand and left-hand sides of (7) by using the criterion of the squared differences sum minimization:

$$J(u) = (\overline{z} - Hu)^T R^{-1} (\overline{z} - Hu) \quad (8)$$

This method is called a method of weighted least squares and minimization problem solution can be obtained from a normal system of equations with a square matrix:

$$\left(H^T R^{-1} H\right) u = H^T R^{-1} \overline{z} \quad (9)$$

Estimates of the state variables obtained by solving (9)

$$u = \left(H^T R^{-1} H\right)^{-1} H^T R^{-1} \quad (10)$$

are used for calculation of estimates of both measured variables (nodal current and voltage magnitudes in our case) and unmeasured variables (load flows).

The matrix in equation (9) written for three phases is very big, which creates additional computational difficulties as compared to calculations of one phase at balanced loads. Experience of calculating the load flows in the low-voltage four-wire distribution network with unbalanced phase loads [1] shows that in the case of zero mutual inductances between phase, neutral and earth, calculation of load flow for each phase can be carried out independently. Currents and voltages in the zero wire and in the ground can be determined in the second stage of calculations. This approach can also be used for state estimation of each phase individually. Another advantage of the iteration method over the Newton method is that it is unnecessary to re-calculate the matrix in expression (9) in the course of iterations.

IV. Selection of the number and localities for measurements in the secondary distribution network

Ensuring the topology observability of the active model of a distribution network phase that includes a power supply node and *N-1* load nodes under the absence of transit nodes in it, requires at least one measurement of real voltage component and *N-1* measurements of active power. Out of *2·(N-1)* smart meter measurements taken at the load or generator nodes, *N-2* measurements are redundant. Similarly, for reactive model observability it suffices to fix the imaginary voltage component and measure *N-1* reactive power. Thus, there are no redundant measurements in the reactive model.

For the cases where it is impossible to install smart meters at all the nodes with loads and/or generations to ensure observability of nodal voltage magnitudes only, which is of special importance for the networks with renewable generation, the authors of [18] proposes using the algorithm [19] of selecting the minimum number of single-channel PMU to select the minimum number of smart meters. Additional constraints were introduced into this algorithm that prohibit installation of meters at the transit nodes and installation of more than one smart meter at any node. To provide the reactive model observability it was proposed to specify the zero values of measurements of transverse voltage components. It is worth noting that transit nodes neighboring two branches and leaf nodes without nodal power at them are not included into the phase equivalent circuit when selecting the mix of measurements.

In [20], the authors demonstrate that at minimum set of measurements as well as at location of meters at all the load and/or generator nodes, estimates of voltage

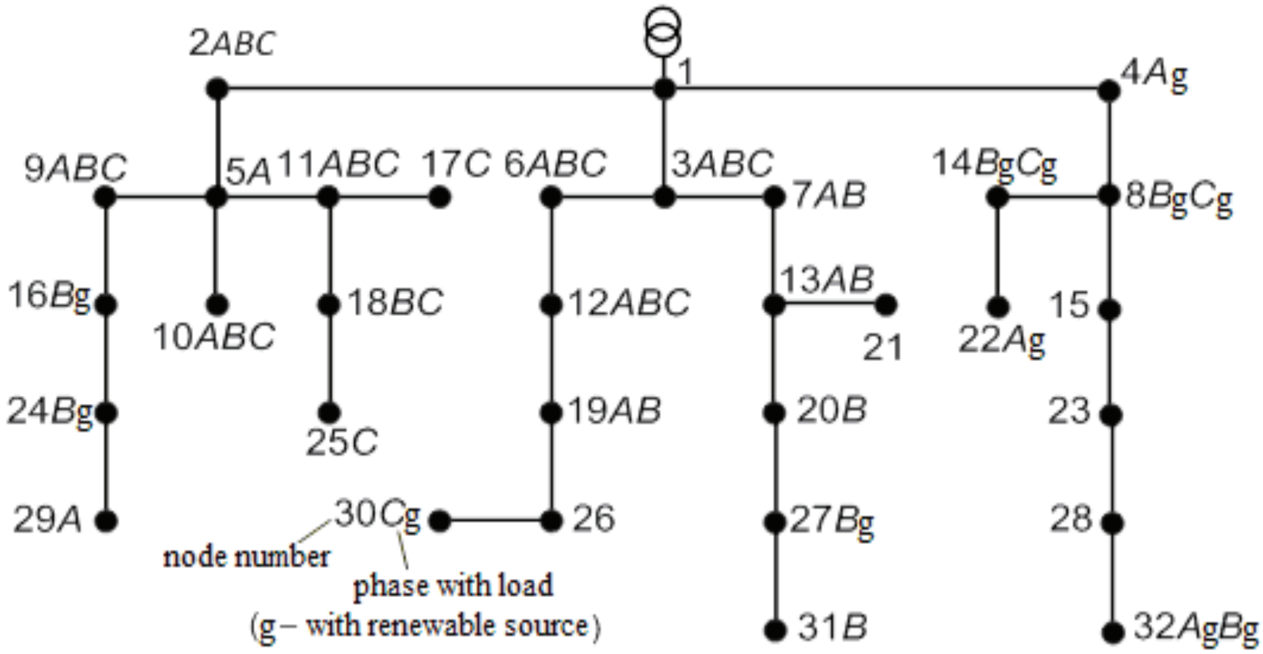

Fig. 2. Scheme of the secondary distribution network

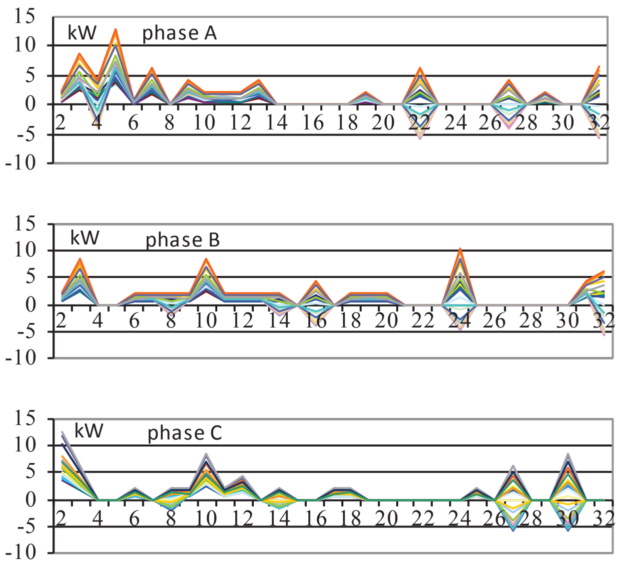

Fig. 3. Active nodal powers in phases A, B, C

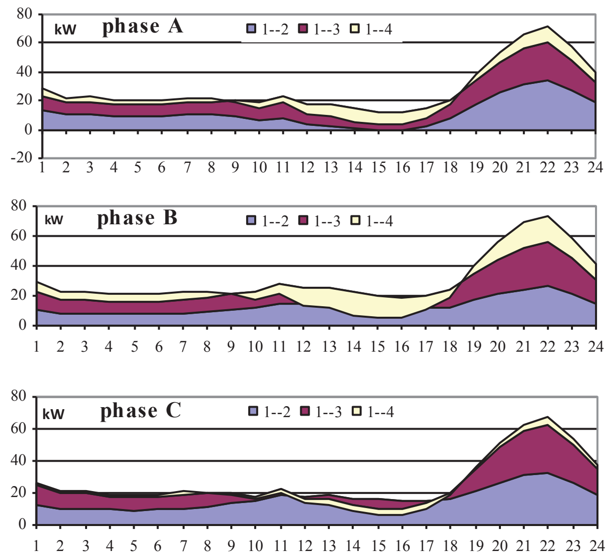

Fig. 4. Measurement of load flows over time in feeder sections 1-2, 1-3, 1-4 the sum of which equals load in the primary distribution network for phases A, B, C

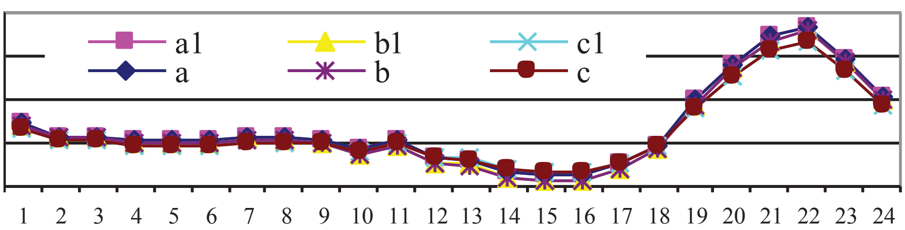

Fig. 5. Test values a1, b1, c1 and estimates of loads in the primary distribution network a, b, c in phases A, B, C (kWh)

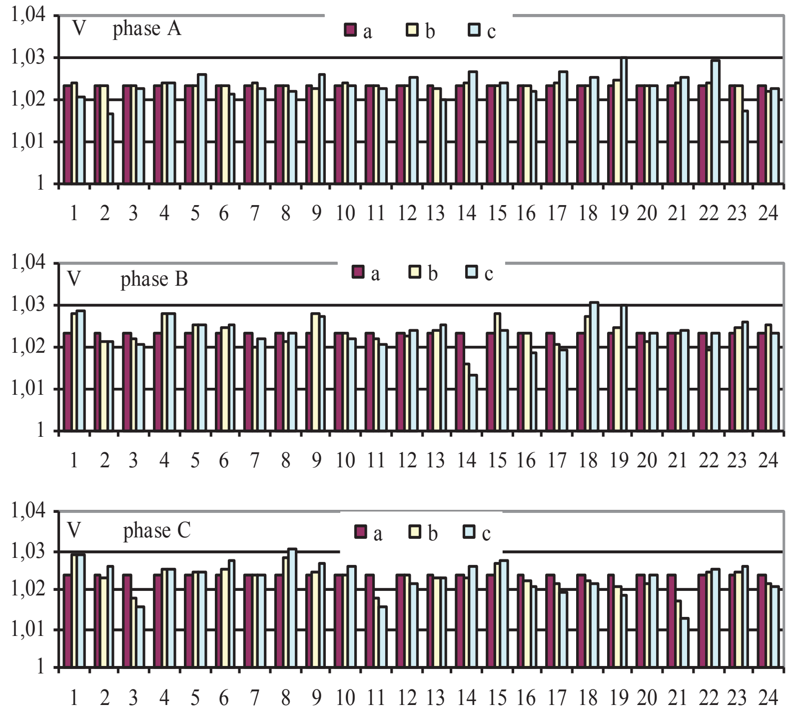

Fig. 6. The change in the relative values of phase voltage magnitudes at the first network node, test values (a); estimates of phase voltage magnitudes obtained from measurements at all load and generator nodes (b), and from the minimum set of measurements (c)

magnitude obtained during state estimation can be used to monitor voltage levels at the nodes of the secondary distribution network. Equating the 'measurements' of imaginary voltage components to zero results in significant errors in the assessment of both reactive and active current (power) components in branches and current (power) injections. Therefore, the authors of [20] concluded that the observability of all the state variables of the distribution network by measurements from smart meters that include measurements of nodal currents (powers) and voltage magnitudes is ensured provided smart meters are installed at all the load nodes.

V. Determination of phase loads in the primary distribution network

Let us illustrate an option of using the estimates of load flows in each phase of a test secondary distribution network that includes 32 nodes (Fig.2) for determination of phase loads in the primary distribution network. Data on hourly values of nodal capacities of each phase in the three-phase network were taken from [21].

Fig. 3 shows the values of active nodal powers in phases A, B, C for each hour of a daily curve. In phase A, there are 15 transit nodes, 12 load nodes, and four (4) generator nodes. The number of transit, load and generator nodes for phase B is equal to 13, 13 and 5, respectively, and those for phase C are 17, 10 and 4, respectively.

Data on loads and generation formed the basis for calculation of load flow at each phase of a test network. The values typical of low-voltage distribution network were taken for resistance and reactance of phase wires. Results of load flow calculations, referred to as test ones, were used for preparing the measurements of nodal power and voltage magnitudes that were to include measurement errors.

For modeling the measurement errors, the errors whose root mean square deviations were taken equal to 0.66W and 0.4V were introduced into the test values of nodal powers and voltage magnitudes.

For phases A, B, and C, Fig. 4 demonstrates the diagrams reflecting the change in time of both separate values of load flows in sections 1-2, 1-3, 1-4 of feeders that were obtained based on the state variables estimates, and their total values that can be considered as a change in the total phase load of the primary distribution network over time.

Graph in Fig. 5 illustrates test values and estimates of phase loads in the primary distribution network.

Fig. 6 shows the time variation of the test relative phase values of the voltage magnitudes at the first network node, estimates of phase values of the voltage magnitudes obtained from measurements at all load and generator nodes and for the minimum set of measurements: phase A - measurements at nodes 2, 6, 7, 10, 11, 19, 22, 27, 29, 32; phase B - measurements at nodes 2, 6, 10, 13, 14, 18, 19, 24, 31, 32; phase C - measurements at nodes 2, 10, 12, 14, 17, 25, 27, 30.

As the graphs in Fig. 6 show, although the estimates of the phase voltages obtained from the minimum set of measurements are less accurate than the estimates obtained from measurements at all load and generator nodes, they can be used to monitor the voltage at all the nodes of secondary distribution network, as noted earlier.

VI. Conclusion

We have demonstrated an option for determination of phase loads in the primary distribution network by using the results of estimation of load flows in the feeders of the secondary distribution network that were obtained by smart meters. Loads and voltages at all the nodes of the primary distribution network can be estimated in a similar manner and can be further used for calculation of three-phase state estimation. Additional measurements, if any, should also be included in the measurement set. Similarly to the linear state estimation procedure, the use of a simple iteration method for non-linear state estimation of distribution network makes the estimation procedure rather simple and time efficient.

Acknowledgment

The study is conducted in the framework of the project III.17.4.2. Program of Fundamental Research of SB RAS, Registration number AAAA-A17-117030310438-1

References

[1] O.N. Voitov, I.I. Golub, L.V. Semenova, “Algorithm for determining energy losses in electrical networks,” in Elektrichestvo (Electricity), no. 9, pp. 38-45, 2010 (In Russian)

[2] W.H. Wellssow, D. Waeresch, “Identification of topology faults by smart meter data in meshed low voltage grids,” in PSCC, Wroclaw, Poland, Aug. 18-22, 2014, pp. 1-7

[3] Ismerenie.RU, no. 16, Mar. 2013. [Online]. Available: https://www.izmerenie.ru/ru/number-15-6-12 Accessed on: Oct. 30, 2018 (In Russia)

[4] Ismerenie.RU, no. 17, Dec. 2013. [Online]. Available: https://www.izmerenie.ru/ru/izmerenie_ru-17 Accessed on: Oct. 30, 2018 (In Russia)

[5] T.N. Le, W-L. Chin, D.K. Truong, T.H. Nguyen, “Advanced Metering Infrastructure Based on Smart Meters in Smart Grid,” in Smart Metering Technology and Services - Inspirations for Energy Utilities, London, UK: InTech, 2016, ch. 3, pp. 37-61. [Online]. Available: https://www.intechopen.com/books/

[6] A. Bahmanyar et al., “Emerging smart meters in electrical distribution systems: opportunities and challenges,” in 24th ICEE, Shiraz, Iran, 10-12 May2016, pp. 1082-1087

[7] S. Ma, H. Zhang, X. Xing, “Scalability for Smart Infrastructure System in Smart Grid: A Survey,” in Wireless Pers Commun, vol. 99, pp. 161-184, 2018. DOI: 10.1007/s11277-017-5045-y

[8] R.R. Mohassel, A.S. Fung, F. Mohammadi, K. Raahemifar, “A survey on Advanced Metering Infrastructure and its application in Smart Grids,” in IEEE 27th CCECE, Toronto, ON, Canada, May 4-7, 2014, pp. 1-8

[9] A. Sendin, I. Berganza, A. Arzuaga, X. Osorio, I. Urrutia, P. Angueira, “Enhanced Operation of Electricity Distribution Grids through Smart Metering PLC Network Monitoring, analysis and grid conditioning,” in Energies, vol. 6, pp. 539-556, 2013, DOI: 10.3390/en6010539

[10] S-W. Luan, J-H. Teng, S-Y. Chan, L-C. Hwang, “Development of a Smart Power Meter for AMI Based on ZigBee Communication,” in PEDS 2009, Taipei, Taiwan, Nov. 2-5, 2009, pp.661-665

[11] K. Billewicz, “The use of Cloud Computing in AMI System Architecture,” in MEPS’15, Wroclaw, Poland, Jul. 6-9, 2015, pp.1-6

[12] H. Pezeshki, P.J. Wolfs, “Consumer phase identification in a three phase unbalanced LV distribution network,” in ISGT Europe, Berlin, Germany, Oct. 14-17, 2012, pp. 1–7

[13] Sioe T. Mak, “Smart Meters serving as synchro-sensors for smart distribution grid applications” in IEEE PES General Meeting, Detroit, MI, USA, Jul. 24-29, 2011, pp. 1-3

[14] S. Röhrenbeck, “Construction, commissioning and use of a test bench for smart meter accuracy verification,” in IEEE PESS, Dortmund, Germany, Jan. 13-14, 2015 [Online]. Available: https://eldorado.tu-dortmund.de/handle/2003/33956 Accessed on: Oct. 30, 2018

[15] Ni F., P.H. Nguyen, J.F.G. Cobben, H.E. Van den Brom, D. Zhao, “Three-phase state estimation in the medium-voltage network with aggregated smart meter data,” in INT J ELEC POWER, Elsevier, vol. 98, pp. 463-473, 2018. DOI: 10.1016/j.ijepes.2017.12.033

[16] A.Z. Gamm, I.I. Golub, D.IA. Keselman, “Nabliudaemost elektroenergeticheskikh system [Observability of electric power systems],” Elektrichestvo [Electricity], no. 1, pp. 12–18, 1975 (In Russian)

[17] A.Z. Gamm, I.I. Golub, Nabliudaemost elektroenergeticheskikh system [Observability of electric power systems], Mocsow: Nauka Publ., 1990, 200 p. (In Russian)

[18] I.I. Golub, Y.I. Kuzkina, “Mathematical models and methods of the analysis and optimal synthesis of the developing pipeline and hydraulic systems,” in Mathematical Models and Methods of the Analysis and Optimal Synthesis of the Developing Pipeline and Hydraulic Systems, Irkutsk, Lake Baikal, Russia, Jun. 26 – Jul. 2, E3S Web of Conferences, vol. 39, 2018,

DOI: 10.1051/e3sconf/201839013001

[19] R.F. Nuqui, A.G. Phadke, “Hybrid Linear State Estimation Utilizing Synchronized Phasor Measurements,” in IEEE Lausanne Power Tech, Lausanne, Switzerland, Jul. 1-5, 2007, pp. 1665-1669

[20] I.I. Golub, Y.I. Kuzkina, “Smart meters as a key component of modern measuring infrastructure providing observability and state estimation of low-voltage distribution networks,” Green Energy and Smart Grids 2018, E3S Web of Conferences, vol. 69, 2018, DOI: 10.1051/e3sconf/20186902012

[21] P.C. Olival, A.G. Madureira, M. Matos, “Advanced voltage control for smart microgrids using distributed energy resources,” in Electric power systems research, vol. 146, pp. 132-140, May 2017, DOI: 10.1016/j.epsr.2017.01.027

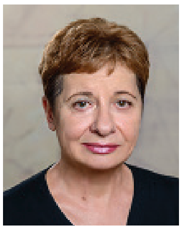

Golub I.I. Professor, Dr.Sc. in Engineering. She is a Leading Researcher at MESI SB RAS. She graduated from Moscow Power Institute as electrical engineer. Her scientific interests are connected with power system state analysis.

Boloev E.V. Ph.D. in Engineering. He has been a senior researcher at MESI SB RAS, since 2015. He graduated from Angarsk Technological Institute as electrical engineer. His research interests are problems of analysis and development of probabilistic power flow.

Kuzkina Y.I. Second category engineer of Relay Protection and Automation Department, LLC “Engineering Center “Irkutskenergo”. She graduated from Irkutsk National Research Technical University as electrical engineer. She has been a postgraduate student at MESI SB RAS, Irkutsk, since 2015.

A Fiducial Approach To Comparing The Electric Power Objects Of The Same Type

E.M. Farhadzadeh*, A.Z. Muradaliyev, Y.Z. Farzaliyev, T.K. Rafiyeva, S.A. Abdullayeva

Azerbaijan Scientific-Research and Design-Prospecting Power Engineering Institute, Baku, the Republic of Azerbaijan

***Abstract* — An increase in service life of equipment and plants (objects) in electric power systems makes it more appropriate to relate the organization of a system of maintenance service and restoration of wear and tear to their technical condition. This, in turn generates the need to quantitatively estimate the indices of their individual reliability. There can be no data on failures and defects of concrete objects, therefore, in practice we often calculate generalized reliability indices. An intuitive understanding of the varied significance of varieties of attributes is reflected by classifying statistical data for some varieties of attributes. For example, they can be classified according to voltage class, design, service life, etc. At the same time, the question on the appropriateness of the statistical data classification is not considered. Initial assumptions of known methods and criteria of checking if it is expedient to classify the statistical data on failures of the electric power system objects in most cases are unacceptable, since they are not relevant to this data set. We have developed a new method and an algorithm to assess the appropriateness of the statistical data classification. Their novelty lies in the application of a fiducial approach to estimation of critical values of a sample from a set of multivariate statistical data.**

***Index Terms* — reliability indices, varieties of attributes, classification, expediency, risk of the erroneous decision.**

I. Introduction

The need to improve the methods for a quantitative estimation of reliability indices of electric power system equipment and devices (objects) has become increasingly more pressing over time [1]. This is largely associated with a recommended transition from a system with regulated term and scope of planned maintenance to wear and tear restoration depending on technical condition of an object [2]. Thus, it is obvious, that this concerns reliability indices of a certain object, in other words, an individual reliability of an object with set varieties of attributes (VA). The varieties of attributes are established on the basis of nameplate data, operation conditions, statistical data on operation, results of tests and repair.

Since the data on failures and defects of concrete objects can simply be absent, in practice we calculate generalized reliability indices that are used for approximate calculations rather than the individual ones. The intuitive perception of the interrelation between reliability indices and varieties of attributes, however, leads to the understanding that it is sensible to classify the statistical data by the varieties of attributes. The practice of classifying data by one of the set of varieties of attributes is widespread. For example, classification according to a voltage class, or rated power or design or other attributes. Occasionally, data are classified according to two, and sometimes three varieties of attributes. In this case, the question whether it is appropriate to classify the statistical data is not considered, i.e. the random nature of reliability indices estimates is not taken into account. It is worth reminding that these data are called multivariate, i.e. depending on the set of the variety of attributes.

We will be surprised at such parameters as average temperature of patients in hospital (for continuous random variables) and average academic performance of students at university or at school (for discrete random variables). However, we calculate average duration of idle time of objects in emergency repair, or an average number of disconnected short circuits a year, or availability factor of a set of objects, and use these parameters in further calculations. We unequivocally characterize such parameters, as average temperature of patients from a surgery department in

* Corresponding author.
E-mail: elmeht@rambler.ru

http://dx.doi.org/10.25729/esr.2018.04.0008
Available online February 28, 2019.

hospital or average academic performance of sophomore students as strange. Nevertheless, we are absolutely confident when we calculate the reliability indices, for example, for the objects of various voltage classes and analyze this dependence. In the end, we do not change our mind about strangeness of the estimates of average academic performance of sophomore students of the Energy Department of university or average temperature of patients of a female surgery department in hospital. At the same time, without any doubts, we use the estimates of reliability indices for the objects of a set voltage class and design in calculations. Certainly, someone can object and say that we use the varieties of attributes of different significance. Yes, possibly, but it confirms even more the necessity of a quantitative estimation of the significance of the varieties of attributes.

Application of known methods for checking the appropriateness of classification of the statistical data characterizing reliability of electric power system objects, in most cases is unacceptable, since initial preconditions of these methods are not relevant to them. These preconditions include, first of all, a great number of realizations of samples and the normal law of their distribution [3]. The difficulties also arise when solving practical problems related to the objects comparison and ranking. Fiducial approach in many respects helps overcome these difficulties.

Fiducial probabilities and intervals. Fiducial distributions were proposed by R.A. Fisher in 1935. They determine "to what extent, we can trust (fiducial means based on or having trust) any set value of an unknown index (parameter) of this distribution", and in essence, this is a distribution of possible realizations of distribution parameters of a random sample from a population [4]. According to Fisher:

1. We should trust only the decisions based on empirical data, to be more precise, distribution of an observable sample [5];
2. An acceptable way of constructing fiducial intervals is calculation of probability distribution of possible variable values [5];
3. Confidence and fiducial intervals are identical but only when a single parameter is estimated. If complex parameter is estimated by two or a greater number of parameters, the results can differ [6].

The difficulties in analytical representation of distributions of parameters calculated for small samples from finite population of multivariate data (FPMD) [7] and for complex indices are well known. However, even in 1942, Kolmogorov A.N. noted that at a small size of sample (ns) the best interval estimates are provided by fiducial probabilities [8].

New unlimited opportunities for calculation of statistical functions of fiducial distributions were brought about by the advent of computer equipment and development of computer technologies.

Prior to the algorithm for calculation of statistical function of fiducial distributions, let us specify the specific features of a relationship between confidence and fiducial intervals [9]. Confidence intervals of parameters are determined analytically by the known formulas for some initial preconditions. They characterize a set of possible realizations of a concrete parameter. For example, if to take a random sample of random variables with uniform distribution in an interval [0,1], we can easily enough identify the confidence borders of the arithmetic mean $M^*(\xi)$ with a set significance value. Between lower $\underline{M(\xi)}$ and upper $\overline{M(\xi)}$ boundary values of a confidence interval there is a set of possible realizations . This set does not necessarily include the true value of $M(\xi)=0.5$. However, if we repeat these calculations a set of times (N), then $N(1\text{-}\alpha)$ confidence intervals will contain the value of $M(\xi) = 0.5$. This is a known engineering interpretation of the confidence interval.

In real operation of electric power system objects, there is certainly no opportunity to repeat the «tests». In addition, it is impossible to disagree with Fisher that empirical data characterize these objects. All uniform objects form a FPMD, for example, related to the duration of emergency idle time. A sample from this population characterizes the significance of an attribute according to which the classification is done. The set of possible realizations is determined similarly to an estimation of a set of realizations of a confidence interval (see an example with an estimation of arithmetic mean $M^*(\xi)$), the only difference being that for the confidence interval this set is determined analytically, while for fiducial interval - by simulation modelling. The simulation modelling should be carried out so that the statistical function of fiducial distribution of a calculated parameter completely coincides with distribution of the parameter within the confidence interval.

Thus, the boundary values of confidence and fiducial intervals of parameters coincide when the law of parameter distribution inside of a confidence interval is known, in other words, the law of fiducial distribution. This requirement provides objectivity of simulation modelling algorithm, an opportunity to control operability and estimate the accuracy when the initial preconditions are not met [10]. For example, the boundary values of Pearson correlation coefficient are calculated at a large size of samples and normal law of their distribution. The result of calculation of boundary values of Pearson correlation coefficient based on fiducial approach should completely coincide with its tabulated values. In these conditions, at super small samples [ns=(3÷10)], when boundary values of a confidence interval are erroneous, the fiducial approach provides objective calculation of accuracy.

The condition of correspondence between an analyzed parameter and a group of single parameters [11] is optional, since confidence intervals can be calculated for some complex parameters as well. Vivid examples of such parameters are the correlation factor, linear regression coefficient, etc.

Figure 1 demonstrates a simplified block diagram of modelling a statistical function of fiducial distribution (s.f.f.d.) for an arithmetic mean of random variables with uniform distribution in an interval [0,1] [12].

II. Modeling of possible realizations of objects reliability indices

We will model the reliability index realizations on an example of an average duration of forced idle time for eight circuit breakers of 300 MW oil-and-gas fired units $[M^*(\tau_c)]$. The realizations τ_c are given for illustration in Table 1.All these data are called finite population of multivariate data (FPMD). Their number n_Σ=43 and arithmetic mean $M^*(\tau_{c,\Sigma}) = \sum_{i=1}^{c}\sum_{j=1}^{n_i}\tau_{c,i,j} \Big/ 43 = 72,3\,h$ Estimates of this parameter for each power unit $[M^*(\tau_{c,i})]$ are presented in and allows two groups to be identified. The first group

$$F_S^*(\tau_f) = \begin{cases} 0 & \text{if } \tau_f \le \tau_{f,1} \\ \dfrac{s-1}{n_i+1} + \dfrac{(\tau_c - \tau_{c,s})}{(n_i+1)\cdot(\tau_{c,(s+1)} - \tau_{c,s})} & \text{if } \tau_{f,1} < \tau_f < \tau_{f,(n_i+1)} \\ 1 & \text{if } \tau_f \ge \tau_{f,(n_i+2)} \end{cases} \quad (1)$$

where $s = 1,(n_i+1)$

will include the estimates $[M^*(\tau_{c,i})]$ that exceed $[M^*(\tau_{c,\Sigma})]$, and the second group will include estimates for which $[M^*(\tau_{c,i})]<[M^*(\tau\ \xi_{c,\Sigma})]$ Our task is to determine estimates $[M^*(\tau_{c,i})]$ that randomly differ from $[M^*(\tau_{c,\Sigma})]$

Let us consider three assumptions (hypotheses) H:

1. Estimate $[M^*(\tau_{c,i})]$ randomly differs from $[M^*(\tau_{c,\Sigma})]$ This will be denoted as $H \rightarrow H_1$;
2. Estimate $[M^*(\tau_{c,i})]$ is non-randomly larger than $[M^*(\tau_{c,\Sigma})]$ This will be denoted as $H \rightarrow H_2$;
3. Estimate $[M^*(\tau_{c,i})]$ is non-randomly lower than $[M^*(\tau_{c,\Sigma})]$ This will be denoted as $H \rightarrow H_3$.

where conformity is denoted by →

To make a decision with the minimal risk of erroneous decision, it is necessary to be able to calculate critical values of these parameters $[M^*(\tau_{c,\Sigma})]$ and $[M^*(\tau_{c,i})]$ with i=1.8.

Possible realizations of duration of the forced idle time of circuit breakers $\tau_{f,i}$ are modelled by statistical distribution functions $F^*(\tau_{c,\Sigma})$ and $F^*(\tau_{c,i})$ with i=1,n8. It is worth noting, that one of the basic reasons why the confidence and fiducial intervals are different is the discrepancy between the modelled set of possible realizations of calculated parameters and the real set.

The traditional approach to modeling possible realizations τ_c by $F^*(\tau_{c,i})$ for super small sizes of samples is unacceptable. In [13], we propose a new method. The statistical distribution function $F_s^*(\tau_{c,i})$ is represented by the equation (1):

Realization is calculated by the formula:

$$\tau_c = \tau_{c,s} + (\tau_{s+1} - \tau_{c,s}) \cdot [\xi(n_i + 1) - (s - 1)] \quad (2)$$

Realization τ_c of average duration of forced idle time $M^*(\tau_c)$ is calculated by n_i realizations τ_f.

III. Formation of statistical function of fiducial distribution

According to possible hypotheses we will distinguish three statistical functions of fiducial distributions:

$F^*[M^*(\tau_c / H_1)]$, $F^*[M^*(\tau_c / H_2)]$ and $F^*[M^*(\tau_c / H_3)]$.

For $F^*[M^*(\tau_c/H_1)]$ the sample should be representative.

For $F^*[M^*(\tau_c / H_2)]$ and $F^*[M^*(\tau_c / H_3)]$ the samples are modeled similarly to $F^*[M^*(\tau_c / H_1)]$ with the essential difference being that modeling of realizations τ_c is performed not by statistical distribution function $F^*(\tau_{c,\Sigma})$, but by $F^*(\tau_{c,i})$, where i=1,n8.

Table 1. Data on duration of forced idle time of circuit breakers, h.

i	Conventional numbers of circuit breakers of power units							
	1	2	3	4	5	6	7	8
1			78.59					
2	64.42		3.36				66.29	
3	15.31	46.12	3.48			49.15	47.02	
4	53.5	46.27	42.05	61.36		91.17	93.13	36.05
5	94.55	298.58	45.15	236.3	63.5	99.51	54.03	6.23
6	69.37	134.12	62.36	123.59	38.07	39.11	79.21	15.35
7	5.48	35.51	18.15	358.15		133.24	57.2	
8	185.0		29.42				66.1	
9			7.43				1.3	
10			25.5					
$\sum\tau_{c,i}$, h.	487.1	560.5	320.0	780.0	102.0	412.0	464.0	57.6
$[M^*(\tau_{c,i})]$	69.6	112.1	32.0	195.0	51.0	82.4	58.0	19.2

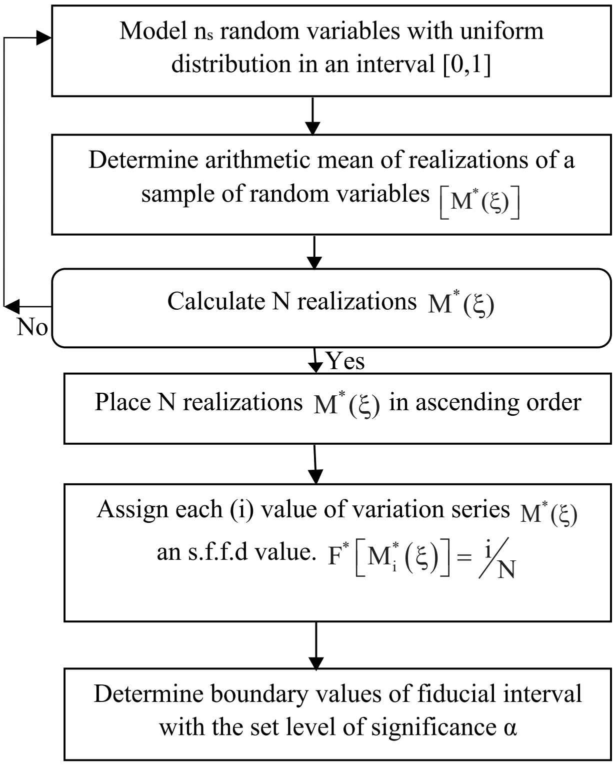

Fig.1. A simplified block diagram of an algorithm for modelling a s.f.f.d. $F^*\left[M_i^*(\xi)\right]$

It is obvious, that number of possible realizations $M^*(\tau_c)$ equal to N should satisfy the requirement of stability of estimates of quantiles of fiducial distributions for set values of Type I and Type II errors.

We will consider the quantiles of these distributions to be steady if the divergence of realizations of critical values does not exceed 1% with an increase in the number of realizations N. Let us note one more feature of the algorithm for decision-making on significance of varieties of attributes:

if $[M^*(\tau_{c,\Sigma})] < [M^*(\tau_{c,i})]$, we compare the distributions $R^*[M^*(\tau_c / H_1)] = [1 - F^*[M^*(\tau_c / H_1)]]$ and $F^*[M^*(\tau_c / H_2)]$;

if $[M^*(\tau_{c,\Sigma})] > [M^*(\tau_{c,i})]$ we compare $R^*[M^*(\tau_c / H_3)] = [1 - F^*[M^*(\tau_c / H_3)]]$ and $F^*[M^*(\tau_c / H_1)]$

Accordingly, we consider:

critical values $\overline{M^*(\tau_{c,(1-\alpha)})}$ and $\underline{M^*(\tau_{c,\beta_k})}$ at $[M^*(\tau_{c,\Sigma})] < [M^*(\tau_{c,i})]$;

critical values $\overline{M^*(\tau_{c,(1-\beta)})}$ and $\underline{M^*(\tau_{c,\alpha_k})}$ at $[M^*(\tau_{c,\Sigma})] > [M^*(\tau_{c,i})]$.

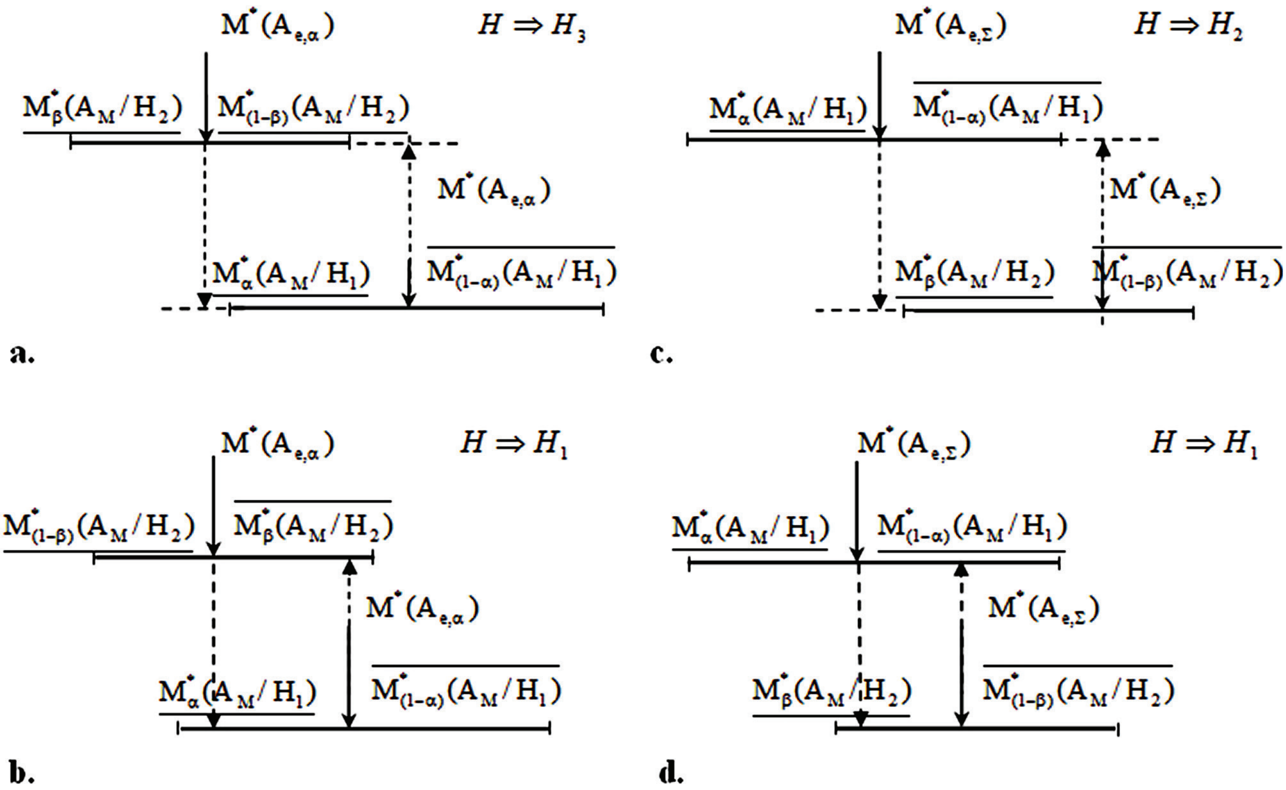

Fig. 2. Graphic illustration of relationships between experimental estimates of reliability indices (A_e) *and their critical values:* (a and b) → $M^*(A_{e,i}) > M^*(A_{e,\Sigma})$; (c and d) $M^*(A_{e,i}) < M^*(A_{e,\Sigma})$

IV. A criterion of decision-making on significance of attribute varieties

The appropriateness of the statistical data classification with respect to a set variety of attributes is assessed to specify the reliability indices of objects. Classification is considered to be appropriate if an estimate of reliability indices calculated after classification of data in a sample non-randomly differs from a reliability index calculated based on an initial data set. A condition, that determines the appropriateness is called criterion. The following criterion is proposed:

$$\left.\begin{array}{l|l} \text{1. If } M^*(A_{e,i}) < M^*(A_{e,\Sigma}) & \text{2. If } M^*(A_{e,i}) > M^*(A_{e,\Sigma}) \\ \text{and } M^*(A_{e,i}) < \underline{M^*_{\alpha}(A_M/H_1)}, & \text{and } M^*(A_{e,i}) > \overline{M^*_{(1-\alpha)}(A_M/H_1)} \\ \text{then } H \Rightarrow H_3 \rightarrow \text{exit} & \text{then } H \Rightarrow H_2 \rightarrow \text{exit} \\ \text{if } M^*(A_{e,i}) > \underline{M^*_{\alpha}(A_M/H_1)} & \text{if } M^*(A_{e,i}) < \overline{M^*_{(1-\alpha)}(A_M/H_1)} \\ \text{then } H \Rightarrow H_1 \rightarrow \text{exit} & \text{then } H \Rightarrow H_1 \rightarrow \text{exit} \end{array}\right\} \quad (3)$$

Here $M^*(A_{e,\Sigma})$ and $M^*(A_{e,i})$ are estimates of any reliability index, A_e, calculated accordingly by set (Σ) of experimental (e) data and sample (v) for the i-th object; $\underline{M^*_{\beta}(A_M/H_2)}$ and $\overline{M^*_{(1-\alpha)}(A_M/H_1)}$ are the lower and upper boundary values of fiducial interval, respectively, calculated by modelled (м) estimates of reliability index on the basis of representative samples of random variables; $\underline{M^*_{\beta}(A_M/H_2)}$ and $\overline{M^*_{(1-\beta)}(A_M/H_2)}$ are respectively the lower and upper boundary values of fiducial interval calculated by modelled estimates of reliability index on the basis of statistical distribution function of experimental sample of random variables.

Figure 2 presents a graphical illustration of the criterion for comparison of estimates of average duration of the forced idle time of the power unit circuit breakers. The estimates were obtained by classifying the statistical data according to the dispatcher numbers of circuit breakers. This method allows us to transition to the estimates of individual reliability indices and reliability indices of clusters of objects. Their basic difference is that the individual reliability indices are calculated by classifying the data according to the significant varieties of attributes out of those set, whereas the reliability indices of clusters are calculated by classifying the statistical data according to the significant varieties of attributes from a specified set of attributes and their varieties.

Table 2 presents the results of an analysis of the appropriateness of the classification of statistical data (Table 1) on the duration of the forced idle time of the 300 MW power unit circuit breakers.

If $H \Longrightarrow H_1$, classification is considered to be inappropriate, while at $H \Longrightarrow H_2$ or $H \Longrightarrow H_3$, it is appropriate. Thus, irrespective of the relationship between the experimental estimates of average idle time of power unit circuit breakers according to the data population and samples, classification of data is inappropriate for four of eight circuit breakers (1, 5, 6 and 7). An analysis of this vivid example confirms the appropriateness of monitoring the significance of a divergence of reliability index estimates before and after classification of statistical data.

V. Conclusion

1. The accuracy and reliability of calculation of the reliability indices of electric power system equipment and devices can be increased by:
   - employing computer technologies based on simulation modeling of fiducial distribution in the statistical analysis of experimental data;
   - determining (based on these distributions) the critical values of reliability indices;
   - applying the recommended criterion of estimation of the data classification appropriateness;
2. Fiducial distributions of reliability indices are modeled for analyzed assumptions: classification, accordingly, is appropriate and inappropriate. This provides the minimal risk of erroneous decision;

Table 2. An analysis of appropriateness of the classification of statistical data on forced idle time of 300 MW power unit circuit breakers according to their conventional number

№	Parameters	Conventional number of circuit breakers							
		1	2	3	4	5	6	7	8
1	n_i	7	5	10	4	2	5	8	3
2	$M^*_{e,i}(\tau_{em})$, h.	69.7	112.1	32	195	51	82.4	58	19.2
3	$\overline{M^*_{M,(1-\alpha)}(\tau_{em})}$, h.	-	108.9	-	113.3	-	108.9	-	-
4	$\underline{M^*_{M,\alpha}(\tau_{em})}$, h.	41.5	-	46.4	-	15.2	-	43.4	24.6
5	$\overline{M^*_{M,(1-\beta)}(\tau_{em})}$, h.	93.4	-	-	-	91.3	-	81.2	-
6	$\underline{M^*_{M,\beta}(\tau_{em})}$, h.	-	-	-	-	-	40.9	-	-
7	H	H_1	H_2	H_2	H_2	H_1	H_1	H_1	H_2

3. Classification of statistical data based on the set varieties of attributes is done until the obtained reliability index estimate randomly differs from an estimate calculated in the preceded stage of the classification;
4. The recommended method makes it possible both to control the statistical data classification when complex reliability indices are calculated, which cannot be done by any of the existing methods, and to operate small samples of multivariate data;
5. For small samples, with the number of realizations varying from 2 to 10, one of the pitfalls is a discrete nature of fiducial distribution. In this case, we propose switching from comparison of the fiducial distribution quantiles, to comparison of experimental values of Type I and Type II errors with their critical values.

References

[1] N.I. Voropai, "A concept of SMART-GRID and reliability of electric power systems. Methodological problems in reliability study of large energy systems." Issue 62, Ivanovo. Press Hundred, 2011, p.321-325.

[2] "Rules of technical operation of power plants and networks of the Russian Federation." Ministry for the Electric Power Industry of the Russian Federation. 2003, 160 p.

[3] M. Kendal, Stuart P.A. "Statistical inference and relations." Publishing House "Nauka", 1973, 900 p.

[4] A.I. Orlov, "Applied statistics." M.: Publishing House "Examen", 2004, 656 p.

[5] R.A. Ficher, "The concepts of inverse probability and fiducial probability referring to unknown parameters" // "Proc.Roy.Soc. (London)" A139, p. 343-348. 1939

[6] R.A. Ficher, "The fiducial argument in statistical inference" // "Annals of Eugenics", 6, p. 391-398, 1935

[7] D.A. Frazer, "The fiducial method and invariance" // Biometrika, 1961,v.48, p. 261-280

[8] A.N. Kolmogorov, "Determination of the center of dispersion and a degree of accuracy for a limited number of observations." Izv. of the AS of the USSR. Mathematics. 1942, 6, p. 3-32

[9] E.M. Farhadzadeh, "About an arrangement of boundary values of confidence and fiducial intervals of reliability indices of systems." Izv. of the AS of the USSR, Technical cybernetics No.5, 1979, p.196-199.

[10] E.M. Farhadzadeh, "Estimation of the influence of differentiation of the initial information on system reliability," *Methodological problems in reliability study of large energy systems*. Issue 7. Irkutsk, 1976, p.24-34.

[11] E.M. Farhadzadeh, "About an estimation of statistical distribution function of duration of serviceable work of power system components," *Journal "Elektrichestvo"*, 1976, No. 6, p.78-80.

[12] E.M. Farhadzadeh, "Statistical modeling of duration of equipment failure-free operation on electronic digital computer," Izv. of AS of the USSR. "Energy and Transport", 1977, No.6, p.174-178.

[13] E.M. Farhadzadeh, Y.Z. Farzaliyev, A.Z. Muradaliyev, "Comparison of methods for modelling of continuous random variables by empirical distributions," Baku, "Energy problems", No.1, 2013, p.25-31.

Elmar M. Farhadzadeh (Professor, Dr. Sc.) was born in 1939 in the city of Baku of the Republic of Azerbaijan. He graduated from the Energy Department of the Azerbaijan Oil and Chemistry Institute in 1961. In 1982, he defended the doctoral thesis "Accuracy and reliability of characteristics of reliability of power plants" in Novosibirsk Electro-Technical Institute. Currently he is the head of the Laboratory for Reliability of the Equipment of Electric Power Systems at ASRDPPEI in Baku. His research interests are: reliability and efficiency of electric power systems.

Aydin Z. Muradaliyev (PhD) was born in 1960 in the city of Baku of the Republic of Azerbaijan. He graduated from Energy Department of the Azerbaijan Oil and Chemistry Institute in 1982 year. In 2013, he defended the doctoral thesis "Development of methods and algorithms for calculation of reliability indices of the electric power system equipment and devices". He is the head of the Department for Reliability of Equipment of Electric Power Systems at ASRDPPEI in Baku. His research interests include: Quantitative estimation of reliability of equipment and devices of electric power systems.

Yusif Z. Farzaliyev (PhD) was born in 1958 in the city of Fizuli of the Republic of Azerbaijan. He graduated from the Azerbaijan State University in 1985, as an applied mathematician. In 2008, he defended the master's thesis “An increase in the accuracy and reliability of calculation of reliability indices of power units”. He is the main expert of the Department for Reliability of Power Equipment at ASRDPPEI in Baku.

Tamara K. Rafiyeva was born in 1950 in the city of Baku of the Republic of Azerbaijan. In 1973 she graduated from Energy Department of the Azerbaijan Oil and Chemistry Institute. In 2007 she defended the master's thesis “Simulation modeling of individual reliability of power units”. She is a senior scientific researcher of the Department for Reliability of Power Equipment at ASRDPPEI in Baku.
Her research interests include: Quantitative estimation of a technical condition of the equipment and devices of electric power systems

Samira A. Abdullayeva was born in 1968 year in the city of Baku of the Republic of Azerbaijan. She graduated from the Energy Department of the Azerbaijan Oil and Chemistry Institute in 1990. She is a leading engineer of the Department for Reliability of Equipment of Electric Power Systems at ASRDPPEI in Baku. She is a post-graduate student.